
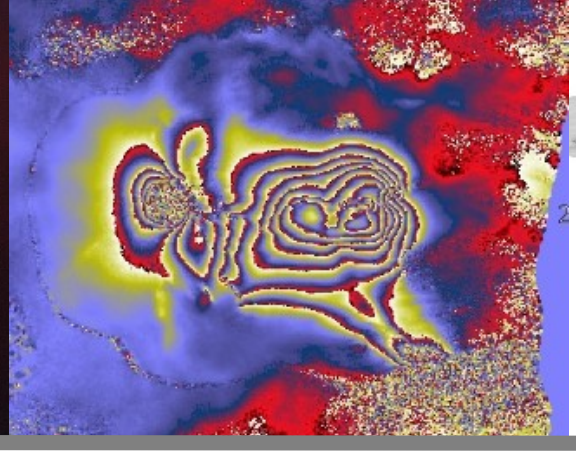
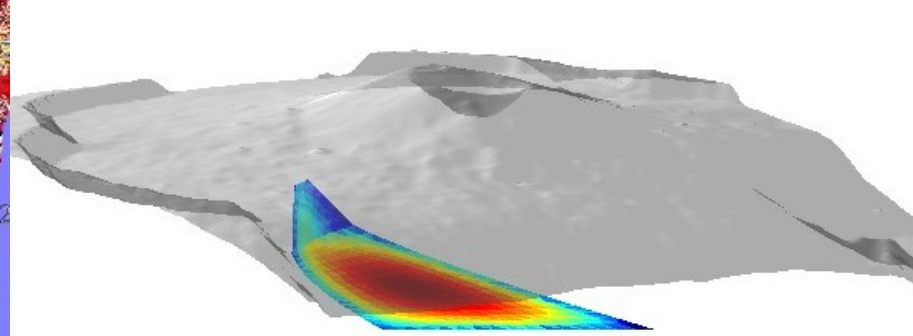

Introduction to inverse modelling of deformation data

Valérie Cayol, valerie.cayol@uca.fr
Laboratoire Magmas et Volcans, CNRS, UCA, IRD, OPGC, F-63000 Clermont-Ferrand, France

Outline

1. Introduction

2. Modelling
   - Most famous simple models
   - More complex models

3. Inversions
   - Linear Inversions
   - Non-linear inversions
   - Discriminating complex models

4. Benchmarking, Validation, Verification

5. Examples of inversions using stress boundary conditions
   - 5.1. Stress inversions as gauges for crustal stress
   - 5.2. Stress inversions for flank failure mechanism

Why do we model deformation ?

InSAR

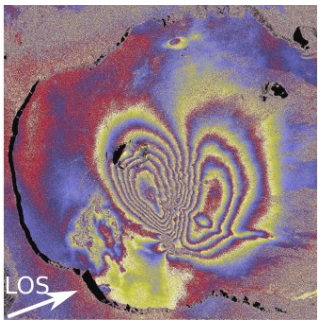

GNSS

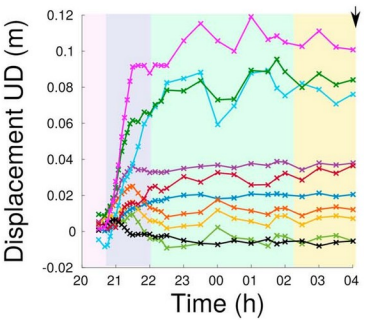

Deformation

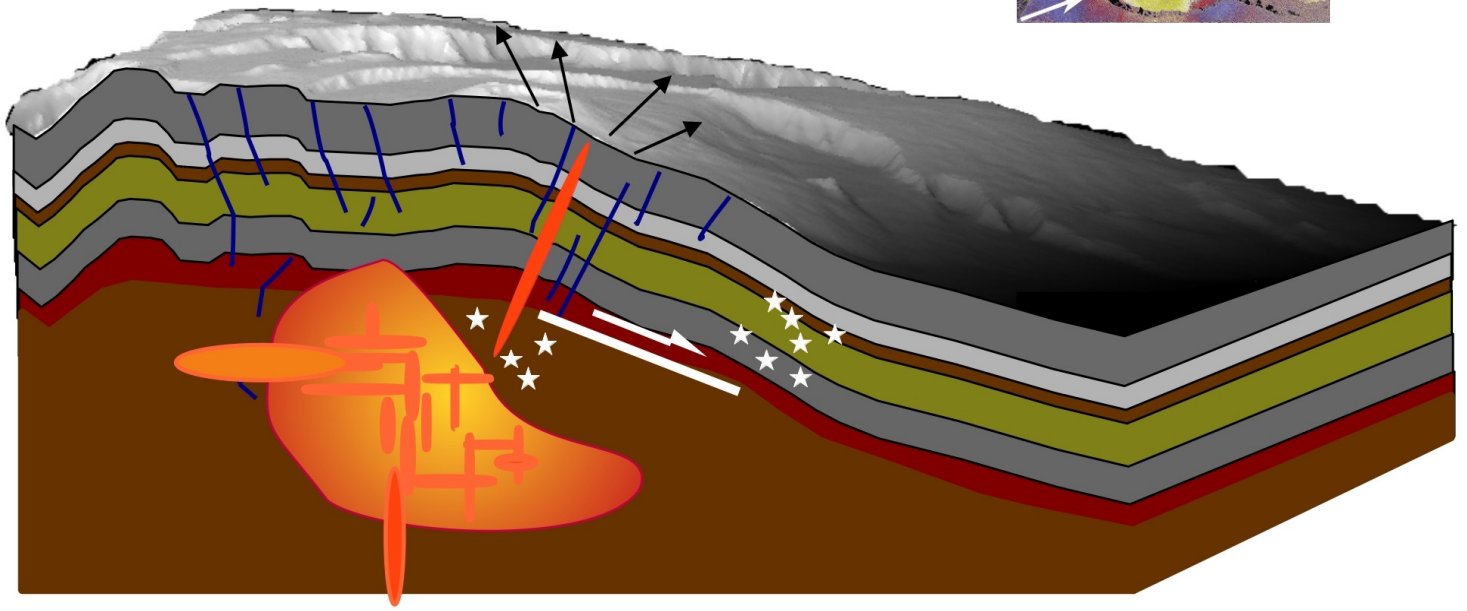

Two objectives of deformation monitoring :

- **To monitor volcanic activity;**
- **To understand volcanic processes through modelling.**

Why do we model deformation ?

InSAR

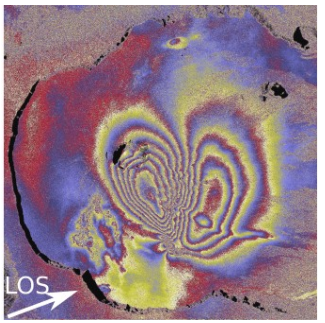

GNSS

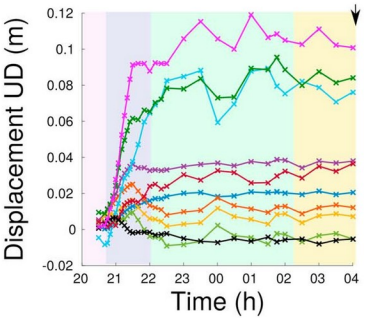

Deformation

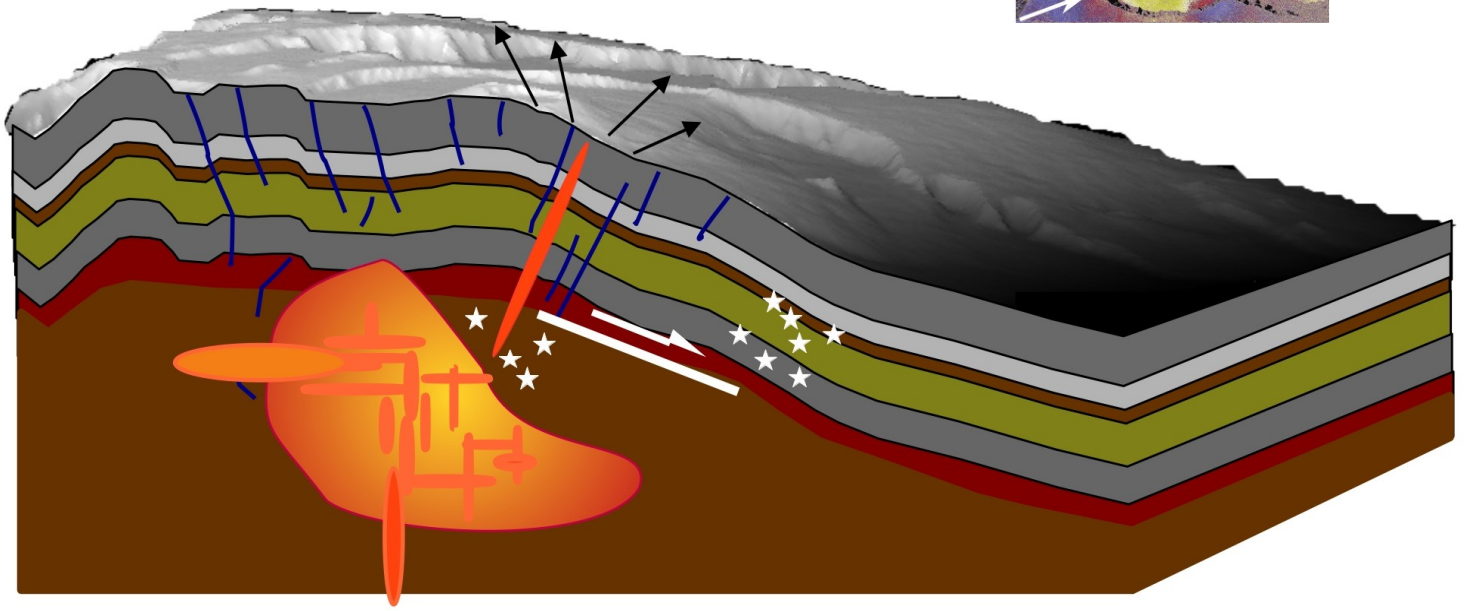

Main questions are

- **Where is magma stored ?**
- **What are the physical and mechanical parameters controlling magma transfer ?**
- **How do edifices grow and collapse ?**

Forward versus inverse models

Direct problem : $\boldsymbol{m} \rightarrow \boldsymbol{u} = G(\boldsymbol{m})$, $\boldsymbol{m}$ = *parameters*
(unique) $\boldsymbol{u}$ = *observations*

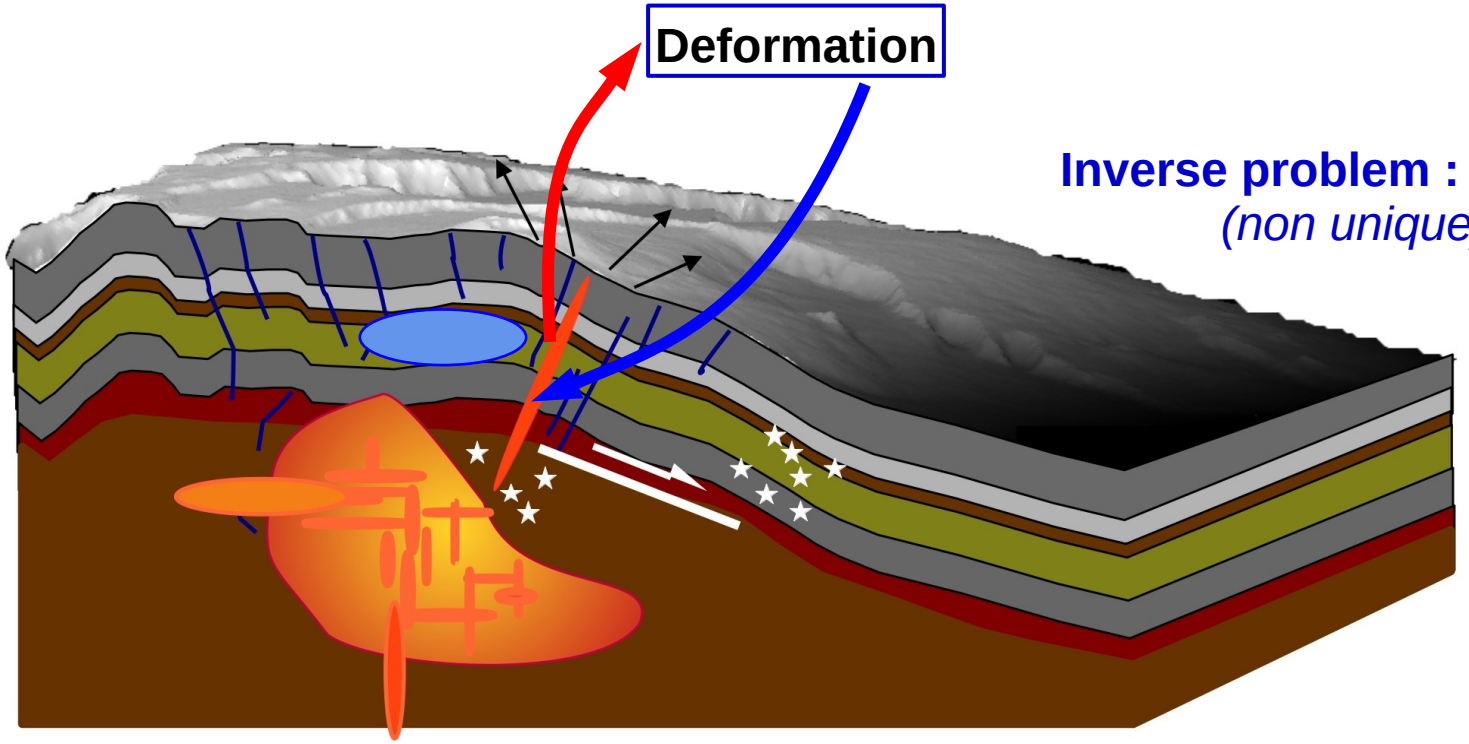

Inverse problem : $\boldsymbol{u} \rightarrow \boldsymbol{m}$?
(non unique)

Adhémar Barré de Saint Venant

St Venant's principle (1855) "the difference between the effects of two different but statically equivalent loads becomes very small at sufficiently large distances from load »

2. Modelling

Direct problem: $\boldsymbol{m} \rightarrow \boldsymbol{u} = G(\boldsymbol{m})$, $\boldsymbol{m}$ = *parameters*
(unique) $\boldsymbol{u}$ = *observations*

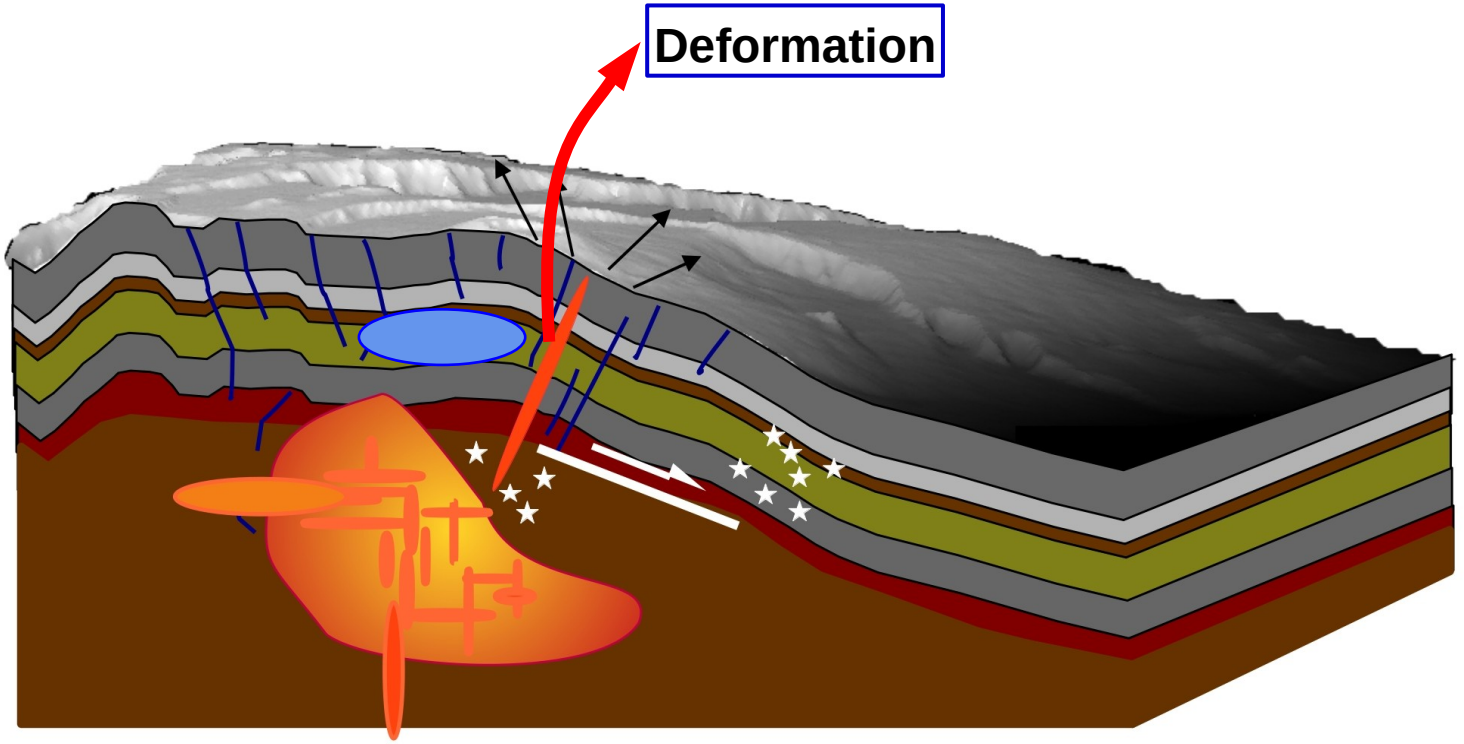

Hypothesis: linear elasticity

1. Linear elasticity : stress is linearly relation to deformation

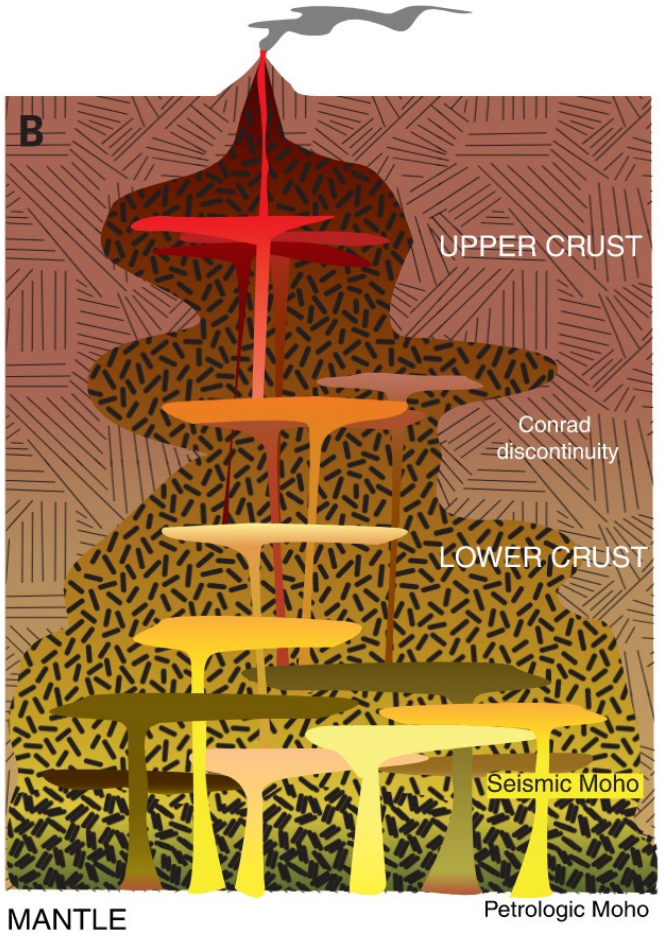

- However, from petrology studies, reservoirs are now considered as being mushes containing magma pockets. Rock behavior is most probably elasto-visco-plastic, or poro-visco elastic over a long time scale.
- St Venant's principle can be used

Cashman et al., Science, 2017

Hypothesis: linear elasticity

1. Linear elasticity : stress is linearly relation to deformation

In situ studies, laboratory experiments and theoretical studies show that inelasticity occurs at the tip of dikes. This zone is small and can therefore be neglected (St Venant's Principle).

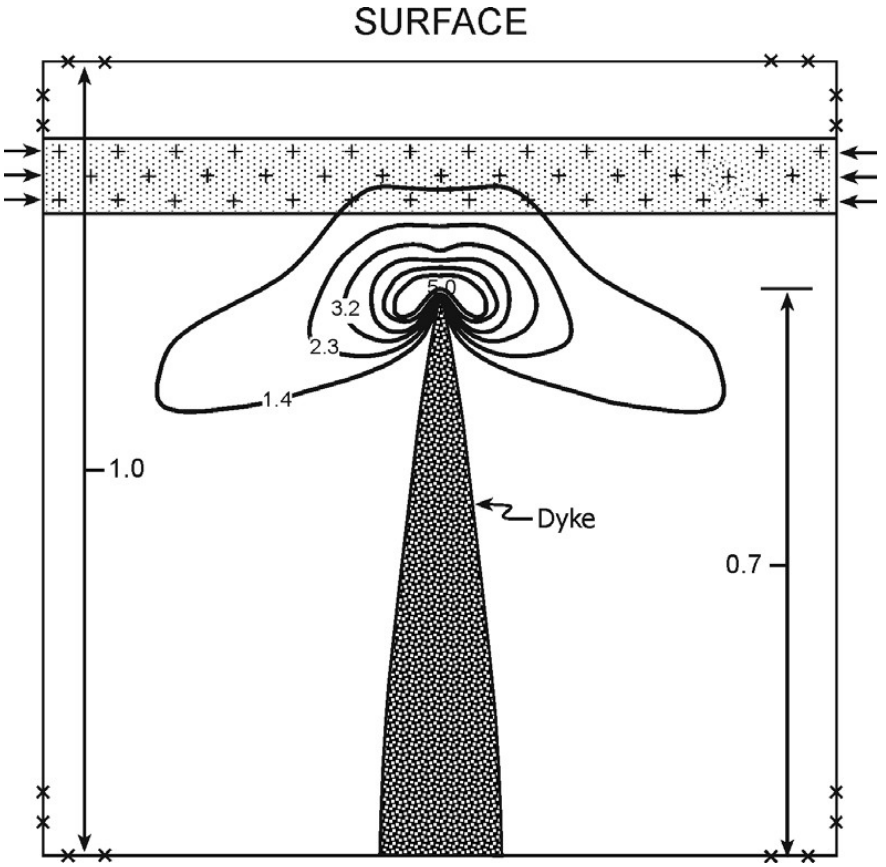

Gudmundsson and Brenner, Annals Geophysica, 2004

Hypothesis: homogeneity

2. Homogeneity (same mechanical properties everywhere)

Tomography of Piton de la Fournaise (*Prôno et al., JVGR, 2009*) :

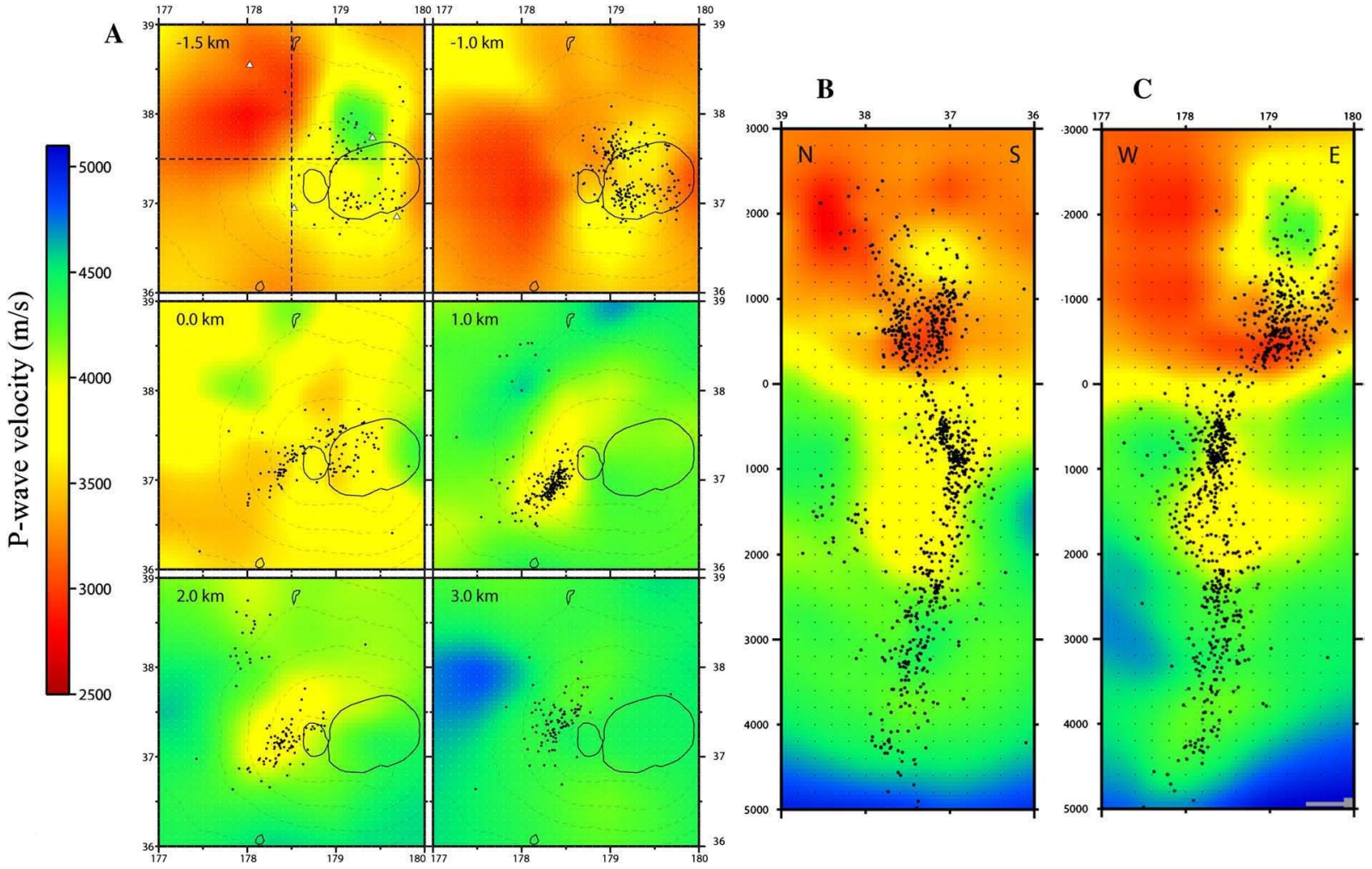

Volcanoes are not really homogeneous,but it is assumed that heterogeneity plays a second-order role.

Most famous simple models

1. Mogi-Yamakawa Model (1958) (Analytic) :
Most widely used model for quantitative interpretation of volcano deformation,
(google scolar > 2000 times)

Sakurajima's 1914 eruption

Most famous simple models

1. Mogi-Yamakawa Model (1958) (Analytic) :
Most widely used model for quantitative interpretation of volcano deformation,
(google scolar > 2000 times)

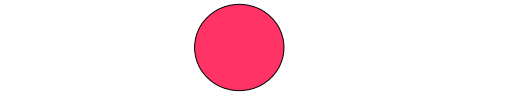

Spherical source in a semi-infinite medium

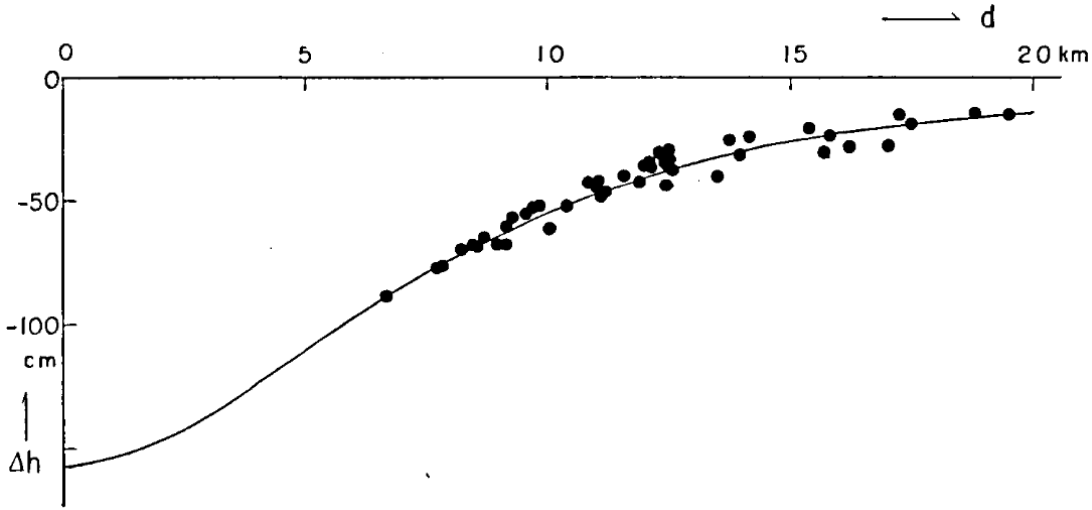

Relationship between vertical displacements (Δh) and distance (d) from the center of the Sakurajima depression during the 1914 eruption

Most famous simple models

1. Mogi-Yamakawa Model (1958) (Analytic) :

a)

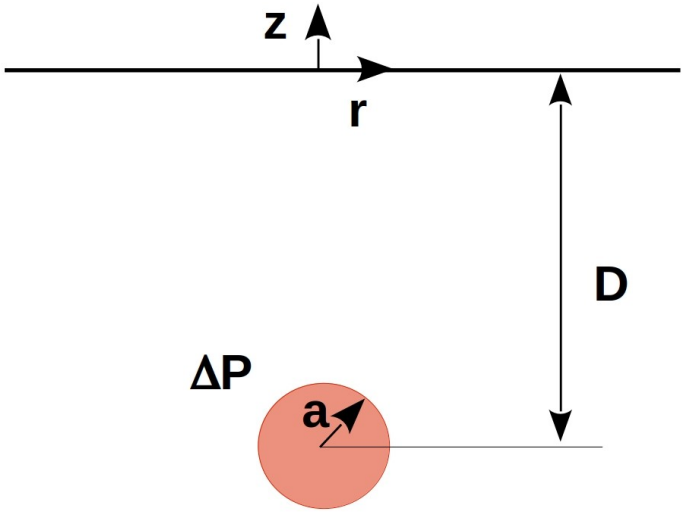

b)

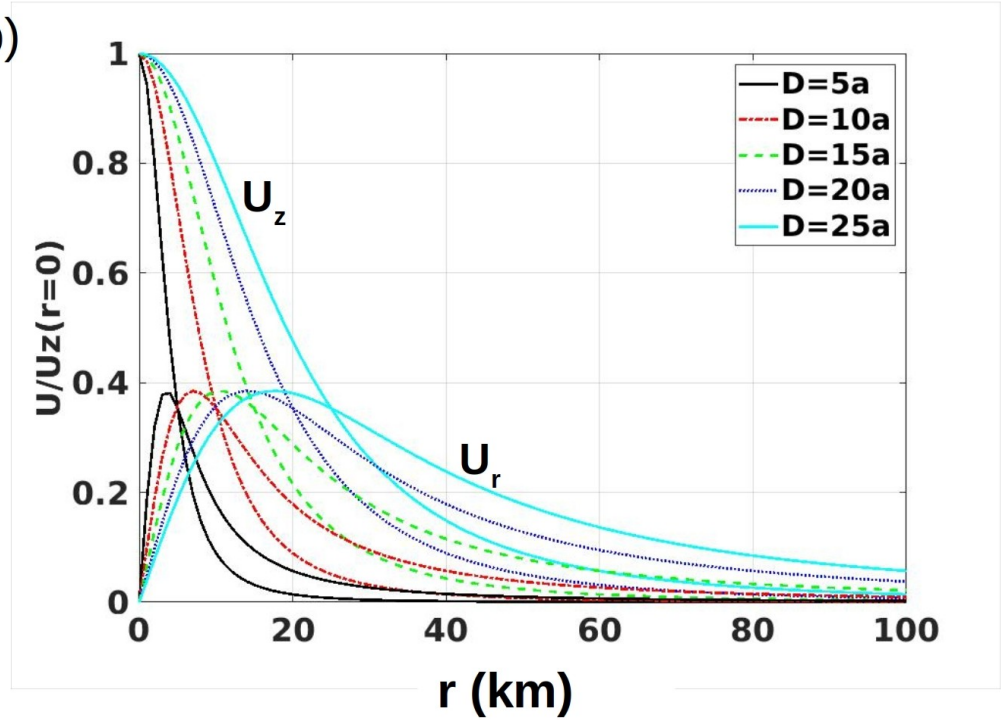

$$U_z(r) = -(1-\nu)\frac{\Delta V}{\pi}\frac{D}{(D^2+r^2)^{3/2}} \qquad U_r(r) = (1-\nu)\frac{\Delta V}{\pi}\frac{r}{(D^2+r^2)^{3/2}}$$

Où $\Delta V = \frac{\pi}{G} a^3 \Delta P$ et $G = \frac{E}{2(1+\nu)}$ Shear moduls

➡ Can be used to determine a spherical reservoir location and volume change

Most famous simple models

1. Mogi-Yamakawa Model (1958) (Analytique) |D/a|>>5

Darwin volcano, The Galapagos
1992-1998

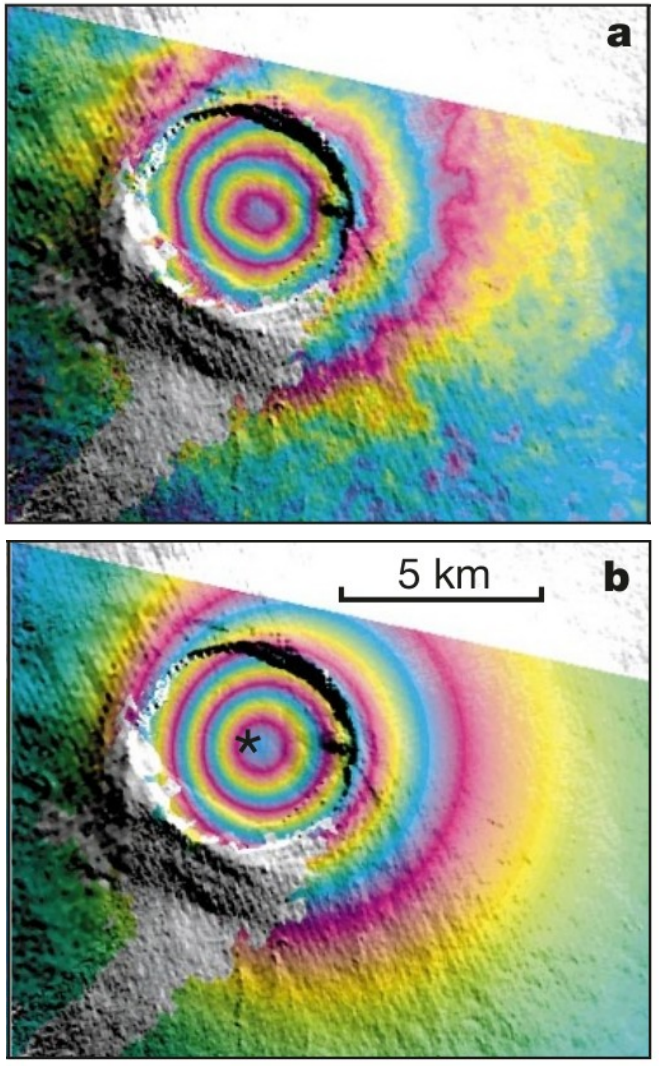

Amelung et al., Nature, 2000

Agung Volcano, Indonesia, Nov-Dec 2017

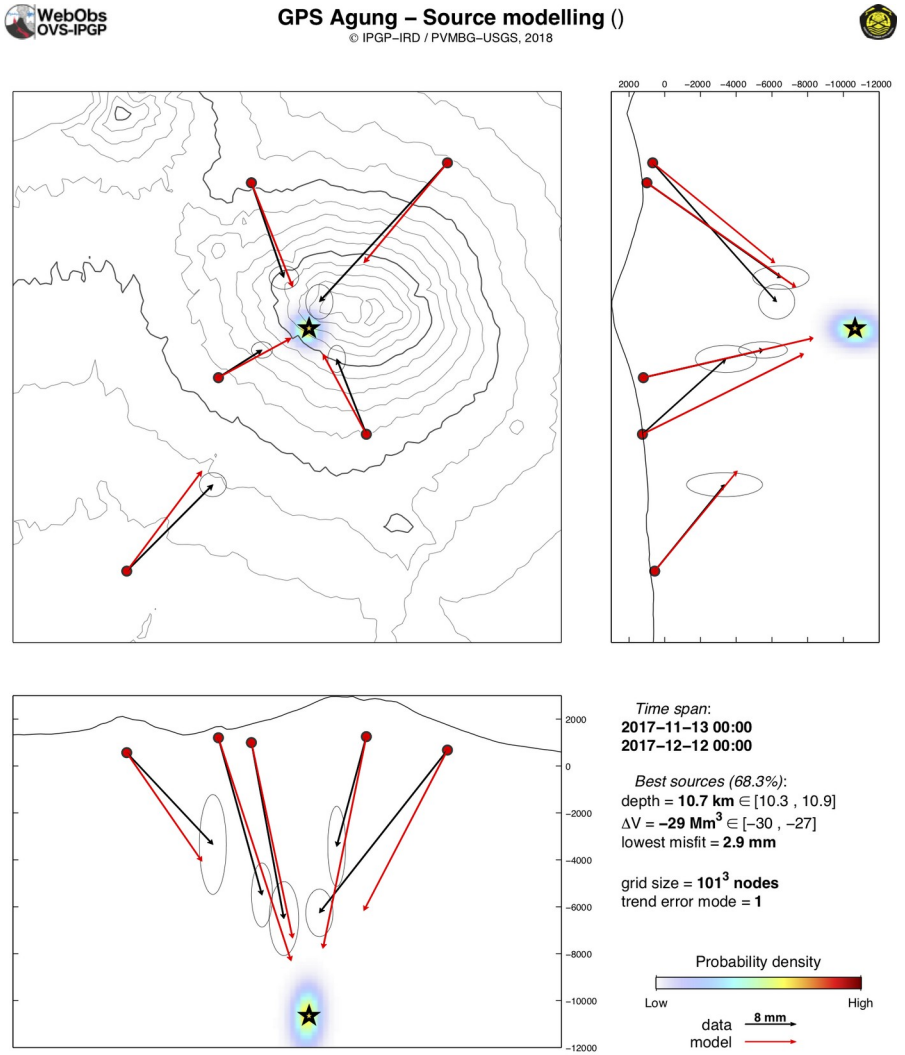

F. Beauducel, Webobs

Most famous simple models

2. Dieterich and Decker's model (1975) (numerical) :
Axisymetrical sources

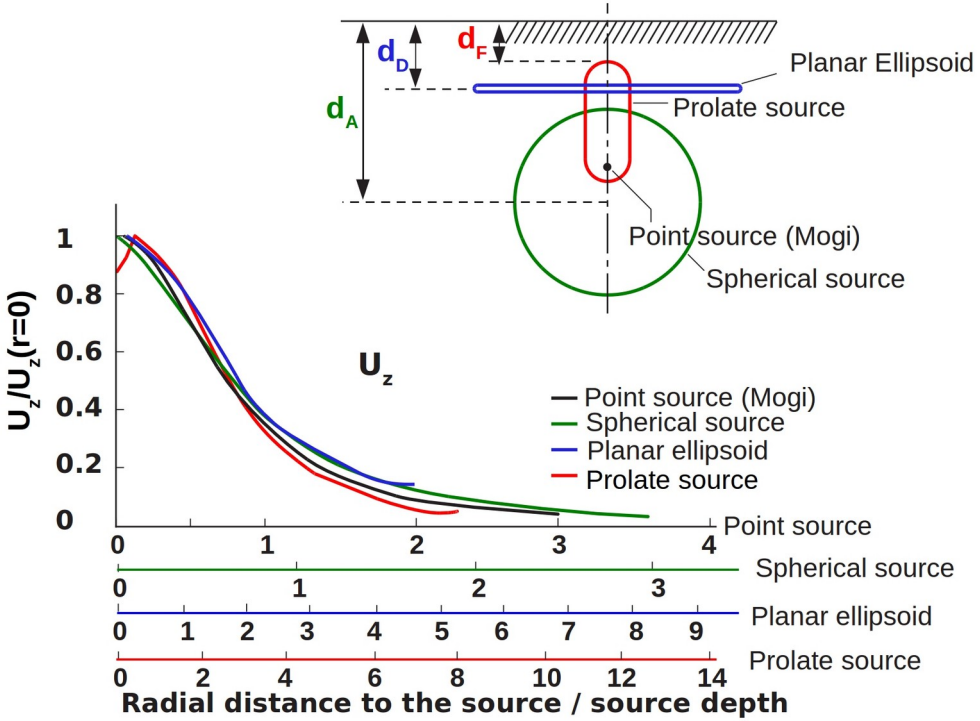

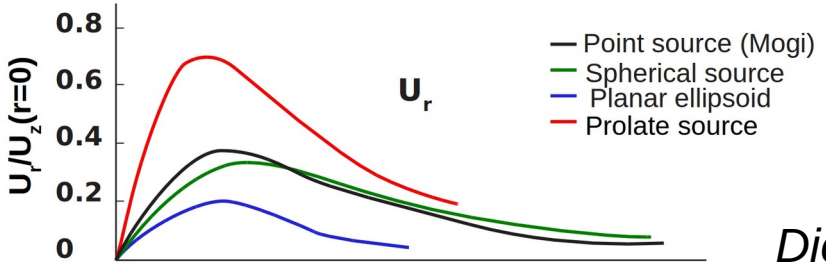

Source depths can be found,
such that the shapes of the normalized displacement resemble each other

Dieterich et Decker, JGR, 1975

➡ **Horizontal and vertical displacements are required to determine the geometry, depth, volume change of a pressure source**

Most famous simple models

3. Okada's model (1985) (analytic): quoted **>** 6700 fois

Openings and slips are constant.

Computation of displacements and inclinations associated with rectangular fractures of any orientation. Ground displacements are a function of **10 parameters**

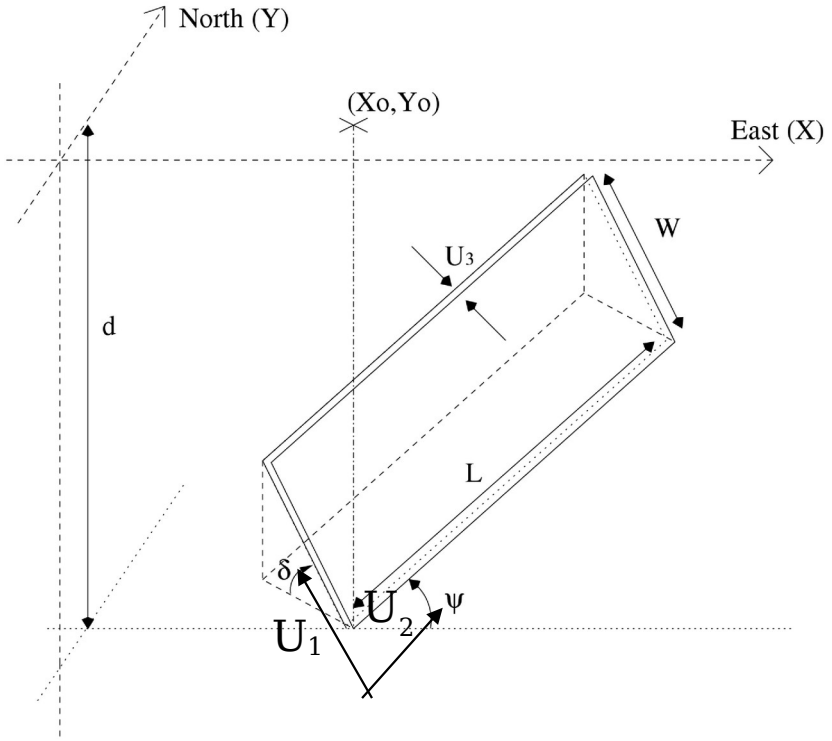

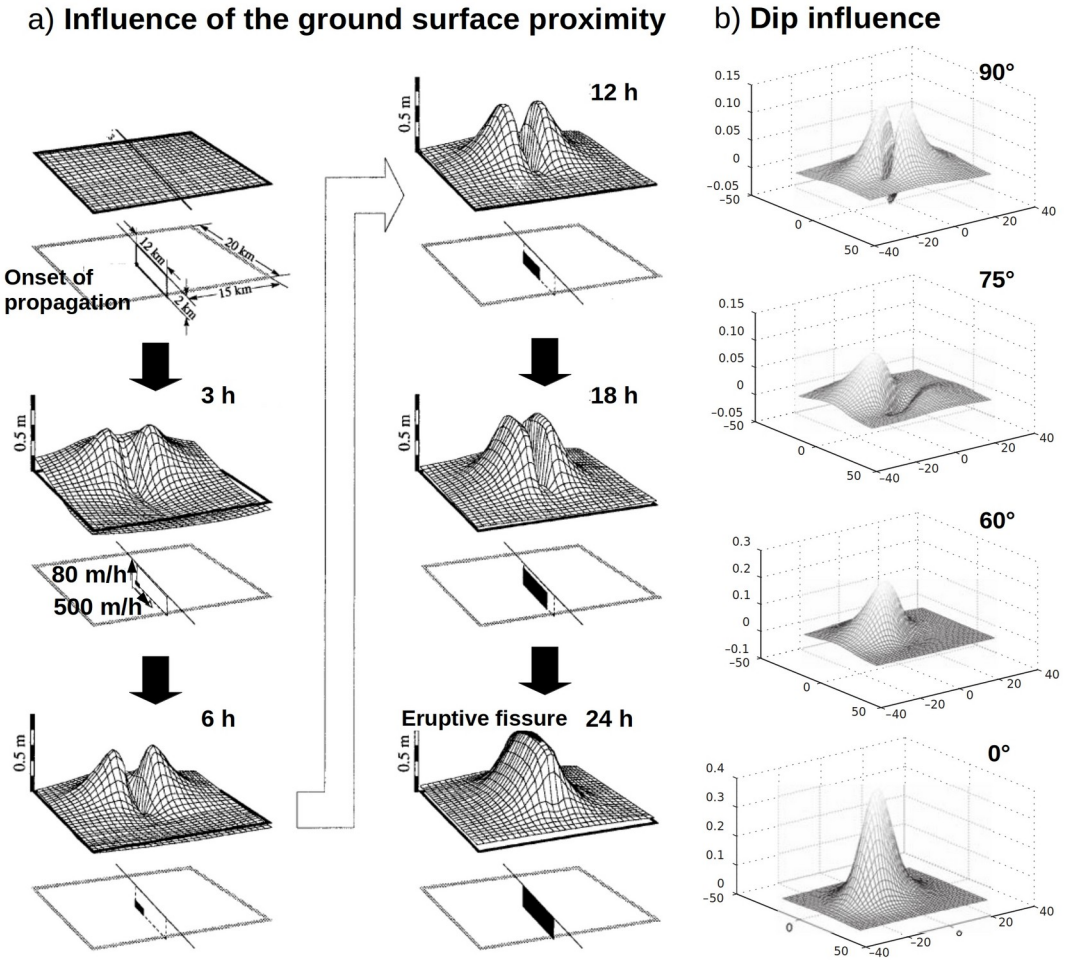

Vertical displacements associated with the propagation of a vertical dike at Kilauea (*Dvorak and Dzurisin, Reviews of Geophysics, 1997*).

Most famous simple models

4. Pollard et al. model (1983) (analytic): pressurized fracture in an infinite medium

Displacement of the elastic medium around the crack under pressure

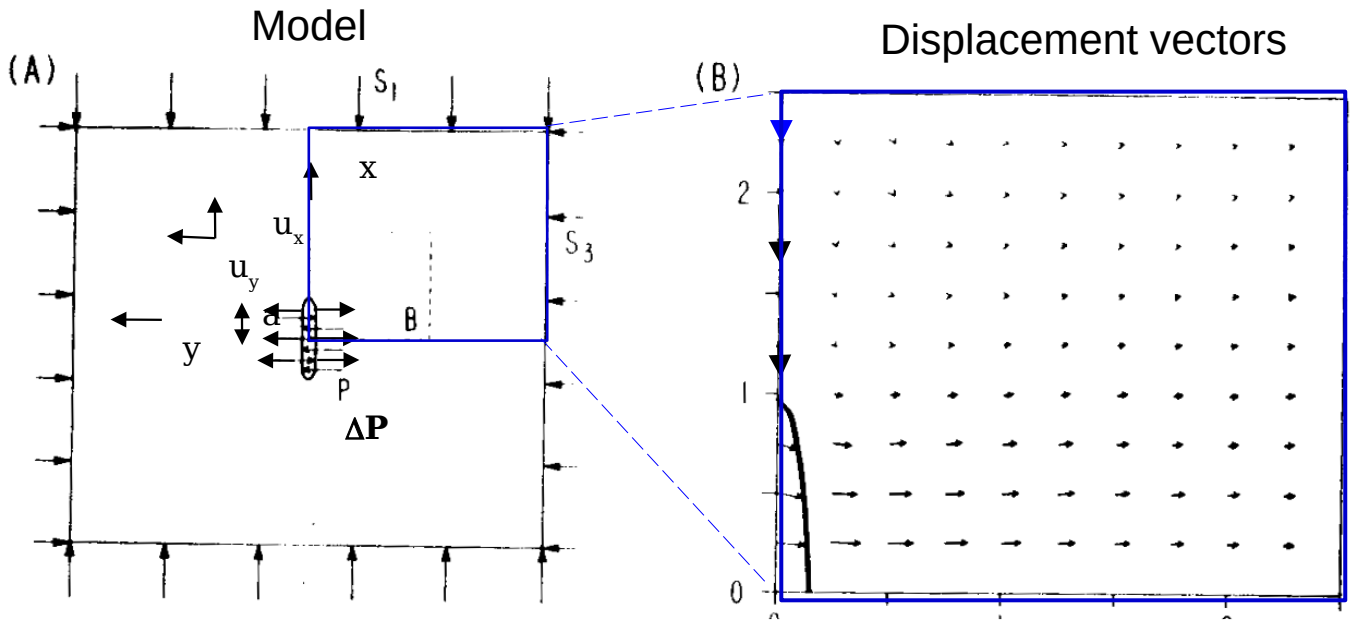

Displacement of each fracture surface

Ux,y = f(?)

Pollard et al., Tectonophysics, 1983

Most famous simple models

4. Pollard et al. model (1983) (analytic): pressurized fracture in an infinite medium

Displacement of the elastic medium around the crack under pressure

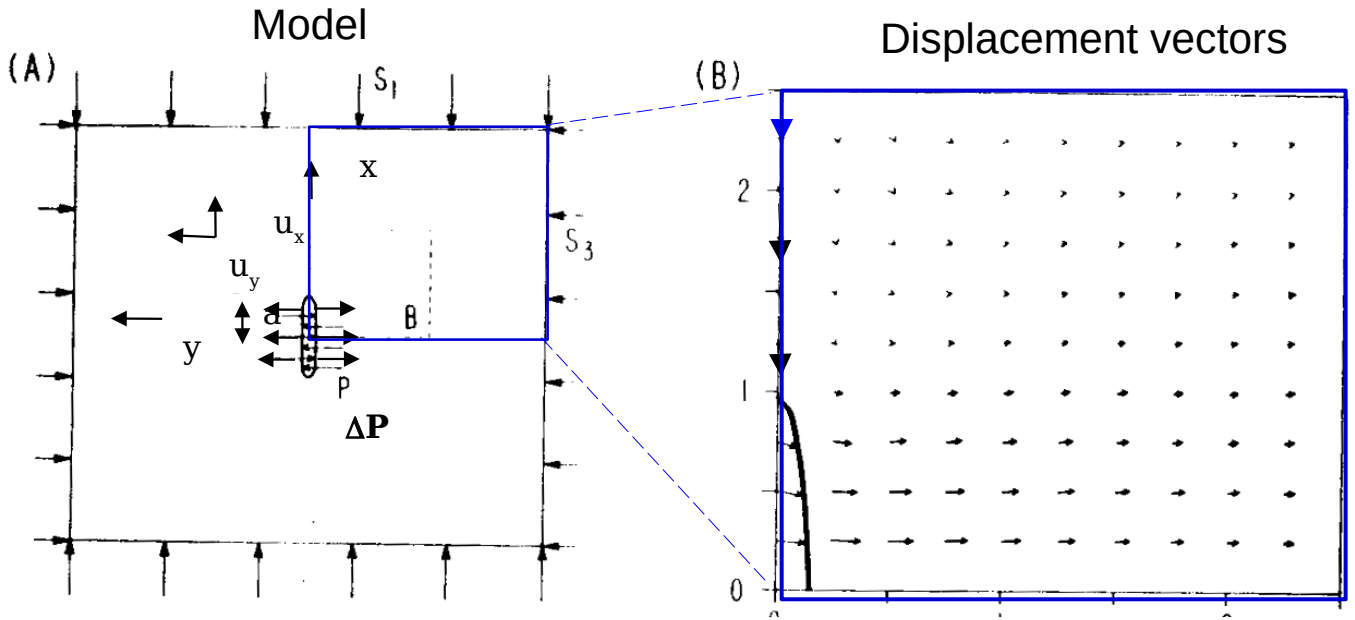

Displacement of each fracture surface :

$$u_x = -\frac{(1-2\nu)(1+\nu)}{2E}\,x\,\Delta P \qquad u_y = \pm\frac{2(1-\nu^2)}{E}\,\Delta P a\left[1-(x/a)^2\right]^{1/2}$$

where ν et E are Poisson's ration and Young's modulus, a is the fracture half-length, P is the fluid pressure, S_1=S_3 are stress in the host medium, and $\Delta P = P - S_3$ is the overpressure.

Pollard et al., Tectonophysics, 1983

These simple models provide a poor fit of InSAR data

Reality

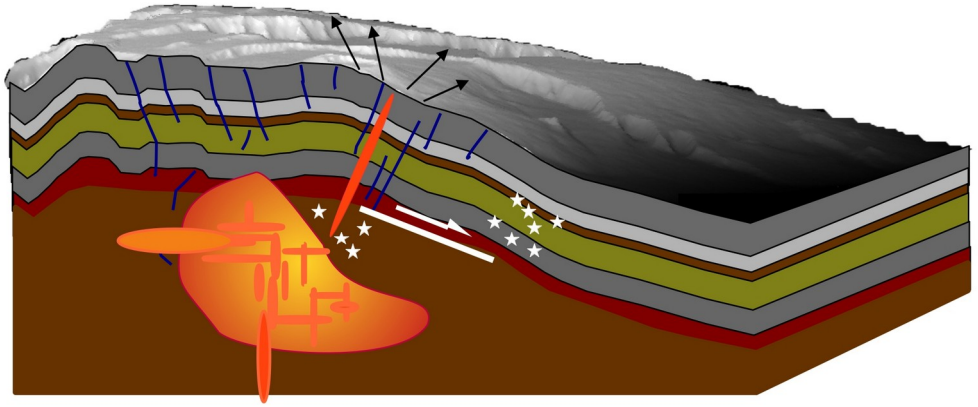

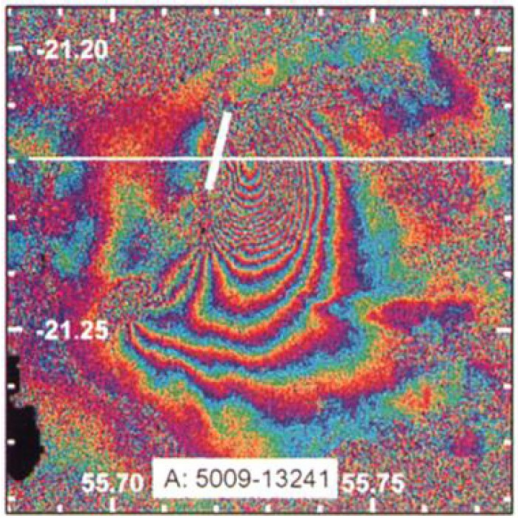

Models

Analytic Models

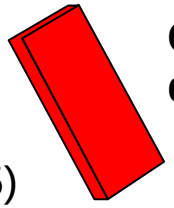

Constant displacement

(Okada, 1985)

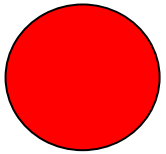

Constant overpressure

(Mogi, 1958)

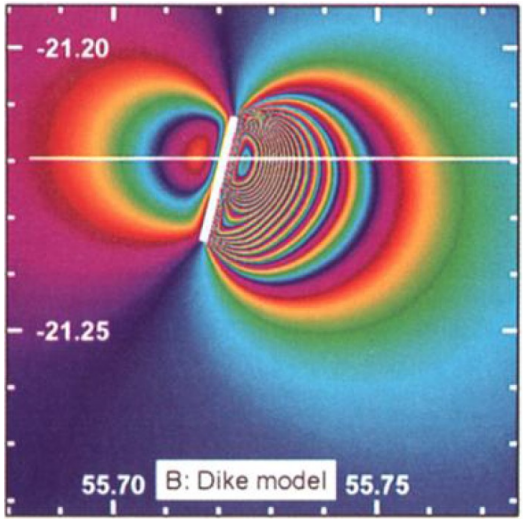

(*Sigmundsson et al., GRL, 1999*)

Numerical models: Example of 3D Mixed Boundary Elements

Cayol et Cornet, Int. J. Rock Mech. Min. Sc., 1997;
Cayol and Cornet, JGR, 1998; Cayol et al., JGR 2014

3D Numerical method:

- **Realistic topographies;**
- **Any number and geometry of fractures and pressure sources;**
- **Treats more than one source appropriately (interactions are taken into account);**

Assumptions:

- **intrusions, faults, reservoirs are submitted to constant stress changes;**
- **Fractures may be curved.**

Example of sources

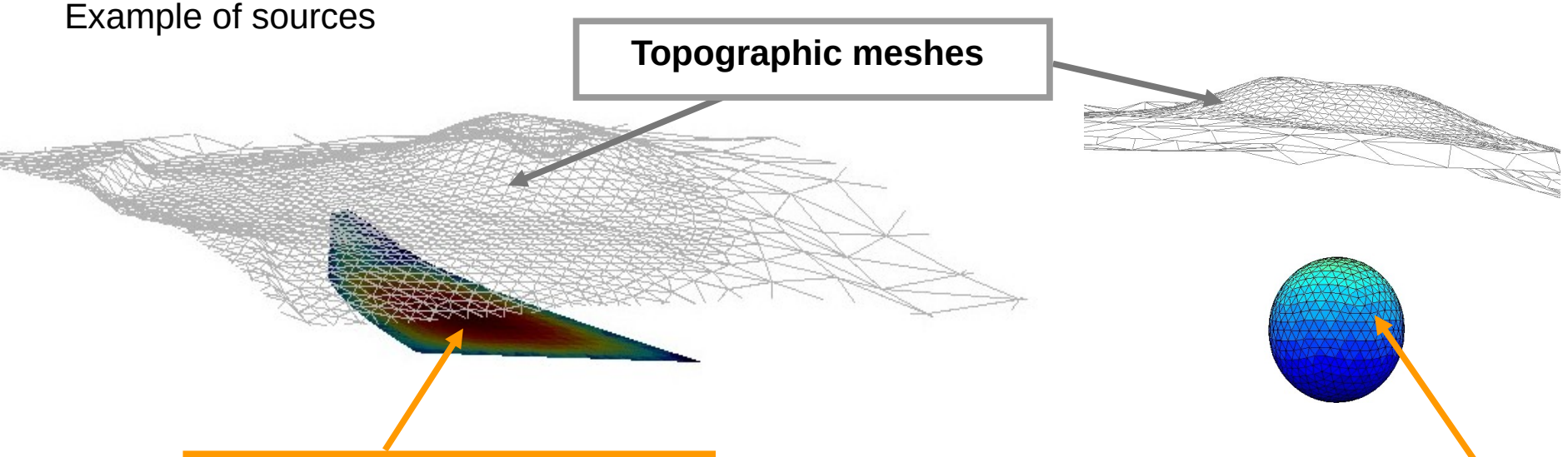

intrusions or faults, curved:
6 to 9 parameters
+
Overpressure or shear stress drops

Reservoirs:
3 to 9 parameters
(sphere-ellipsoid)
+
overpressure

Topography is taken into account

Topographies have an influence of computed displacements

Data | 1/2 space | Mixed BEM

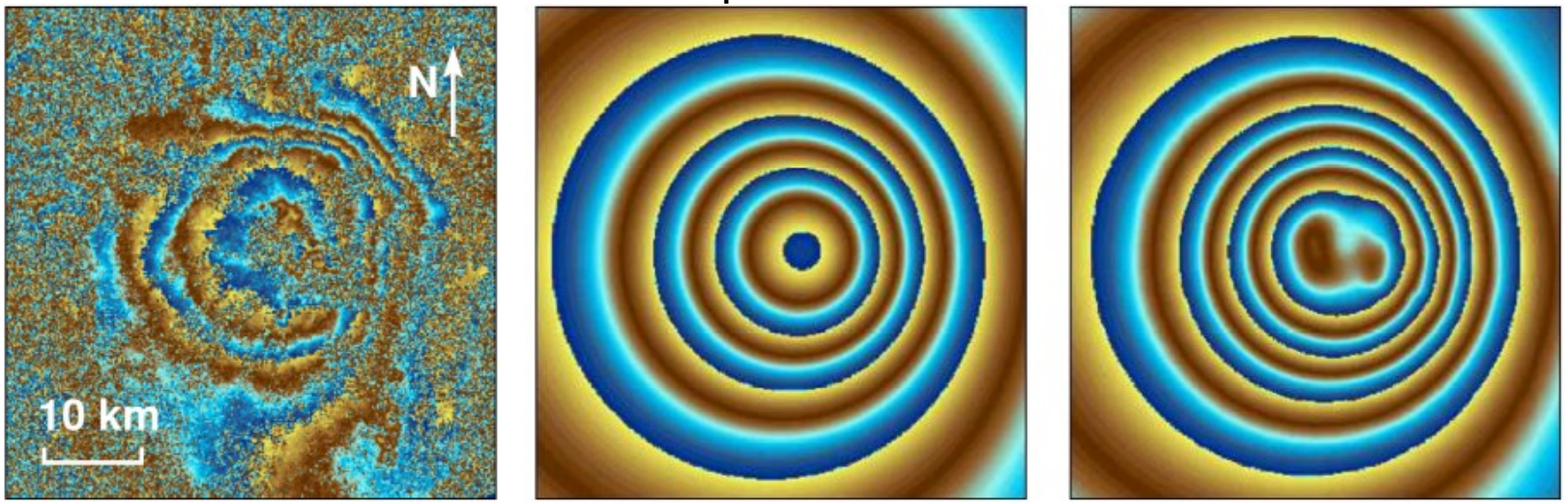

Etna, 1992-1993 eruption,
Massonnet et al., Nature, 1995

Cayol and Cornet, GRL, 1998

Neglecting topographies bias results : volume errors, depths errors

3D Mixed BEM

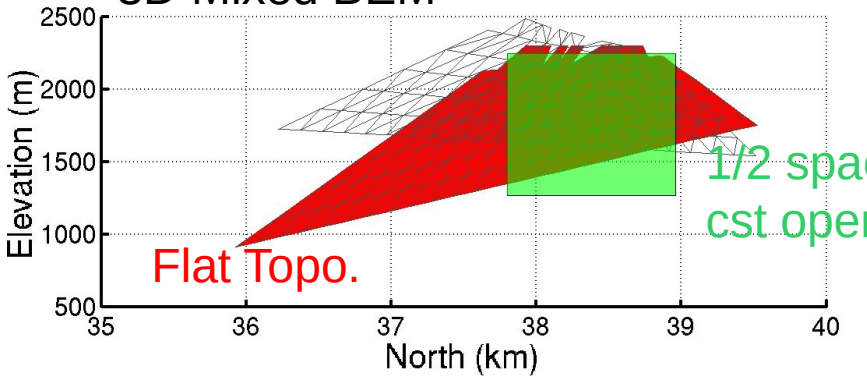

Volume with Okada (1985) : 80 % overestimation

Max depth with Okada : 40 % overestimation

Fukushima et al., JGR, 2005

Source interactions are taken into account

When superposing analytic models, sources interactions are neglected

But:Sources interact when they are close

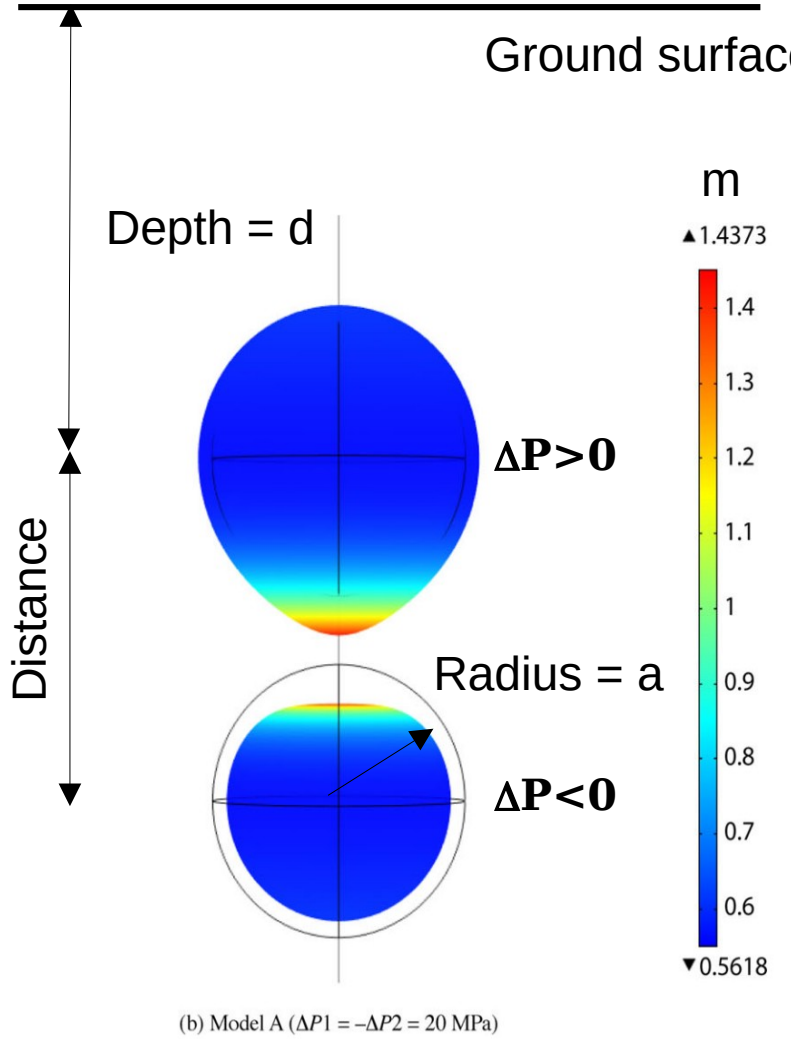

(b) Model A ($\Delta P1 = -\Delta P2 = 20$ MPa)

Finite element computation

Pascal et al., GJI, 2014

Error when neglecting interactions

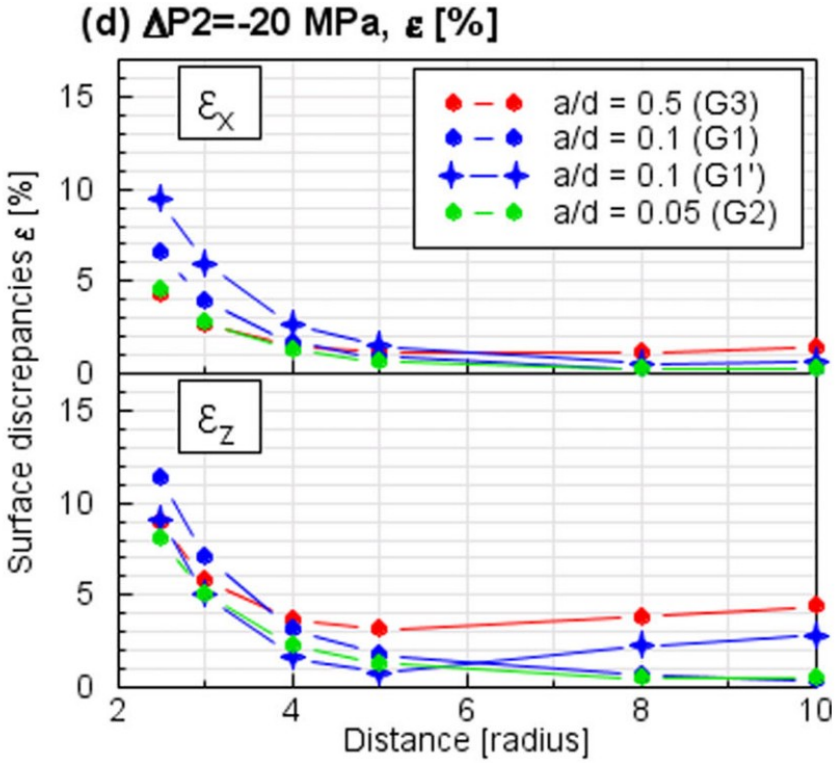

$$\text{with } \epsilon_i = \frac{\sum |U_i^{An} - U_i^{FE}|}{|U_i^{An}|}$$

When sources are closer than 4*radius, they should be taken into account

Models with stress boundary conditions are closer to the physics

Field observation

Models

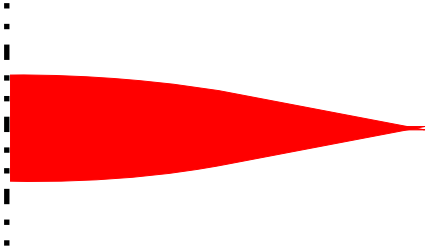

Pressure boundary condition

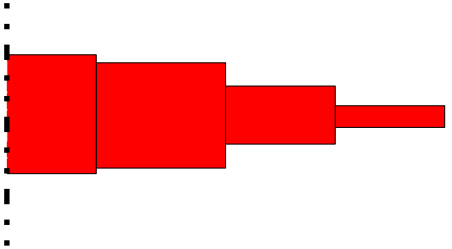

Displacement boundary condition : kinematic models

Fracture stress

Less stress singularities

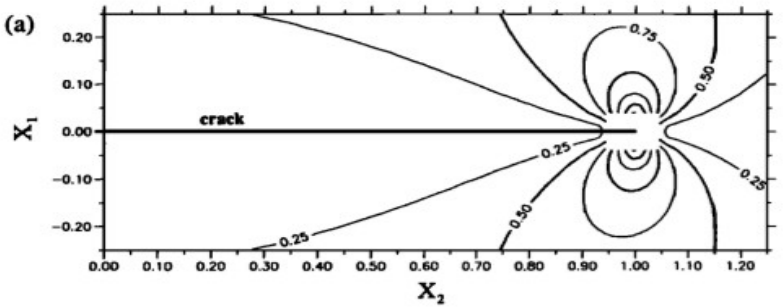

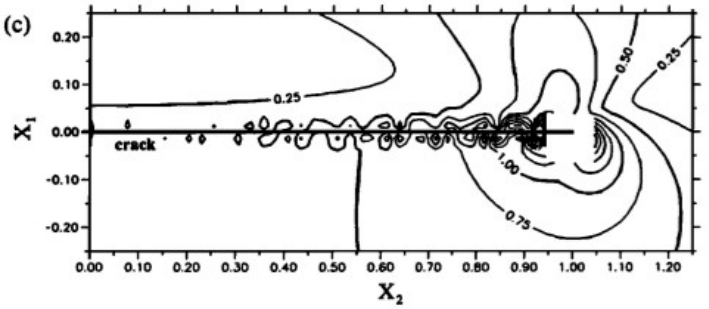

Fracture shear displacement

Shear displacements Are determined

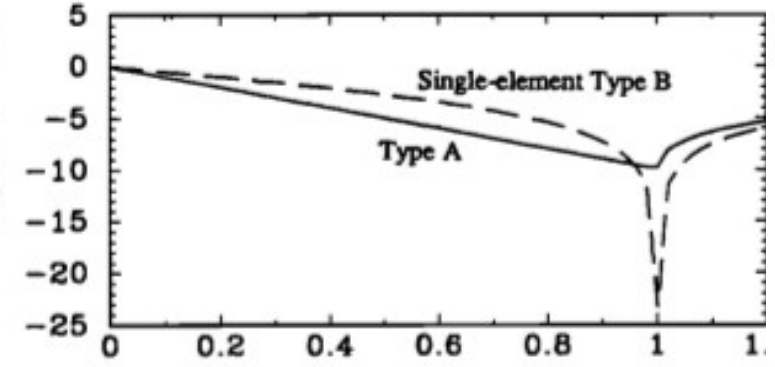

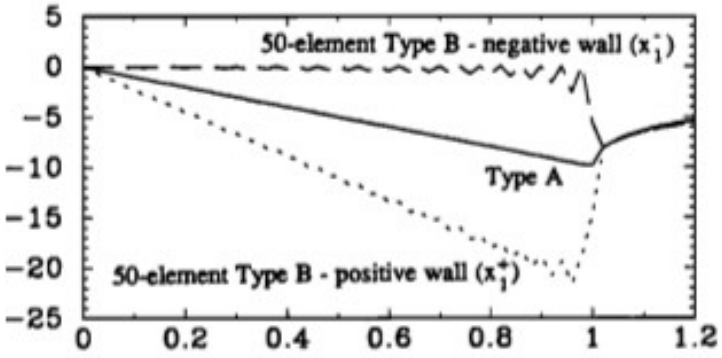

Zeller and Pollard, JGR, 1992

Medium heterogeneities are also important in inversions

Exemple of slow slip events at Kilauea (Hawaii)

Inversion of GNSS data

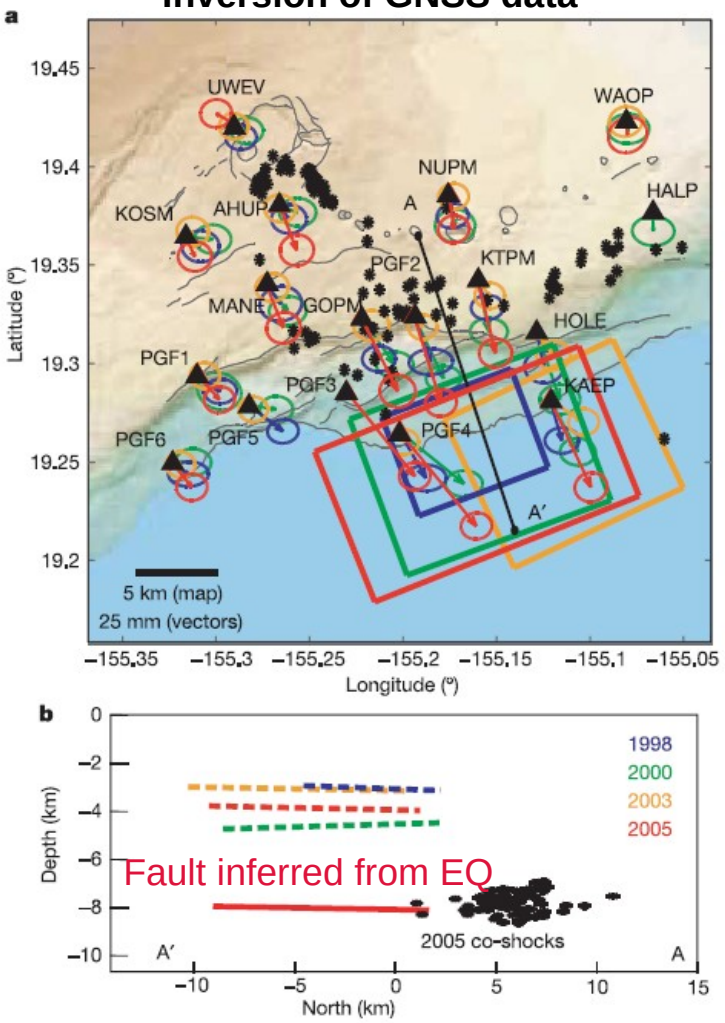

(*Segall et al., Nature, 2006*)

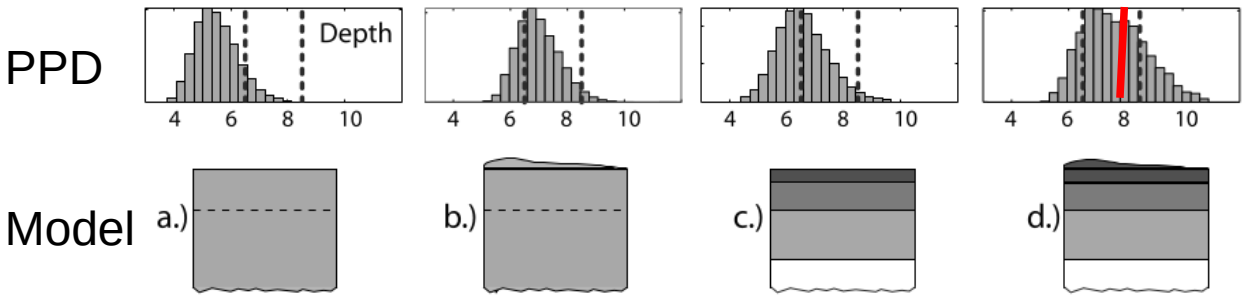

1/2 space Homogeneous | **topography homogeneous** | **½ space heterogeneous** | **topography heterogeneous**

(*modified from Montgomery-Brown et al., JGR, 2009*)

Only models that take into account topography and and heterogeneities reconcile displacement inversions and seismicity

→ **To take heterogenieties into account, finite elements are more suitable Than boundary elements**

Boundary Element Method versus Finite Element Method

Boundary elements
(*DefVolc, Cayol and Cornet, IJRMMS, 1997; Meade, Comput. & Geosc., 2007 Nikkhoo and Walter, GJI, 2015*)

Finite elements
(*Pylith, Aagard et al., JGR, 2013; GALES, Garg. et al., 2021*)

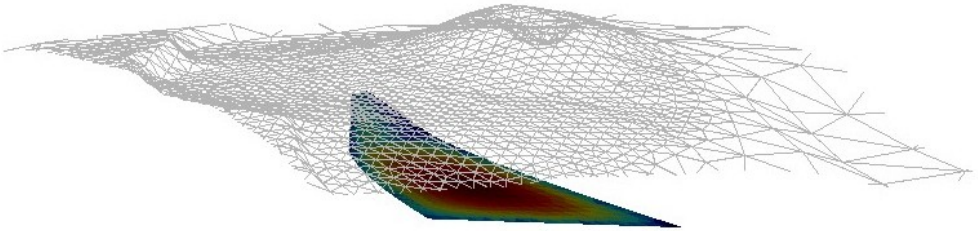

Smittarello et al., JGR, 2019

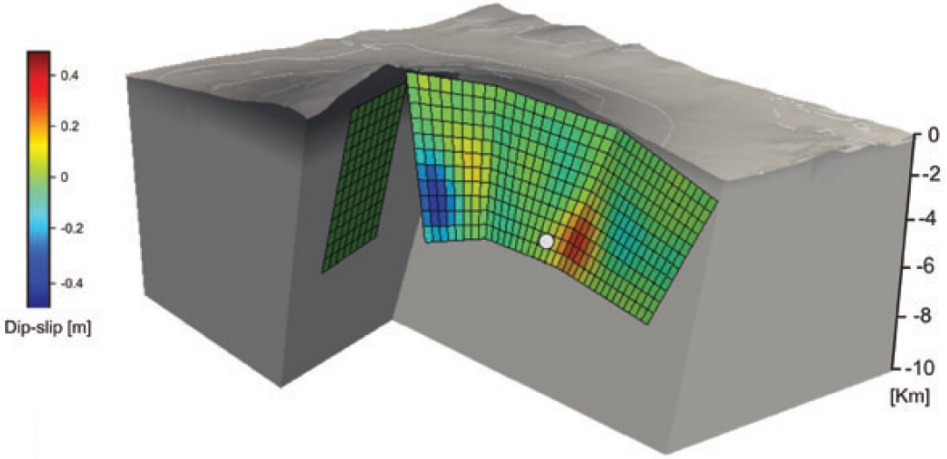

Currenti et al., GJI, 2010

Pros and Cons

- **Assembly & Solving on the boundaries**
- **Homogeneous media**
- **Small symmetric matrices (<10^4x10^4)**
- **Full matrices**
- **Taking fractures into account is straightforward**

- **Assembly & solving in the whole domain**
- **Heterogeneous media**
- **Large matrices (>10^6x10^6)**
- **Sparse & symmetric matrices**
- **Taking fracture into account is not straightforward (Domain decomposition, etc.)**

3. Inversions

Direct problem : $\boldsymbol{m} \rightarrow \boldsymbol{u} = G(\boldsymbol{m})$, $\boldsymbol{m}$ = *parameters*
(unique) $\boldsymbol{u}$ = *observations*

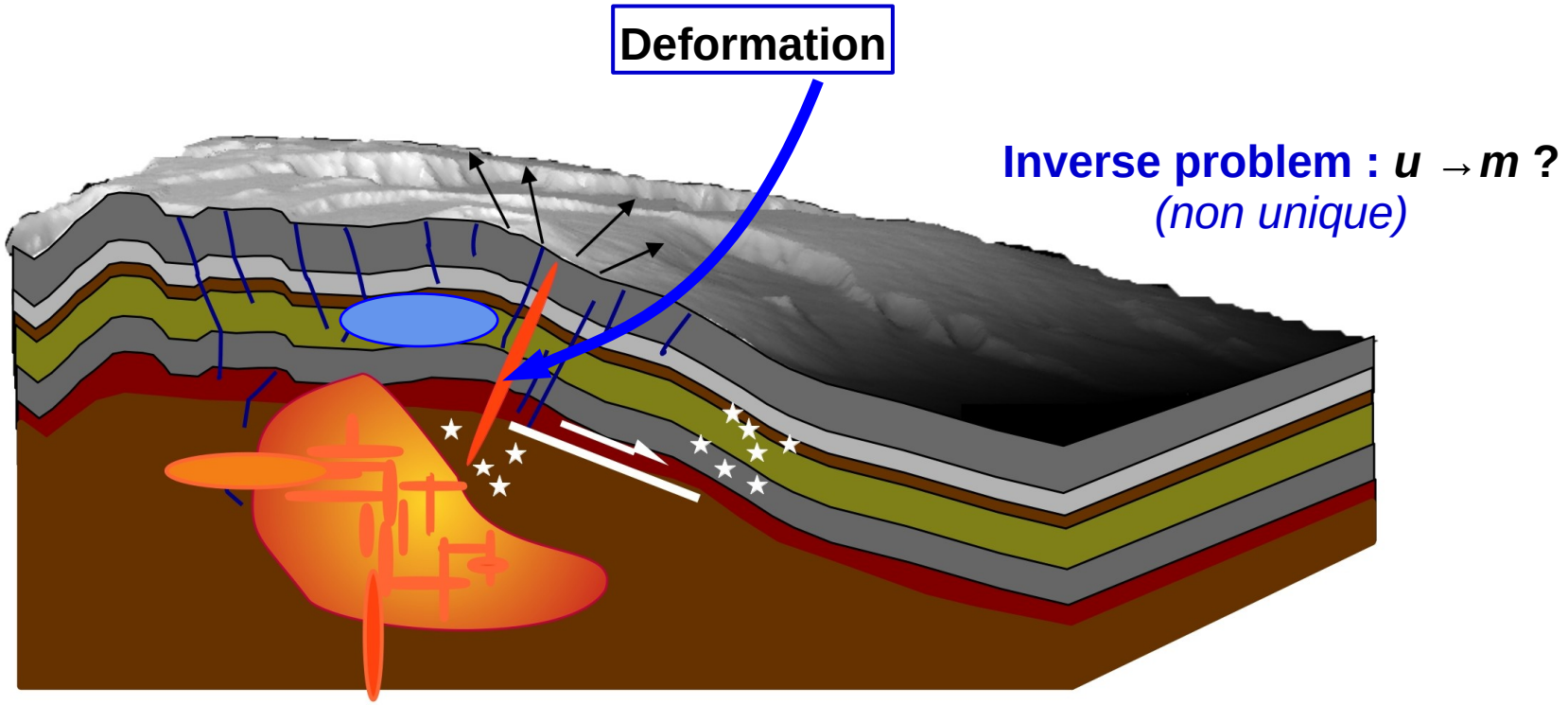

Inverse problem : $\boldsymbol{u} \rightarrow \boldsymbol{m}$?
(non unique)

Which a priori model ?

When inverting displacements, which of the above model should be used ? We need to start with an a-priori model.

To do this, we use :

1. **The context**: has there been an eruption, or have eruptive cracks been observed in the field?

2. **The observed displacement field**: are there any **discontinuities** in the displacement field ? is there any **axisymmetry**?

Which a priori model ?

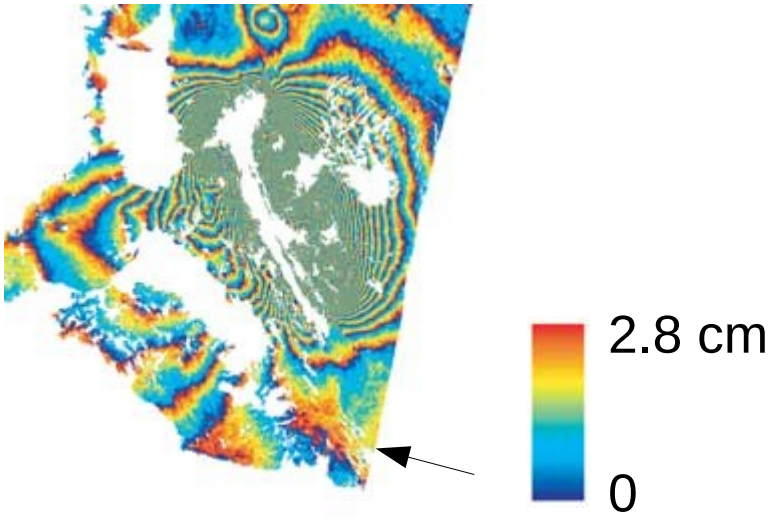

Dike ?
Reservoir ?

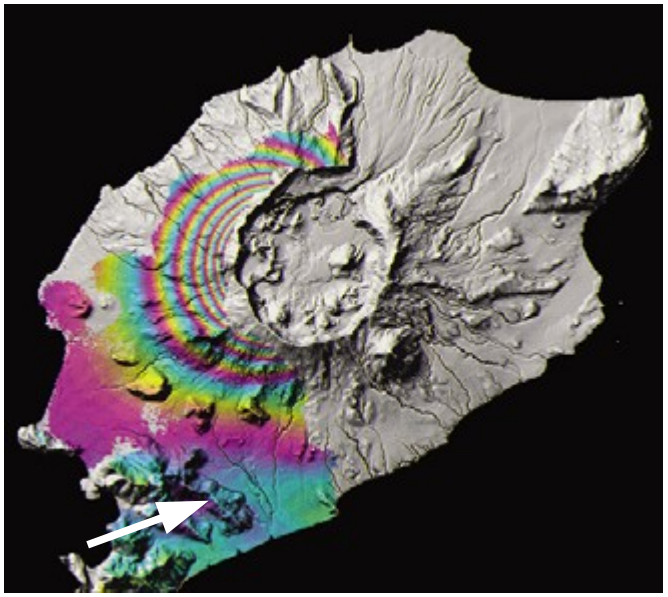

Dike ?
Reservoir ?

Which a priori model ?

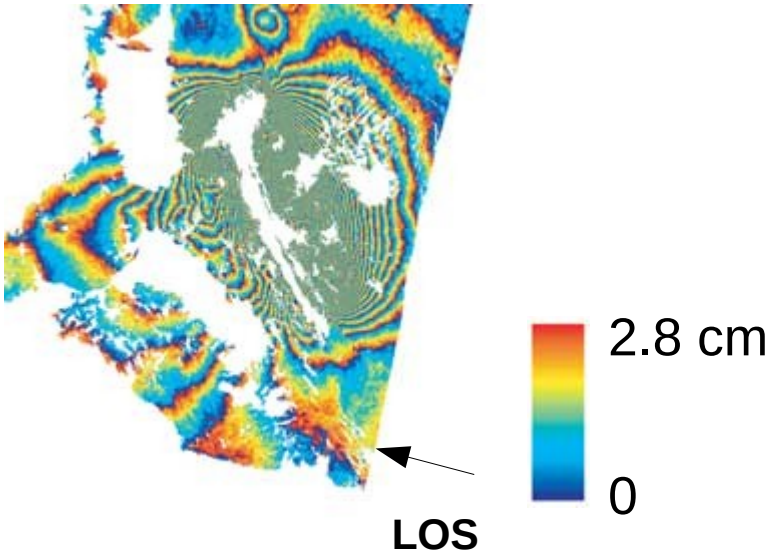

Opening of the Dabbahu rift in 2005
(*Wright et al., Nature, 2006*)

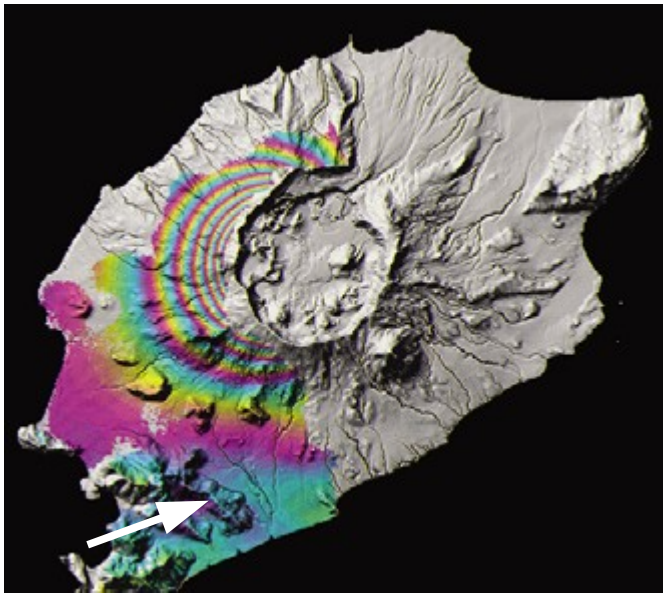

Reservoir deflation during the
Okmok volcano eruption in 2008
(*Lu and Dzurisin, JGR, 2010*)

Analytic inversions of the Mogi model (*Mogi; 1958*) : **Determination of D and ΔV**

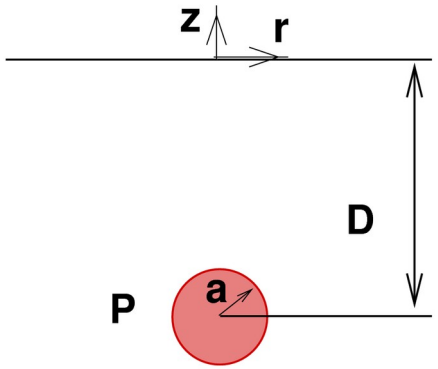

$$U_z(r) = -\frac{3\Delta V}{4\pi}\frac{D}{\left(D^2+r^2\right)^{3/2}}$$

$$U_r(r) = \frac{3\Delta V}{4\pi}\frac{r}{\left(D^2+r^2\right)^{3/2}}$$

$$\Delta V = \frac{\pi}{G}a^3 P$$

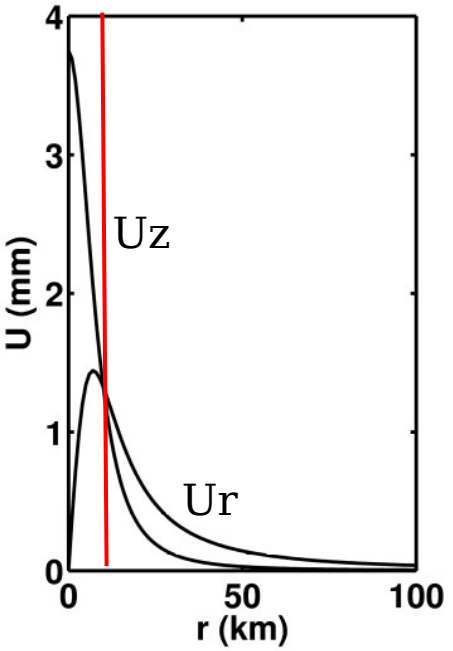

Method using Ur and Uz:

- We determine the distance r such that Uz=Ur. This corresponds to r = D -> r = 10 km
- Knowing the amplitude at r = 0 Uz(r=0)=Umax, we find $\Delta V = \frac{4\pi}{3}D^2 U_{max}$

Numerical inversions:
Definition of a cost-function

Data point undersampling → $\boldsymbol{u}_o$

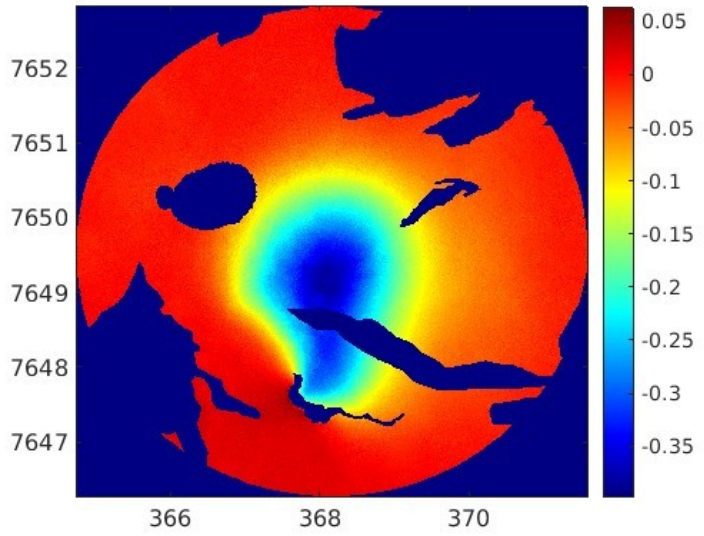

- The simplest cost-function :

$$\chi^2 = \sum_{i=1}^{N} \left(u_o^i - u_m^i \right)^2 = \| \boldsymbol{u}_o - \boldsymbol{u}_m \|^2$$

where u_o^i is the i[th] observed displacement

u_m^i is the i[th] modelled displacements

- Normalized cost function:

$$\chi^2 = \sum_{i=1}^{N} \frac{\left(u_o^i - u_m^i \right)^2}{\sigma_i^2}$$

σ_i Standard deviation or error on the i[th] data

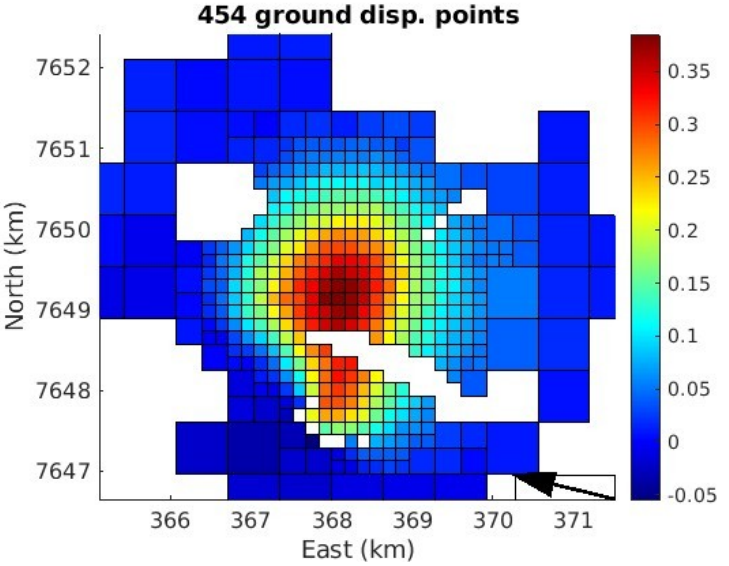

- Taking the data correlation into account:

$$\chi^2 = (u_o - u_m)^T C_d^{-1} (u_o - u_m)$$

where C_d is a full covariance matrix

Inversions: linear versus non-linear inversions

Linear inversions: there is a linear relation between the parameters ***m*** and the observations, $\boldsymbol{u}_m$

$$\boldsymbol{u}_m = \boldsymbol{G}\,\boldsymbol{m}$$

Example: Okada's Model (1985, 1992); Mogi's solution (1958) are linear models

Typically, the location of a source is known, and the amplitude of the source is searched for.

To minimize the cost function: $\chi^2 = \|\boldsymbol{u}_o - \boldsymbol{u}_m\|^2 = \|\boldsymbol{u}_o - \boldsymbol{G}\,\boldsymbol{m}\|^2$

We seek ***m*** such that : $\dfrac{\partial \chi^2}{\partial \boldsymbol{m}} = 0$

Which leads to solving the linear system of equations: $\boldsymbol{m} = \left(\boldsymbol{G}^T \boldsymbol{G}\right)^{-1} \boldsymbol{G}^T \boldsymbol{u}_o$

Pros: fast method

Cons: the source location has to be knows

Example of a linear inversion: “kinematic” models

Uplift at Sierra Negra volcano in 1998-99 (Galapagos)

Minimization of $\chi^2 = \|\boldsymbol{u}_o - \boldsymbol{G}\,\boldsymbol{m}\|^2 + \beta^2 \|\nabla \boldsymbol{m}\|^2$, **where *m* is the opening vector**

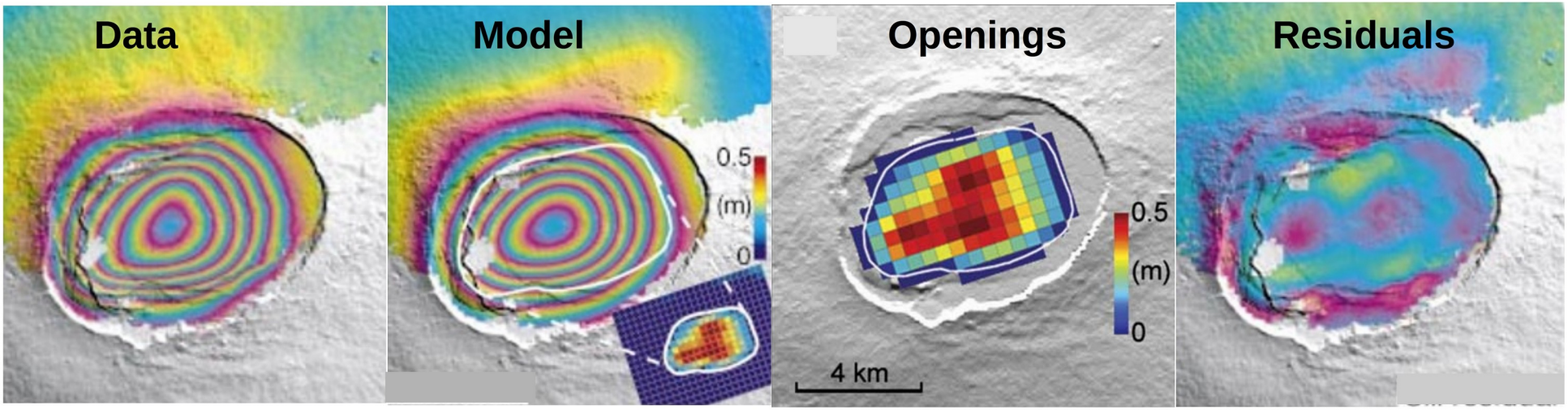

Amelung et al., Science, 2000

Science

Widely used

RESEARCH ART

Check for updates

Cite as: Sigmundsson *et al.*, *Science*
10.1126/science.adn2838 (2024).

Fracturing and tectonic stress drives ultra... flow into dikes

Freysteinn Sigmundsson[1]*, Michelle Parks[2], Halldór Geirsson[1], Andrew Hooper[3], Vincent Dro
G. Ófeigsson[2], Sonja H. M. Greiner[1,4,5], Yilin Yang[1], Chiara Lanzi[1], Gregory P. De Pascale[1], Krist
Valentyn Tolpekin[7], Hildur María Friðriksdóttir[2], Páll Einarsson[1], Sara Barsotti[2]

AGU ADVANCING EARTH AND SPACE SCIENCE

JGR Solid Earth

RESEARCH ARTICLE
10.1029/2019JB019117

Key Points:
- Imaging multidisciplinary continuous deformation data to improve dike ascent modeling
- Detailed temporal model of the 2018 intrusion at Etna volcano

The 24 December 2018 Eruptive Intrusion at Etna Volcano as Revealed by Multidisciplinary Continuous Deformation Networks (CGPS, Borehole Strainmeters and Tiltmeters)

M. Aloisi[1], A. Bonaccorso[1], F. Cannavò[1], G. Currenti[1], and S. Gambino[1]

Inversions: linear versus non-linear inversions

Non-linear inversions: there is a non-linear relation between the parameters ***m*** and the observations, $\boldsymbol{u}_m$

$$\boldsymbol{u}_m = \boldsymbol{G}(\boldsymbol{m})$$

The link between the source location, orientation parameters and the ground displacement is a non linear relation.

Example of a cost-function $\chi^2 = \|\boldsymbol{u}_o - \boldsymbol{u}_m\|^2 = \|\boldsymbol{u}_o - \boldsymbol{G}(\boldsymbol{m})\|^2$,

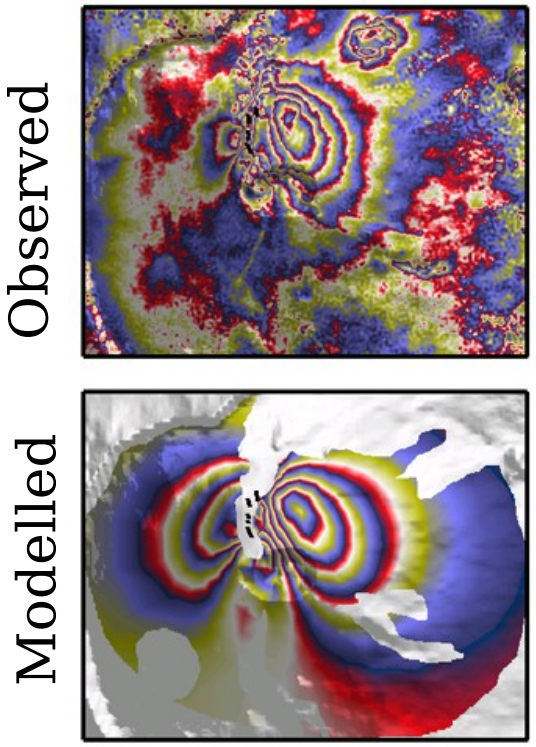

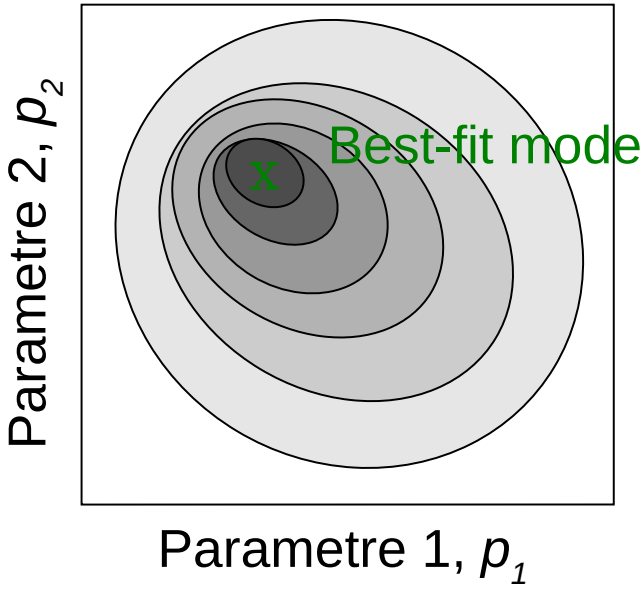

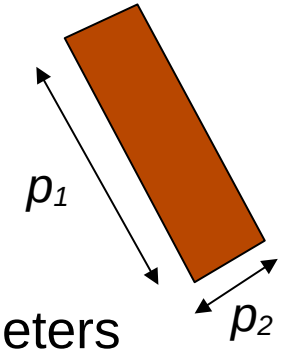

Two parameters source

Non linear inversions

Example of a cost-function $\chi^2 = \|\boldsymbol{u}_o - \boldsymbol{u}_m\|^2 = \|\boldsymbol{u}_o - \boldsymbol{G}(\boldsymbol{m})\|^2$,

Systematic exploration of the parameter space (Grid search method)

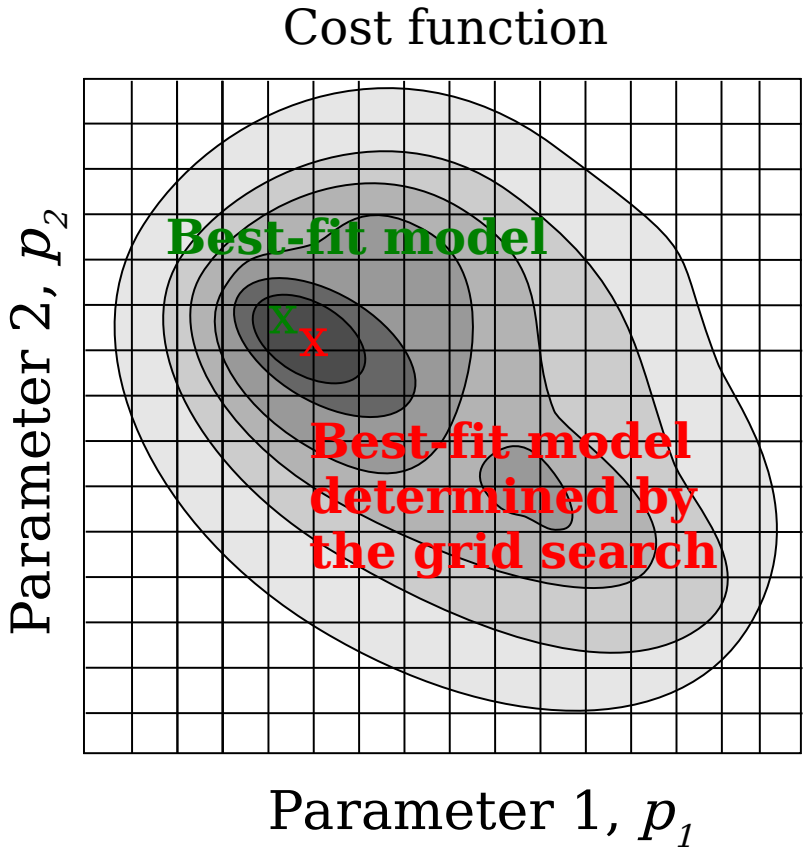

Cons :Numerically costly method

Systematic exploration fixing one parameter after the other

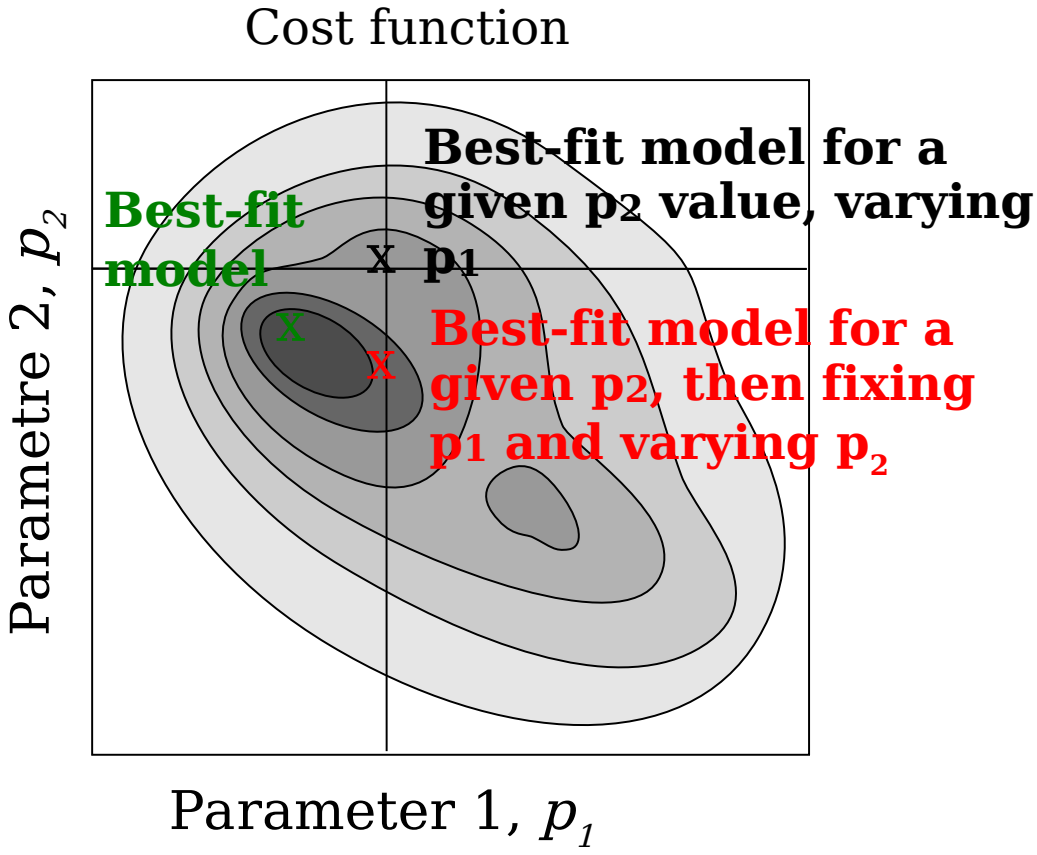

Unreliable method

Non linear inversions

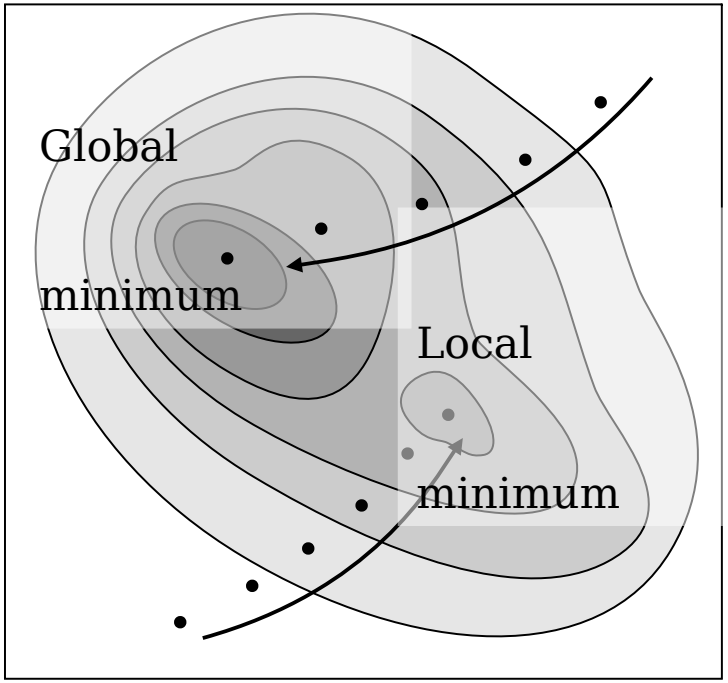

Rapid method

Adapted for functions
with one or two minima

Monte Carlo method

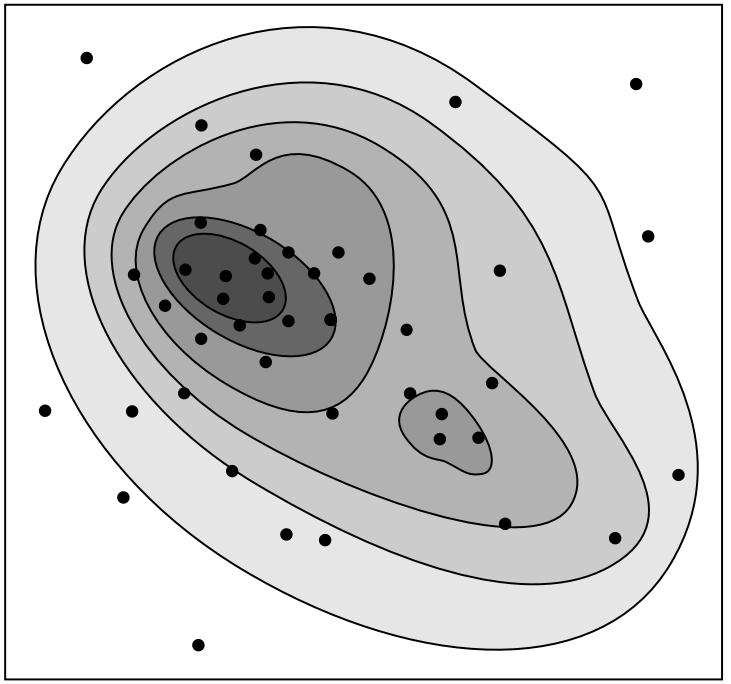

Fairly slow method

Adapted for functions
with multiple minima

Example of the neighborhood Method (Monte Carlo)

(*Sambridge, GJI, 1999*)

Initial step: n initial point are drawn in the model space, their misfits are evaluated

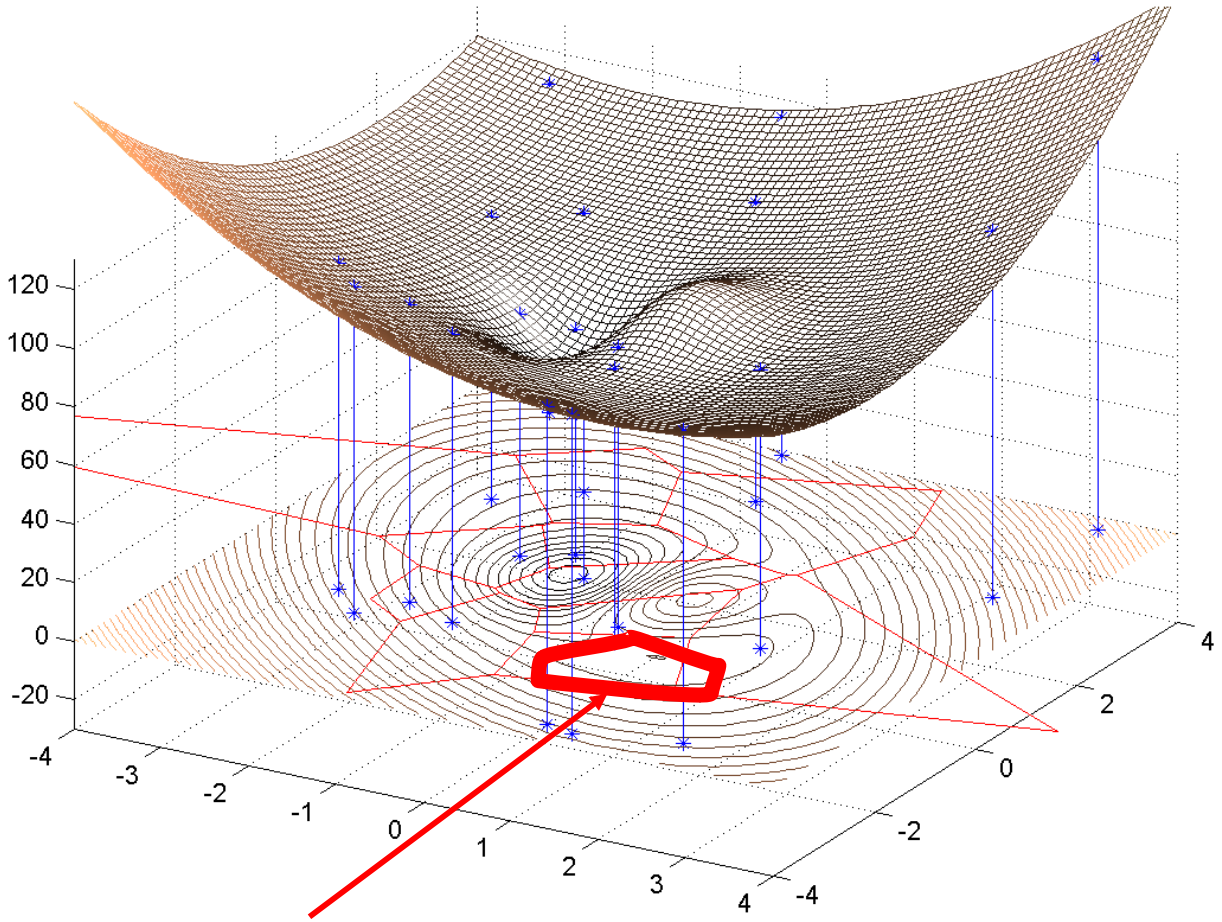

Misfit function in a two parameters space

Voronoi cell (= neighbourhood) : region closer to a point than any region.

Example of the neighborhood Method (Monte Carlo)

(*Sambridge, GJI, 1999*)

Initial step: n initial point are drawn in the model space, their misfits are evaluated

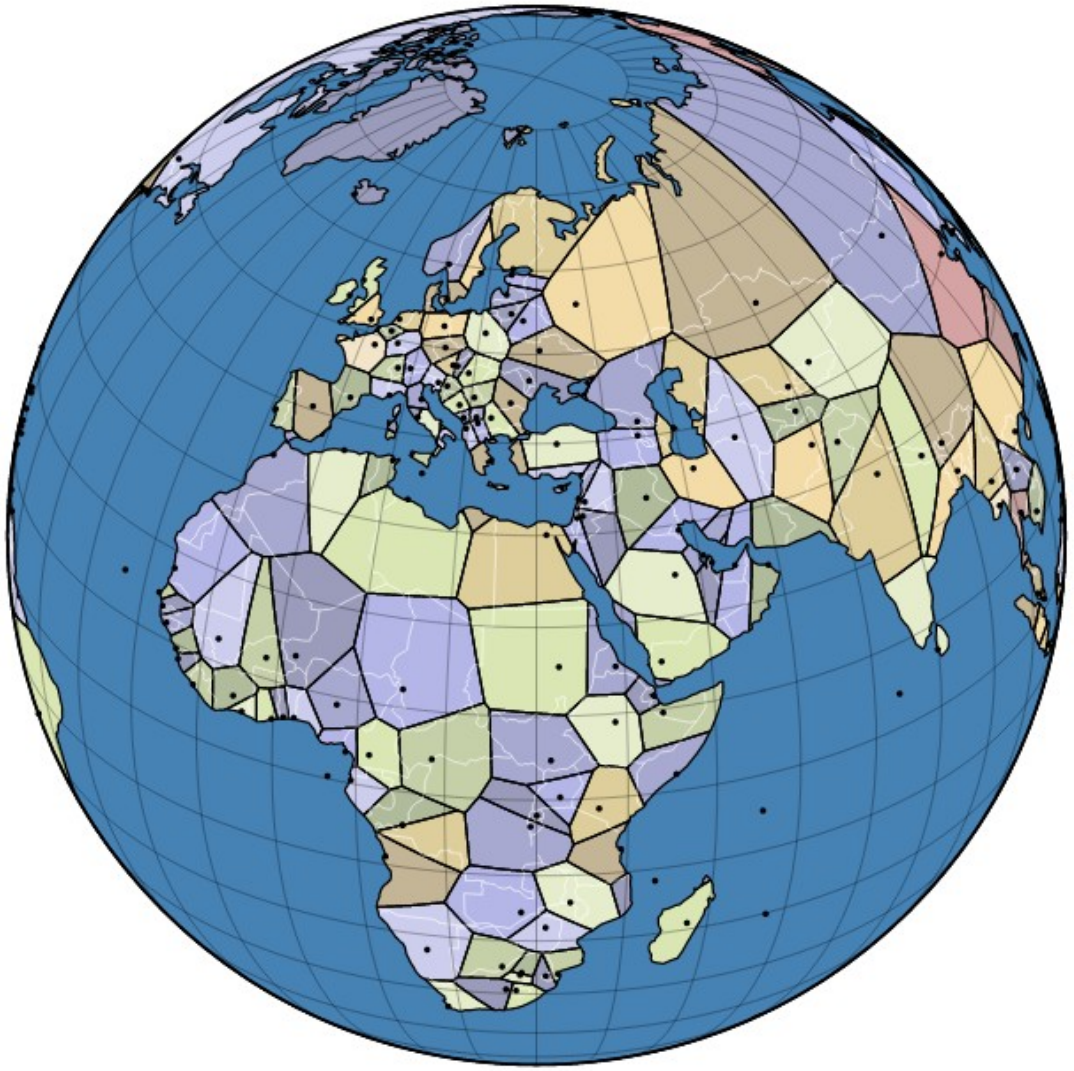

Voronoi cells around the world capitals

Example of the neighborhood Method (Monte Carlo)

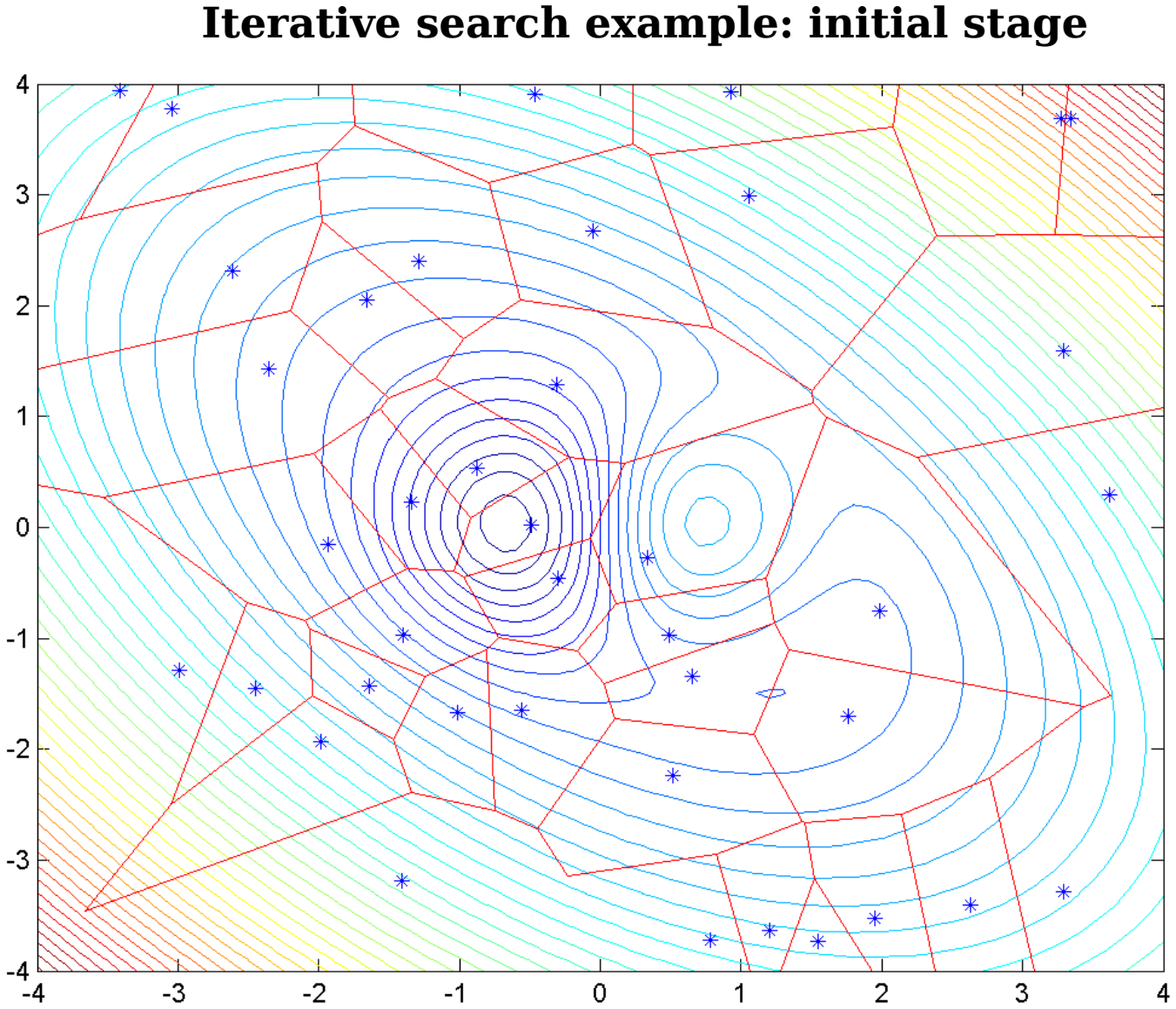

Example of the neighborhood Method (Monte Carlo)

Iterative search example: 1st iteration

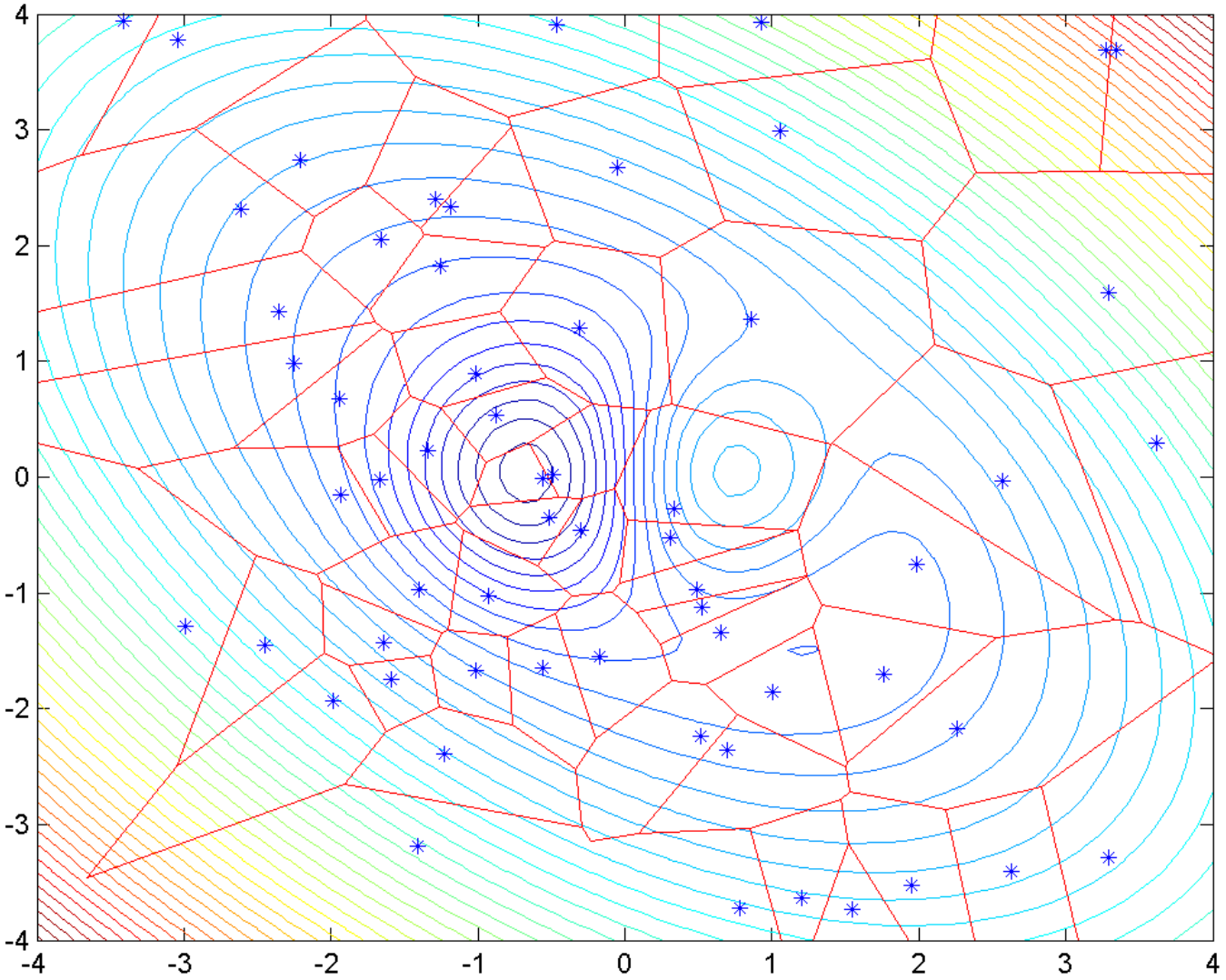

Example of the neighborhood Method (Monte Carlo)

Iterative search example: 2nd iteration

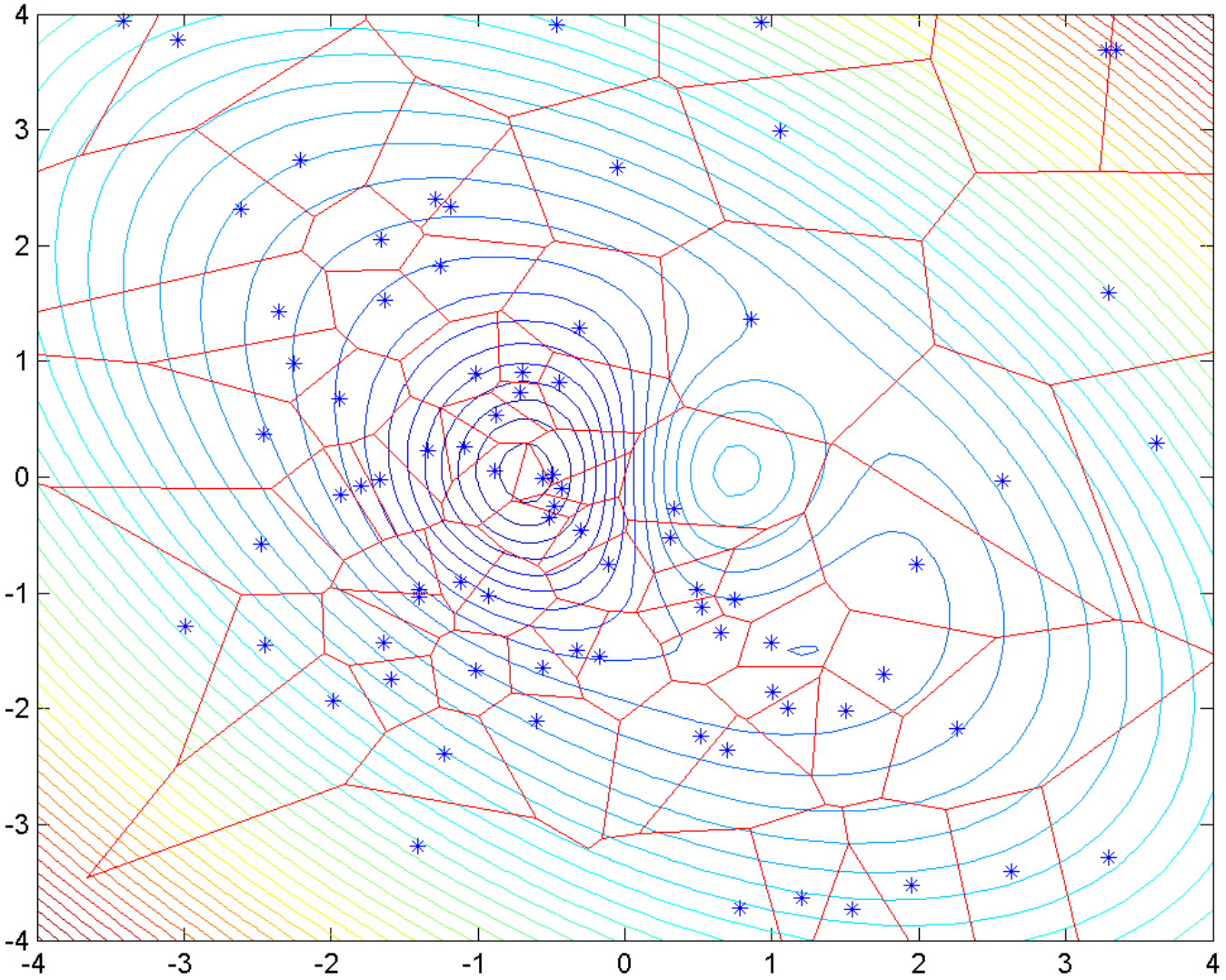

Example of the neighborhood Method (Monte Carlo)

Iterative search example: 3rd iteration

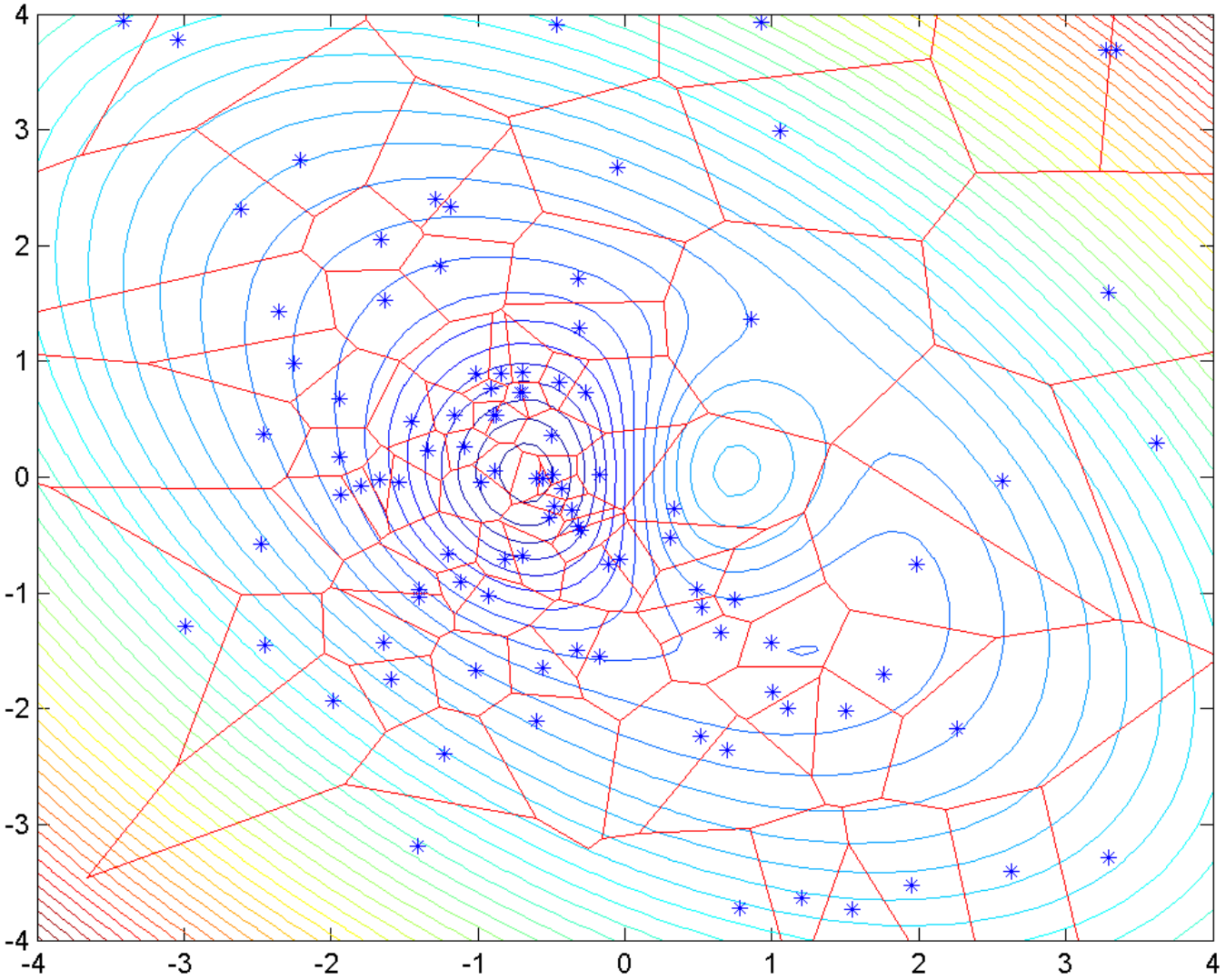

Example of the neighborhood Method (Monte Carlo)

Iterative search example: 4th iteration

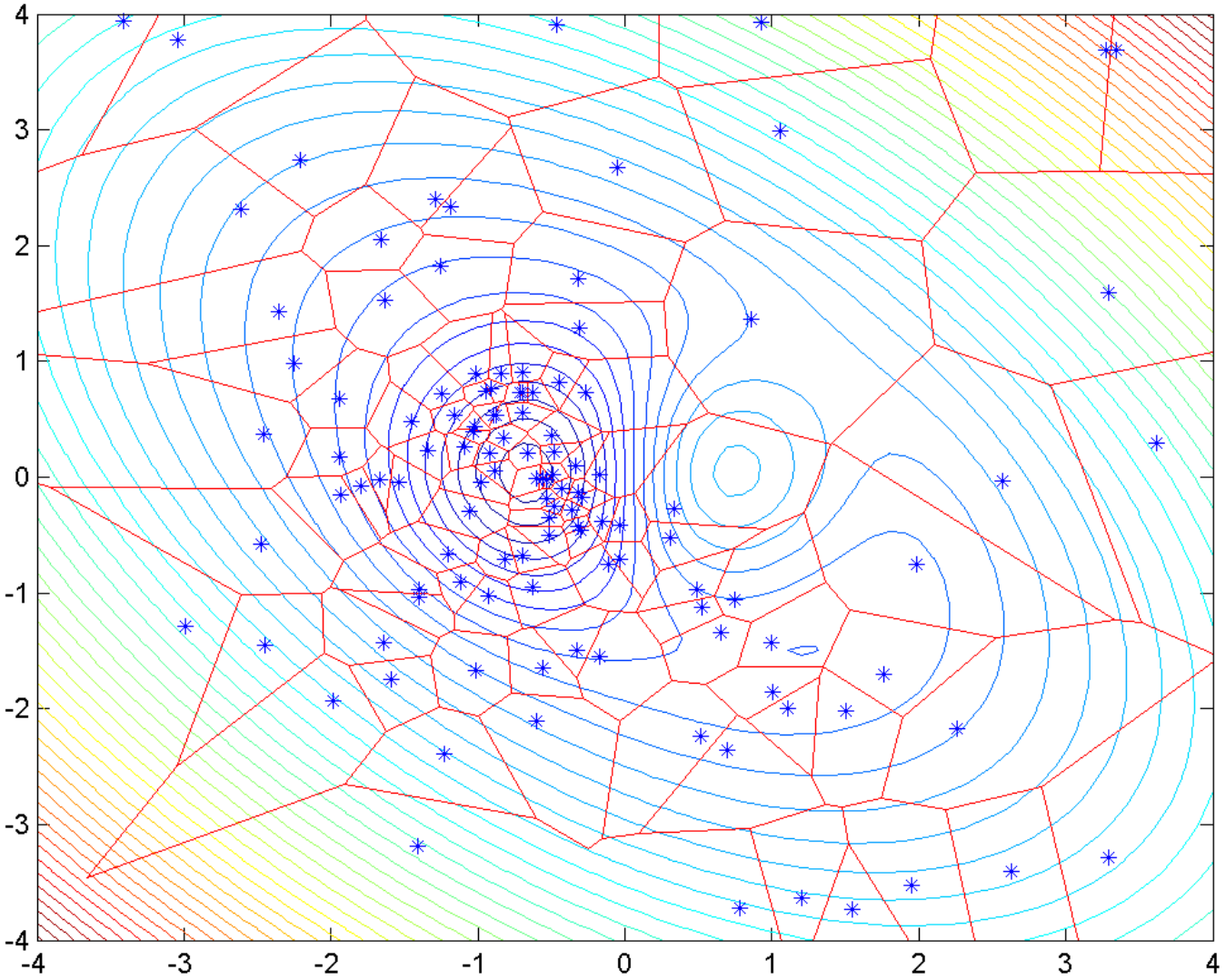

Example of the neighborhood Method (Monte Carlo)

Iterative search example: 5th iteration

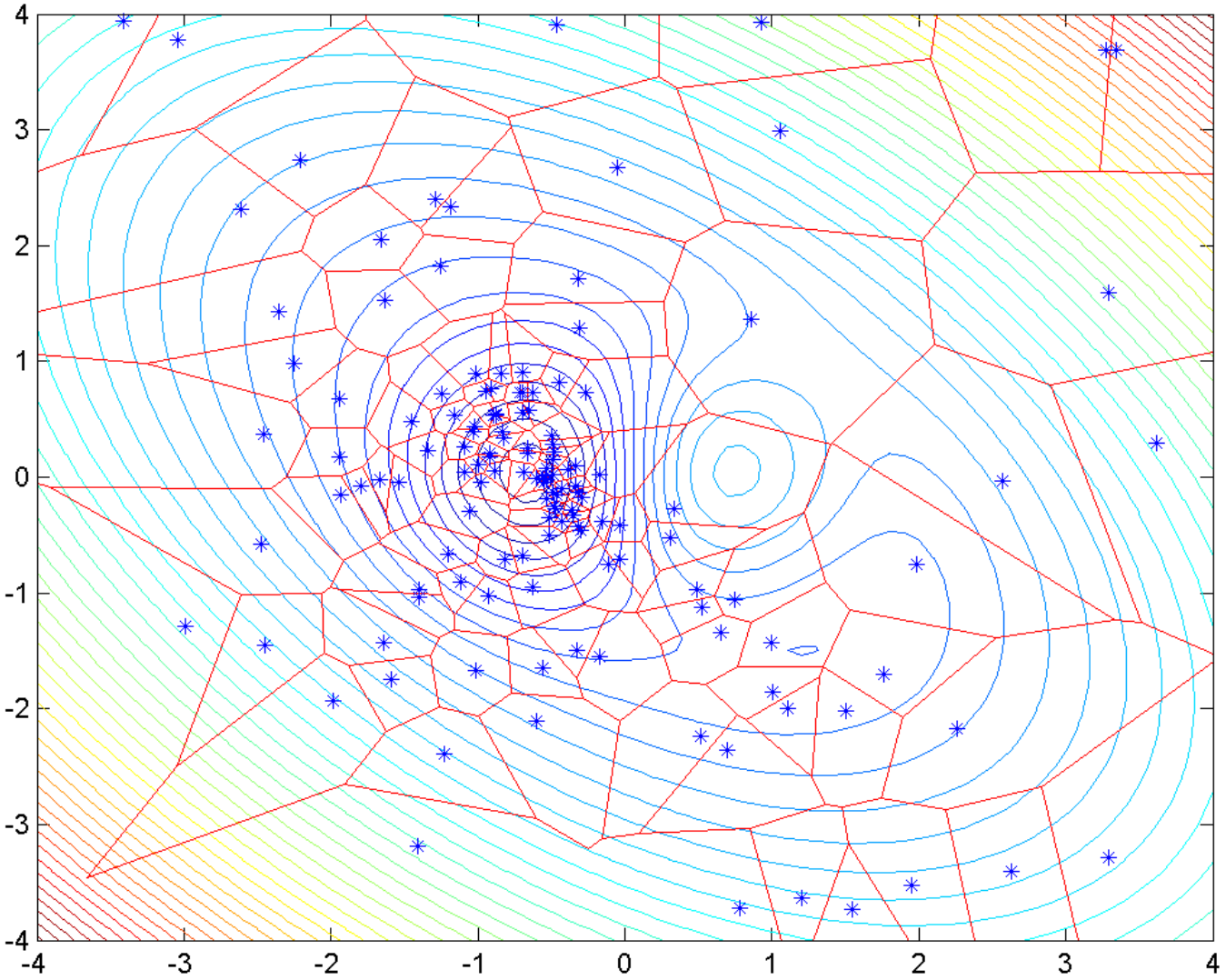

Example of the neighborhood Method (Monte Carlo)

Iterative search example: 6th iteration

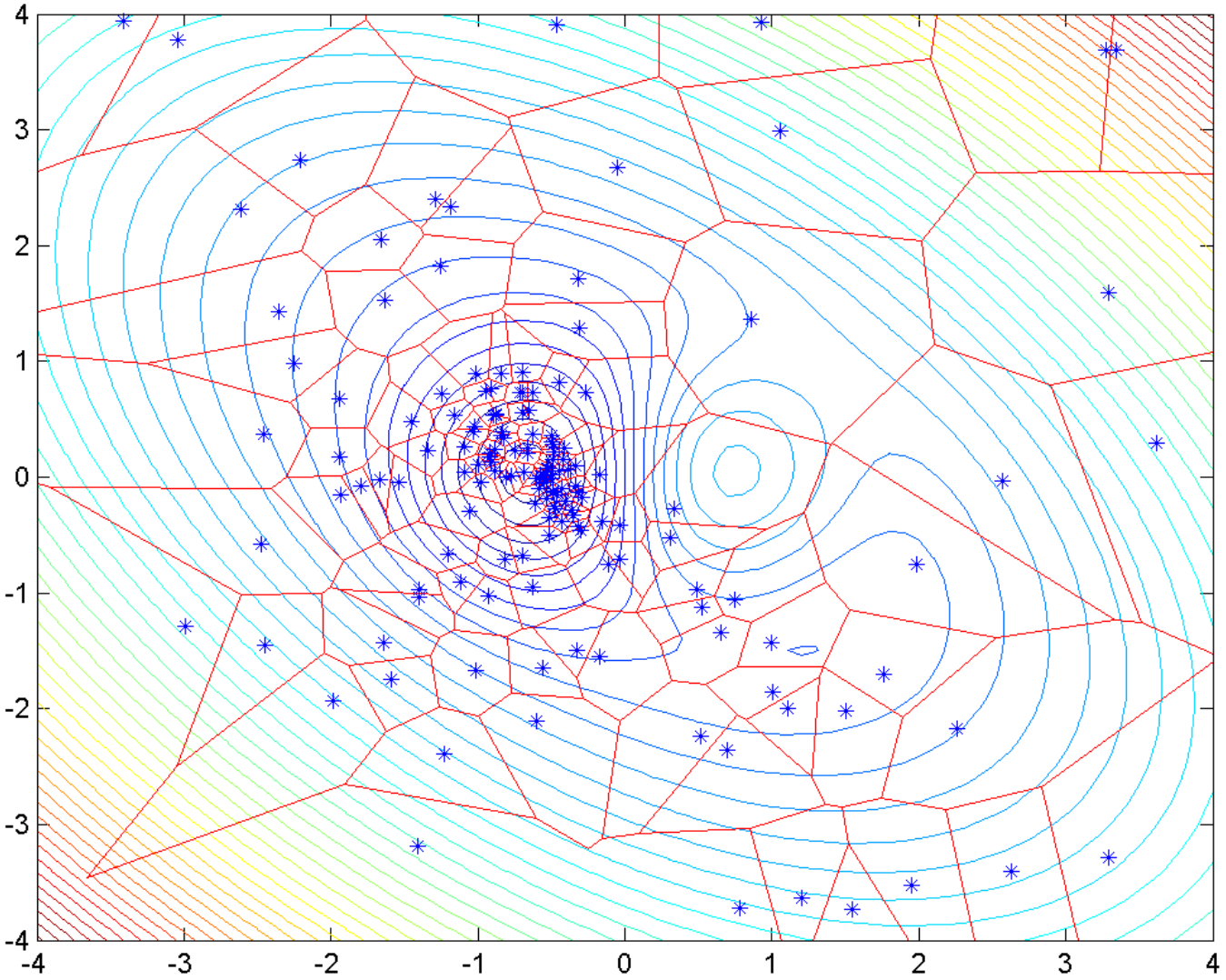

Example of the neighborhood Method (Monte Carlo)

Iterative search example: 7th iteration

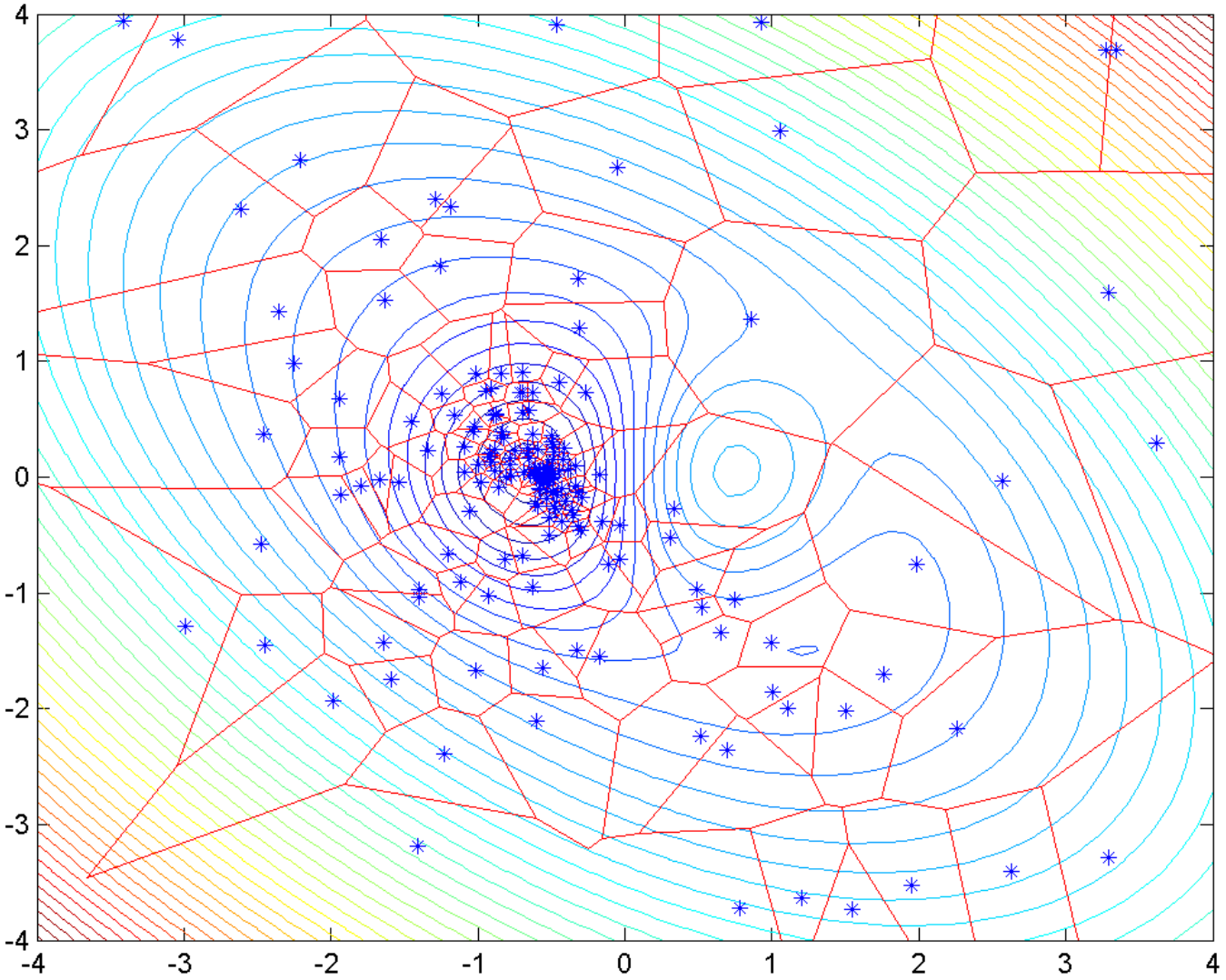

Inverse models based on boundary elements

Fukushima et al., JGR, 2005
Tridon et al., JGR, 2016

Mixed Boundary Element Method

Burried, or not burried curved intrusions

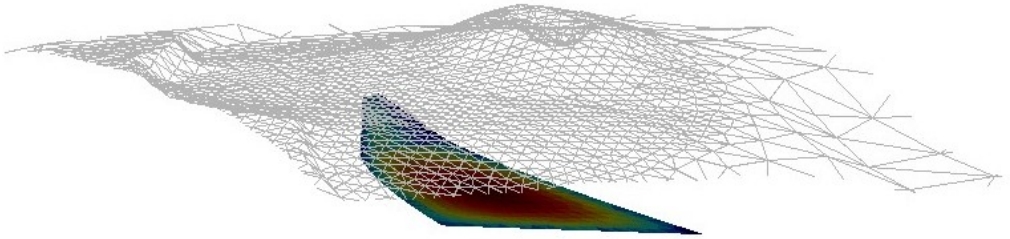

Prolate, oblate, inclined reservoirs

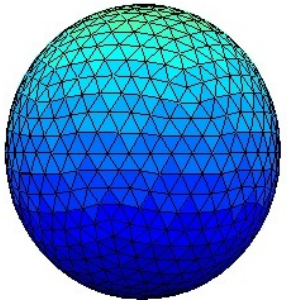

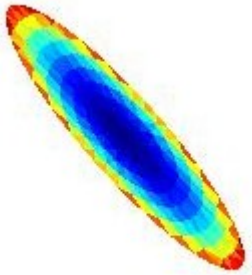

Planar ellipsoids

+

Neighborhood inversions

Misfit function:

$$\chi^2 = (u_o - u_m)^T C_d^{-1} (u_o - u_m)$$

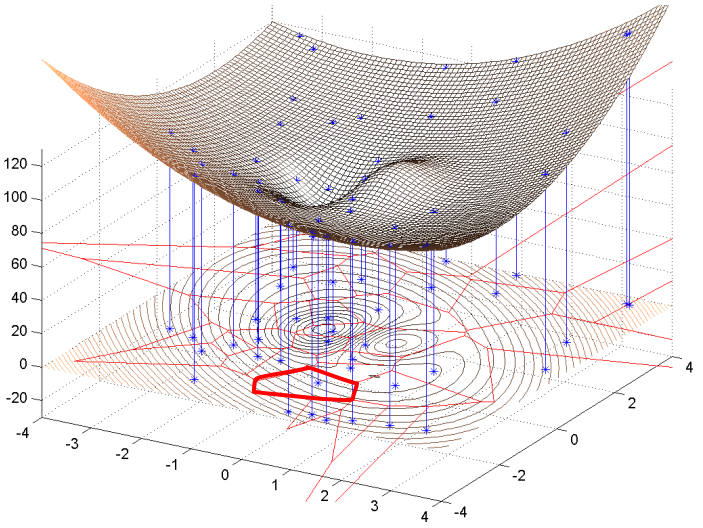

Web service and interface for fast inversions of volcano deformation

Adapted from R. Grandin, HDR

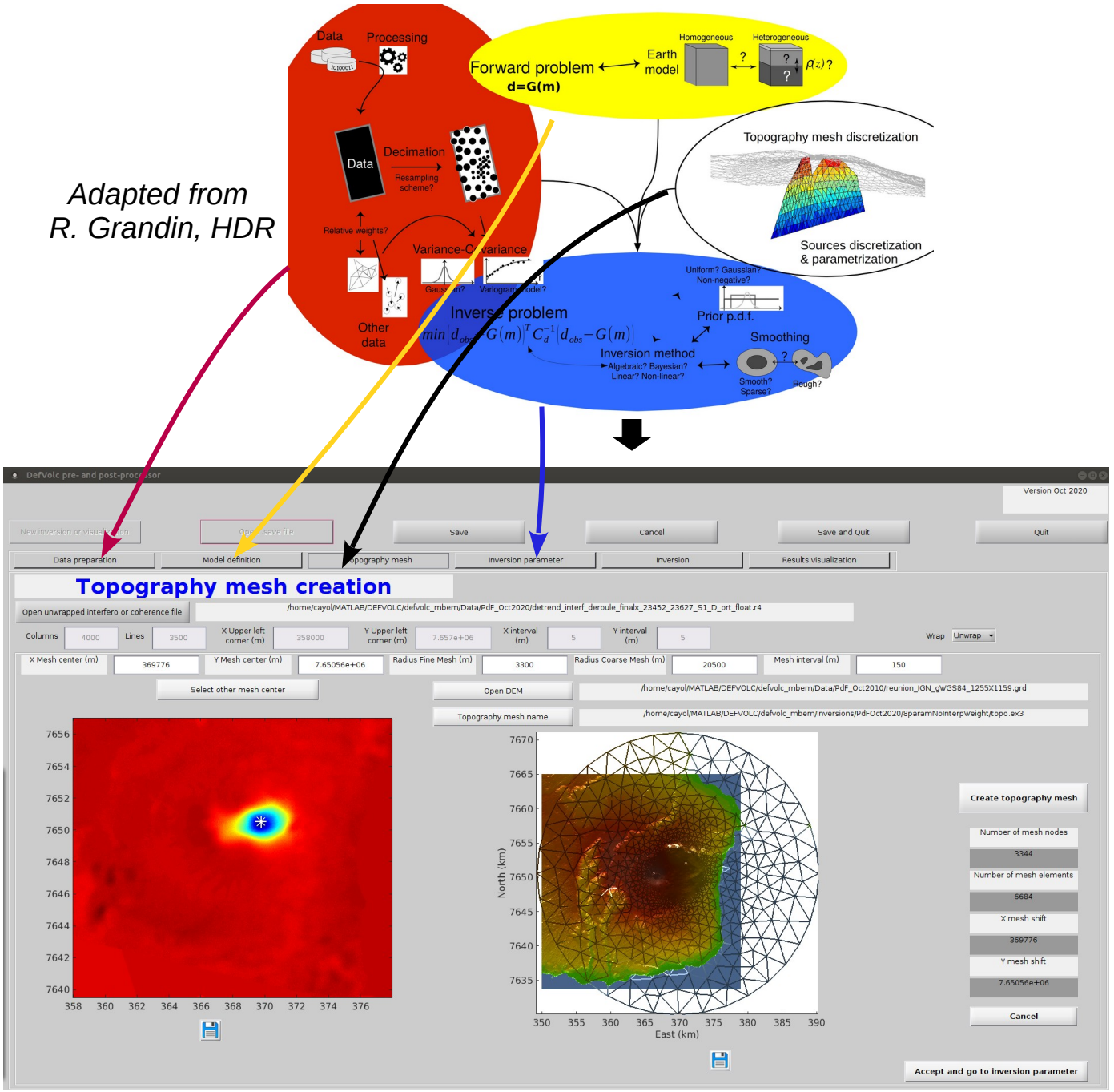

Accessible to registered users http://www.opgc.fr/defvolc/

Non-linear inversion to capture source geometries

Using Okada's model and MCMC inversion

Radial intrusion in 2009 at Fernandina volcano (Galapagos)

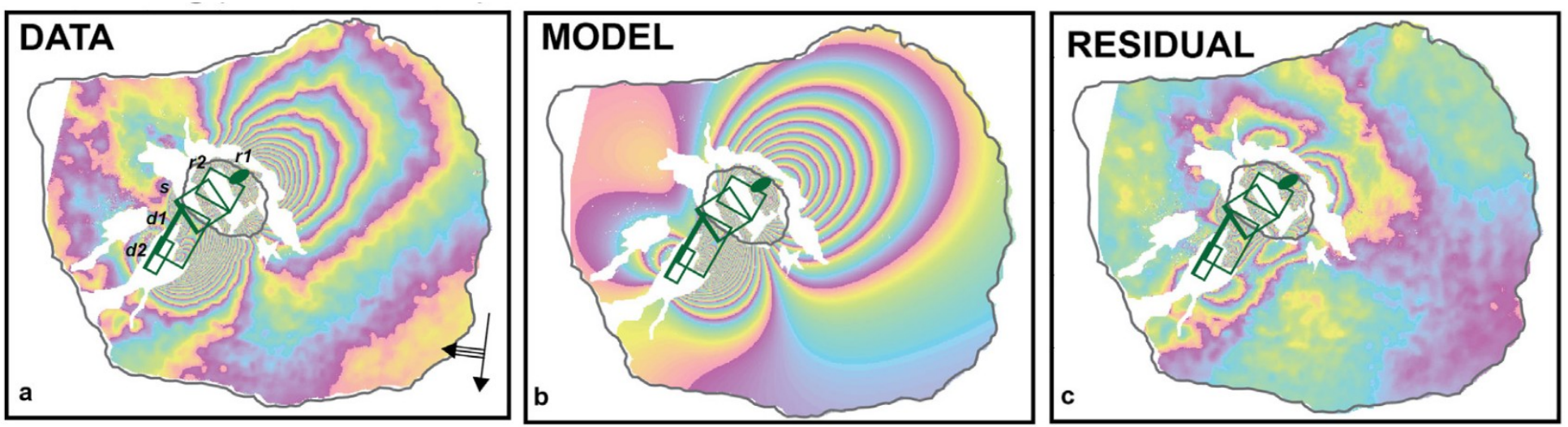

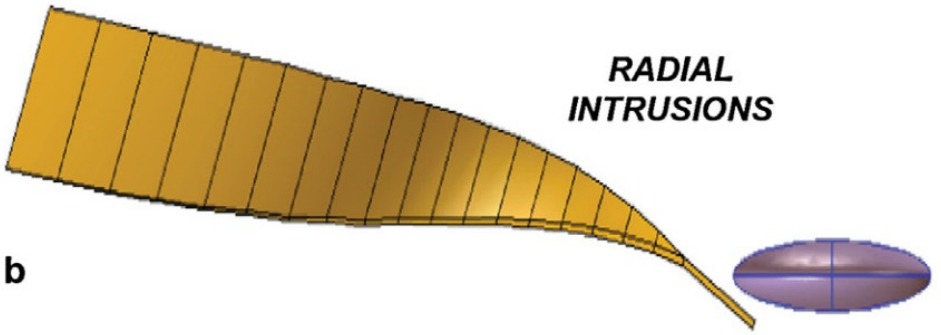

Bagnardi et al., EPSL, 2013

What can be learnt from analytic and kinematic inverse models ?

Intrusion pathways

Bagnardi et al., EPSL, 2013

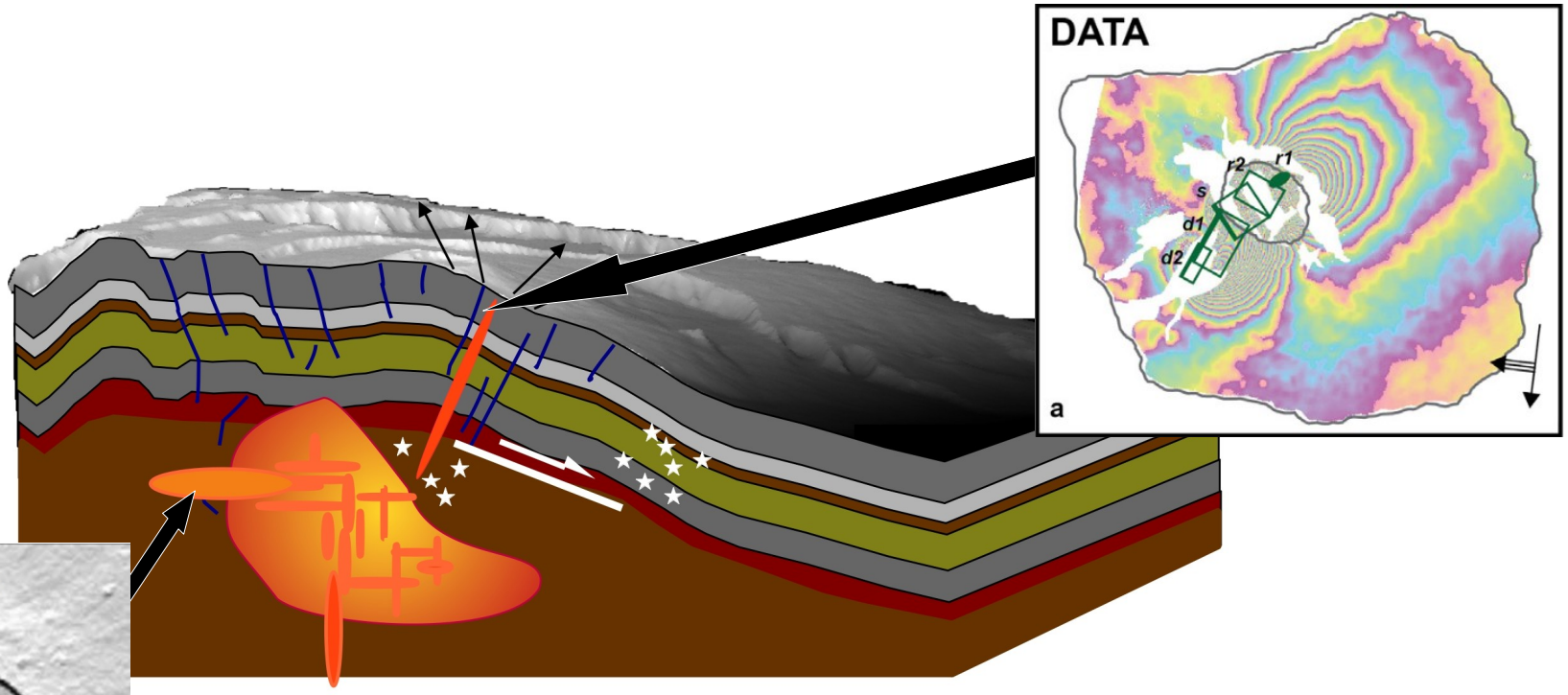

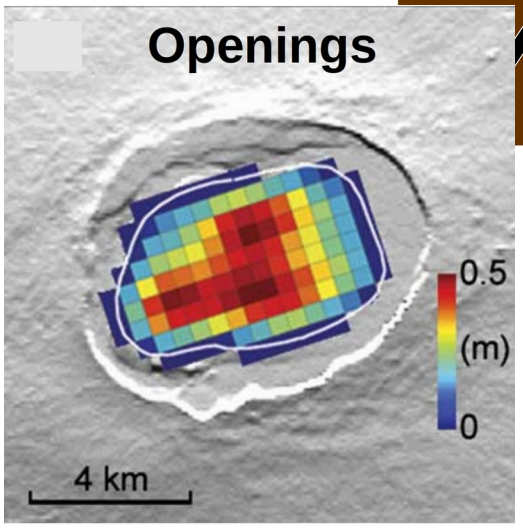

Characteristics of reservoirs

Amelung et al., Science, 2000

Simple analytic and kinematic models require many parameters

- **To better capture openings: linear inversion of 77 parameters**

Uplift at Sierra Negra volcano in 1998-99 (Galapagos)

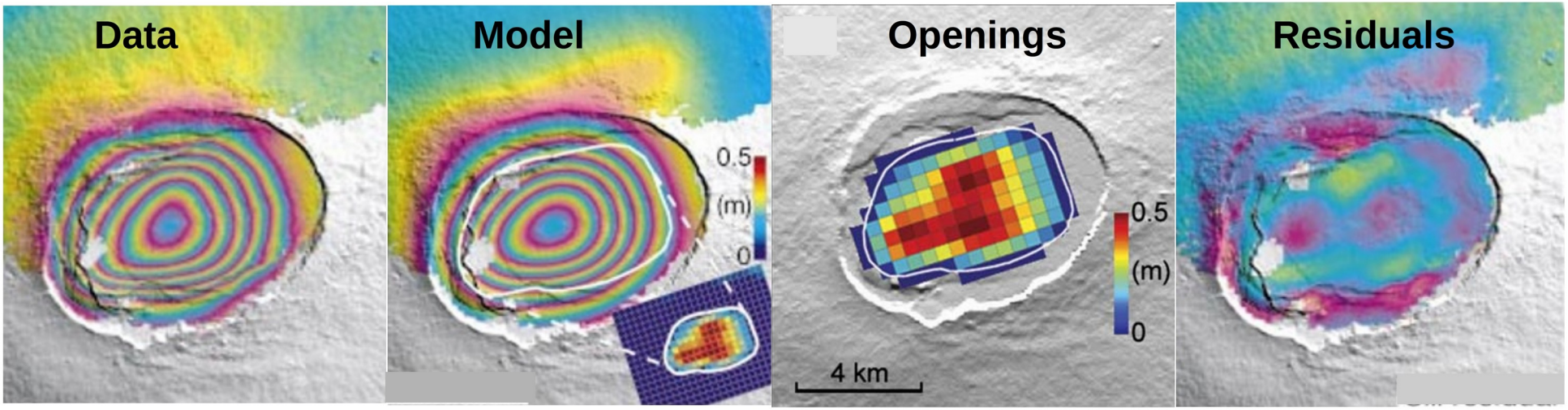

Amelung et al., Nature, 2000

- **To better capture complex geometries: non linear inversion of 22 parameters**

Radial intrusion in 2009 at Fernandina volcano (Galapagos)

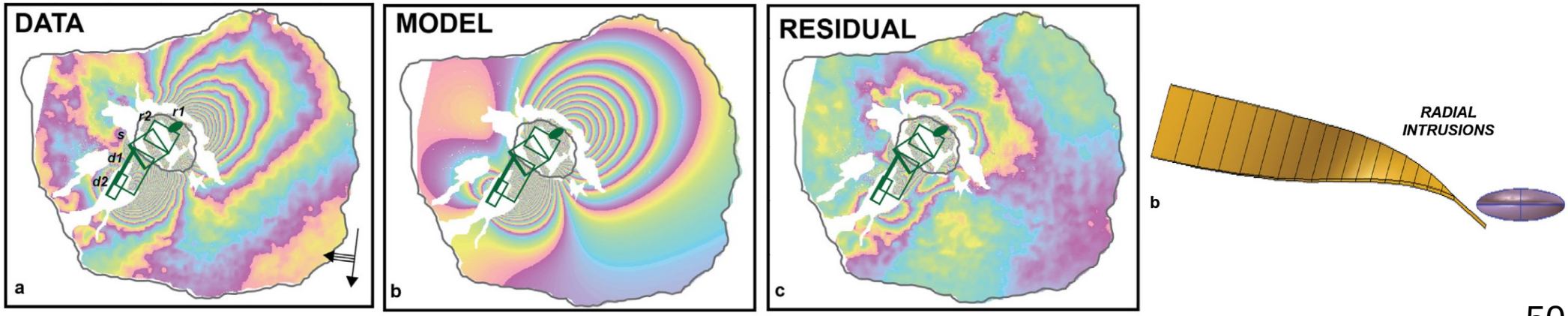

Bagnardi et al., EPSL, 2013

Large numbers of parameters should be avoided

- The probability of finding the best-fit solution decreases with the dimension of the search space ;

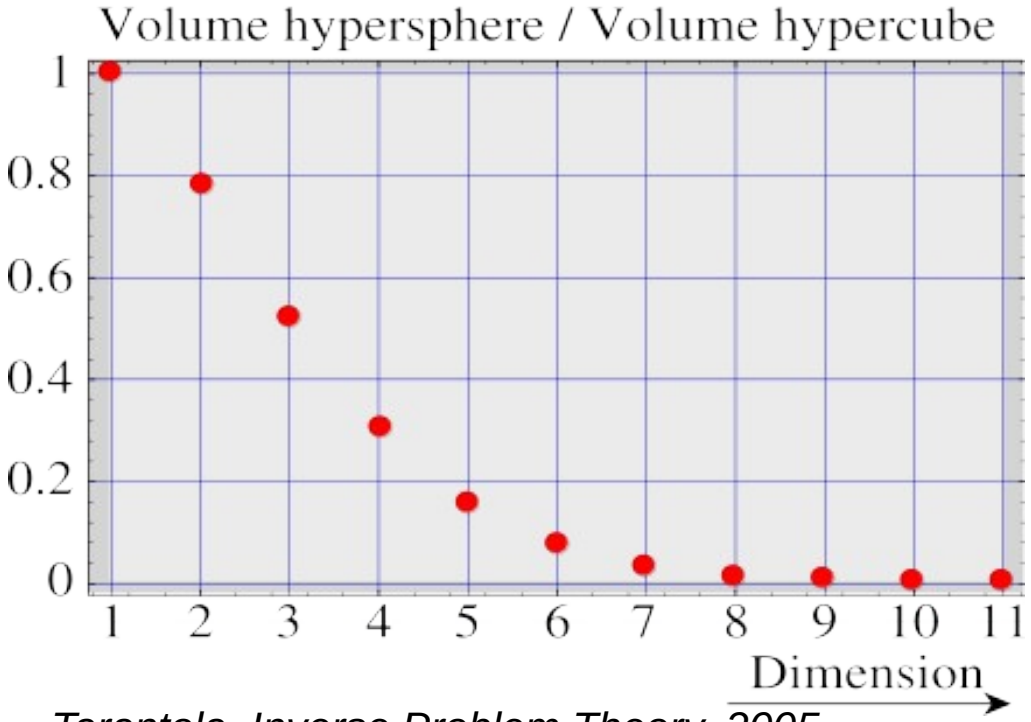

Tarantola, Inverse Problem Theory, 2005

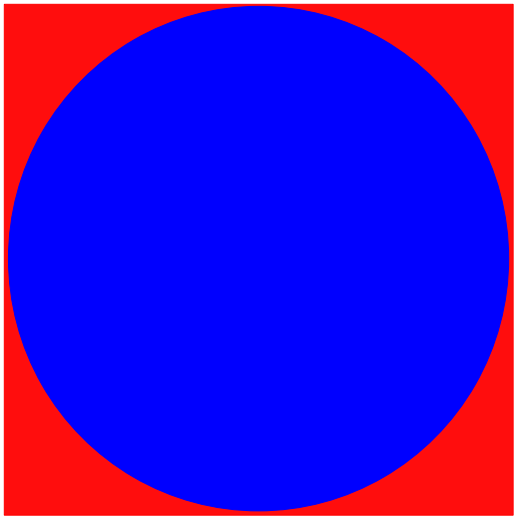

n=2

- With non linear inversions, the search time increases exponentially with the number of parameters ;
- There is a risk of overfitting the data.

→ **Use of Akaike Information Criteria**

AIC = 2*k + χ^2 + cst **with k = Nb parameters and χ^2 = cost-function, cst = a constant, which depends on the number of data**

Large numbers of parameters should be avoided

- The probability of finding the best-fit solution decreases with the dimension of the search space ;

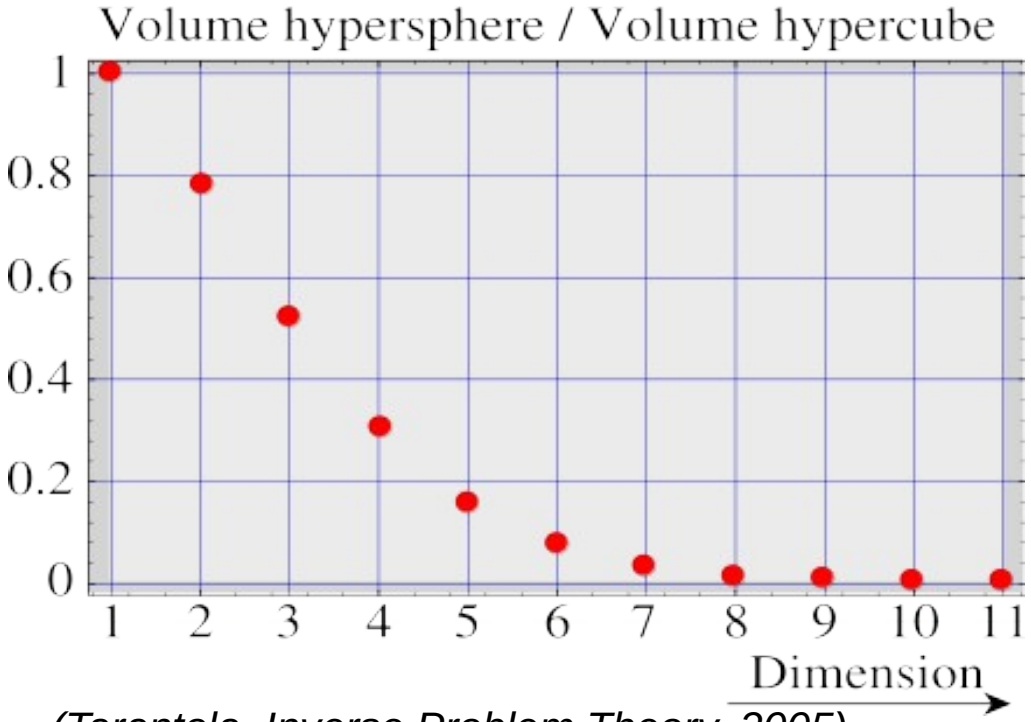

(Tarantola, Inverse Problem Theory, 2005)

n = 12

- With non linear inversions, the search time increases exponentially with the number of parameters ;
- There is a risk of overfitting the data.

→ **Use of Akaike Information Criteria**

AIC = 2*k + χ^2 + cst **with k = Nb parameters and χ^2 = cost-function, cst = a constant, which depends on the number of data**

Non-linear inversion to capture source geometries

Using Mixed Boundary elements and neighborhood inversions

Sill turning into a dike at Piton de la Fournaise Volcano (La Réunion, France)

88% of the data explained

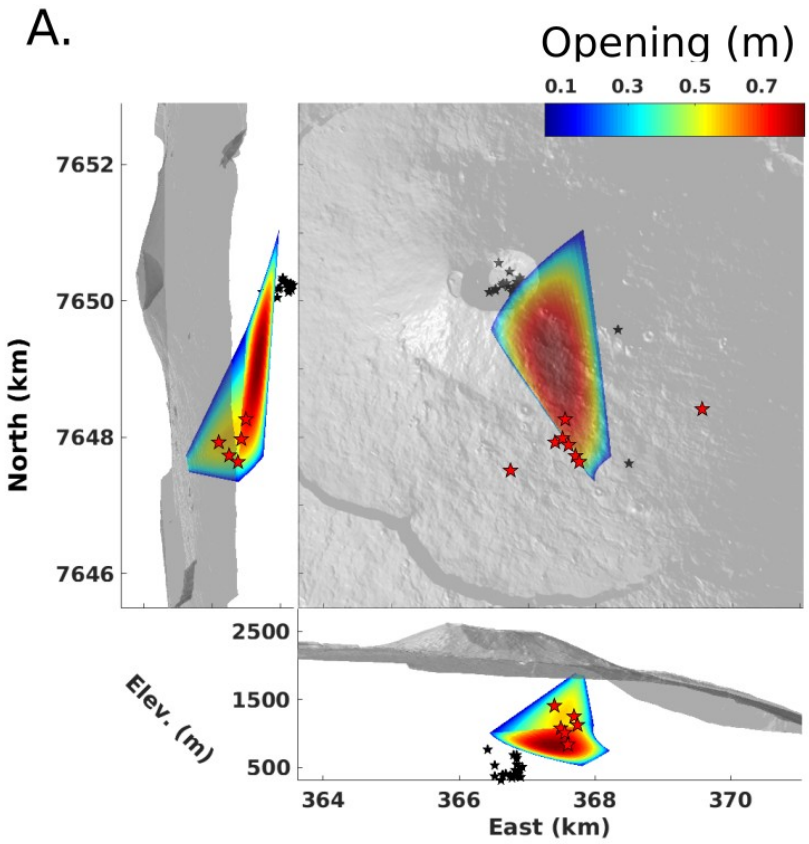

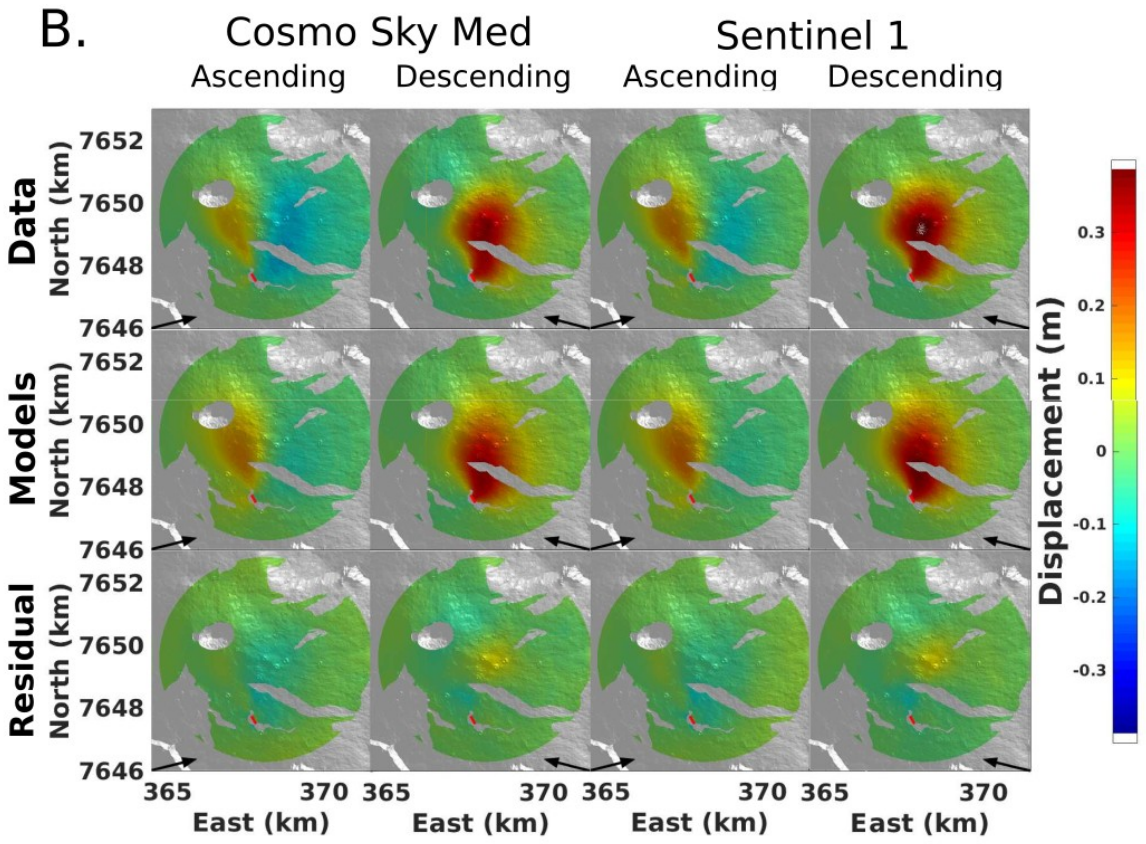

8 geometrical parameters

Smittarello et al., JGR, 2019

Boundary conditions are homogeneous stress

Field observation

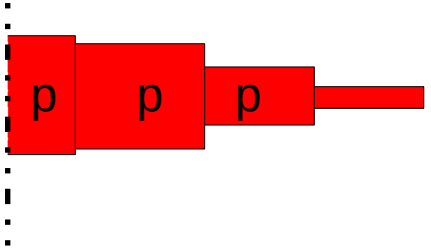

Pressure boundary condition

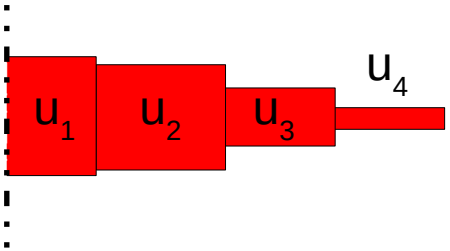

Displacement boundary condition : kinematic models

Inverted openings

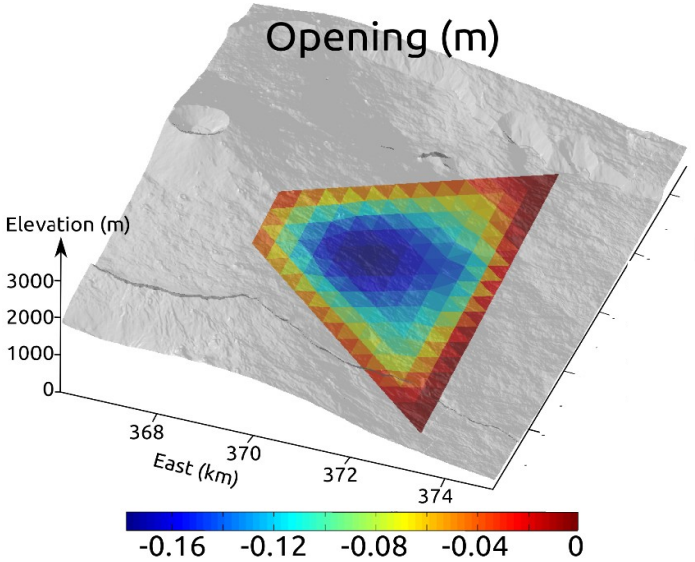

One parameter

~ 5 % of inverse models

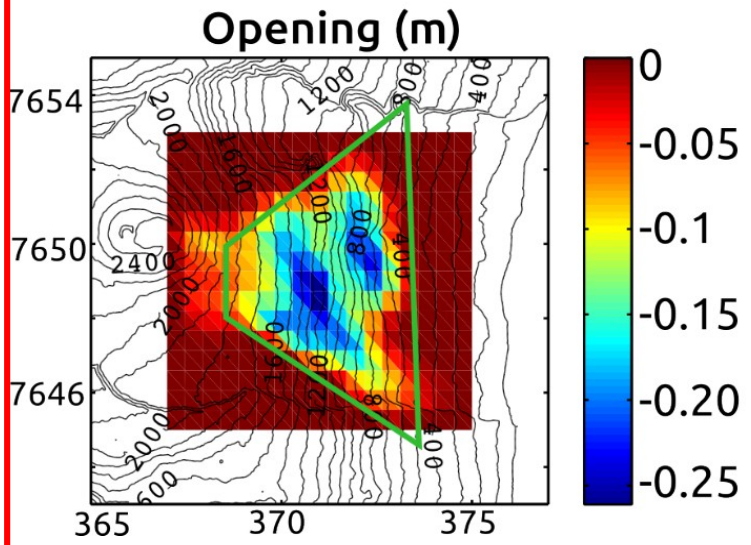

Tridon et al., JGR, 2016

500 parameters

~ 95 % of inverse models

Stress boundary conditions lead to better models

AIC = 2*k + χ^2 + cst with k = Nb parameters and $\chi^2 = (u_o - u_m)^T C_d^{-1} (u_o - u_m)$

Pressure boundary condition | **Displacement boundary condition**

Inverted openings

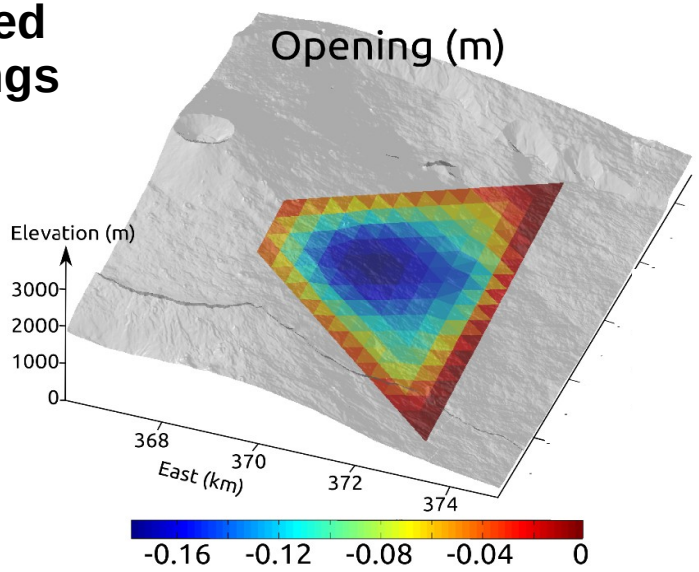

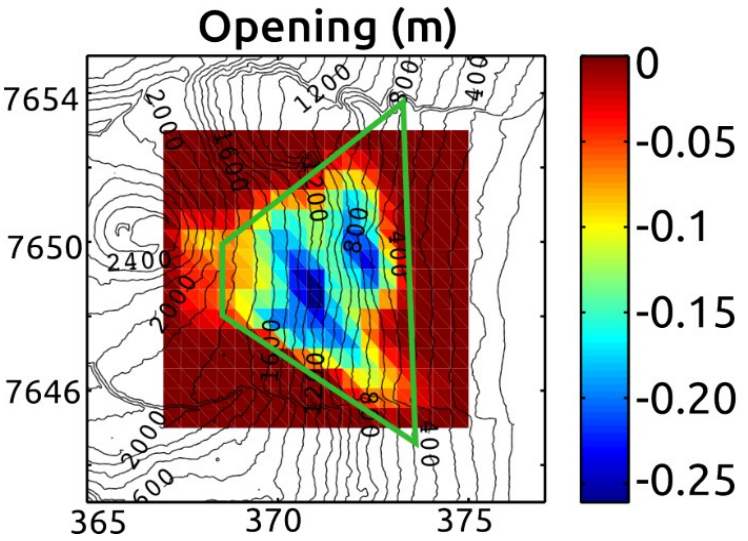

One parameter

$\chi^2 \approx 2784$

AIC ≈ 2800

500 parameters

$\chi^2 \approx 2300$

AIC ≈ 3300

Tridon et al., JGR, 2016

→ **Models with stress boundary conditions require less inversion parameters**

→ **Inverting for stress leads to better models than inverting for dislocation amplitudes**

4. Benchmarking, verification, validation

Modelling benchmarking and verification, inversion validation

Crozier et al., Bull. Volc., 2023

Community exercise: Partnership between
- the IAVCEI geodesy commission,
- Subduction Zones in four Dimensions,
- CONVERSE

IAVCEI VOLCANO GEODESY

SZ4D

CONVERSE
Converging on Eruption Science with Equity

Benchmarking

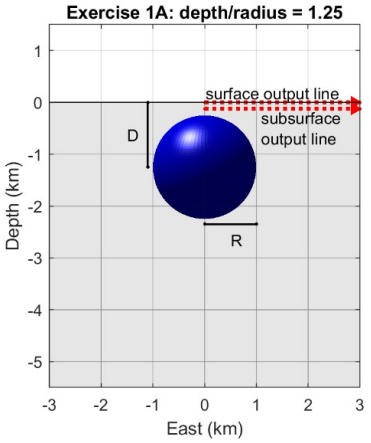

Verification

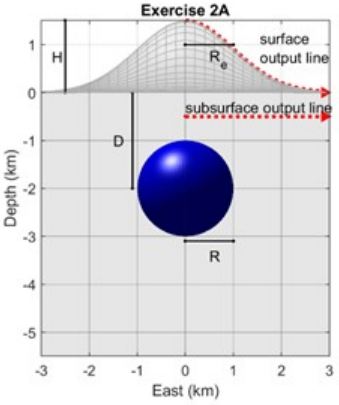

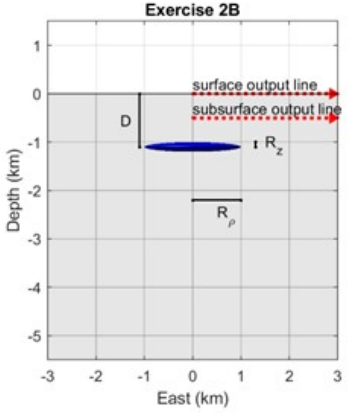

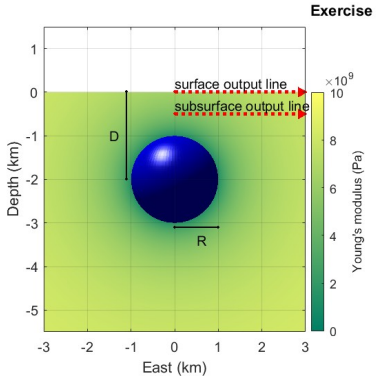

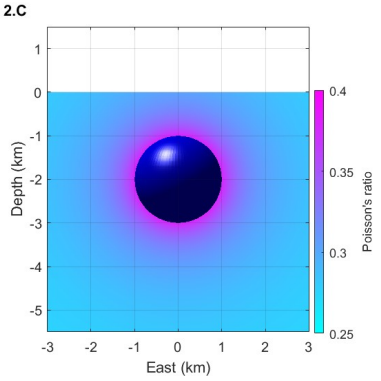

Validation: inversion

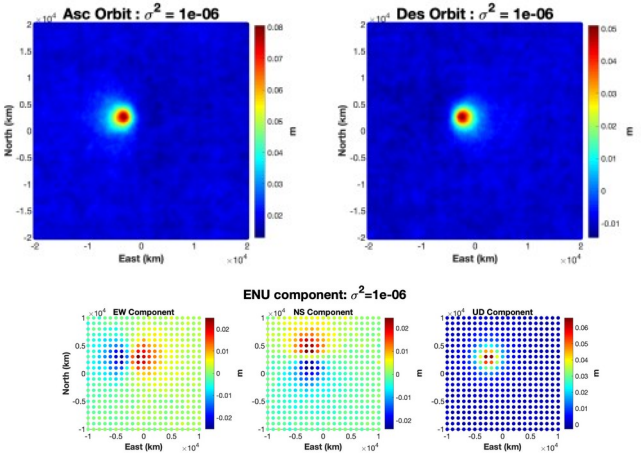

Exercise goal

Inspired by a Southern California Earthquake Center exercises on simulations of fault rupture. Comparison between solutions for reservoirs in **elastic media**.

Built in interface http://www.driversofvolcanodeformation.org/

- Registered users (~25 participants from 4 countries: students, faculty & observatories)
- Still accessible for benchmarking

Benchmarking : sphere in a homogeneous ½ space

Exact solution by *Zhong et al., GJI, 2019*

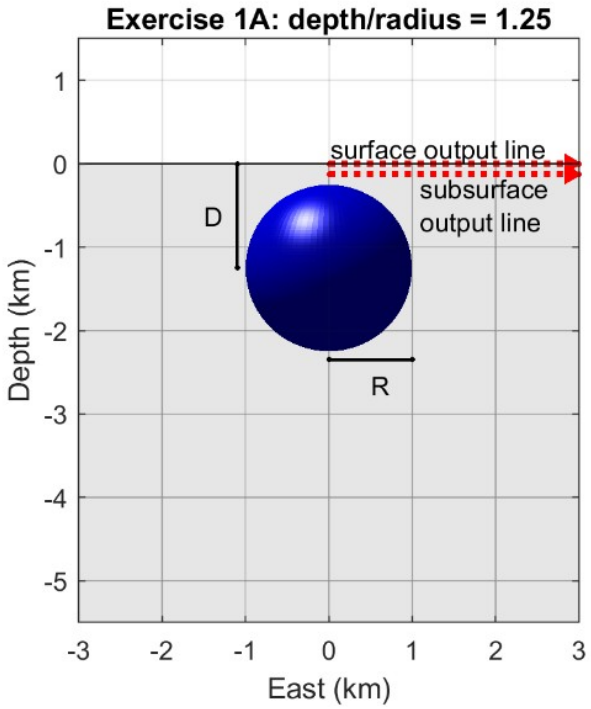

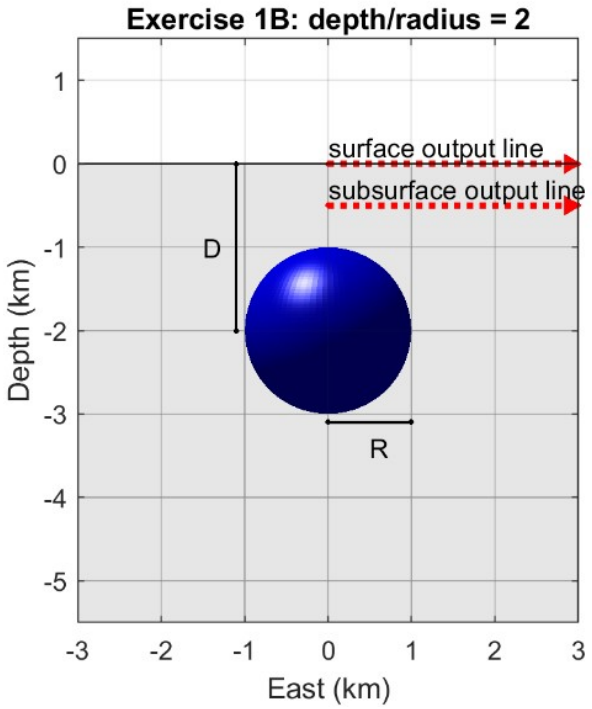

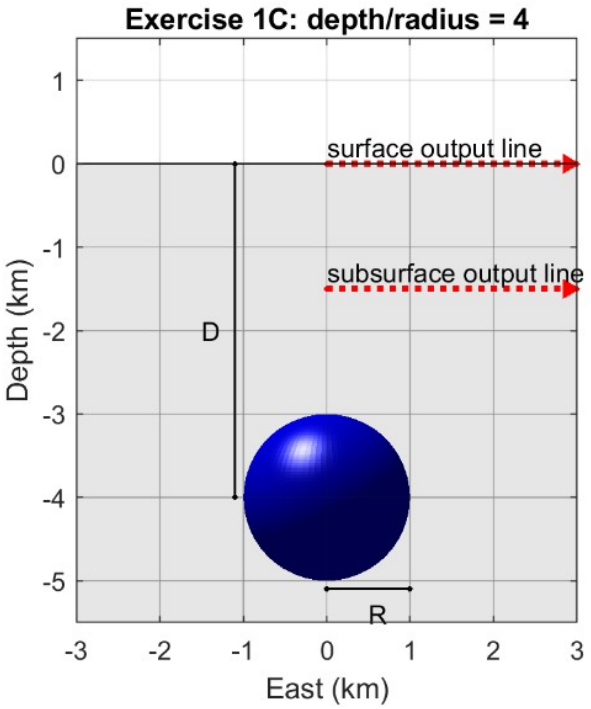

Benchmarking: sphere in a homogeneous ½ space

Errors

17 solutions compared: Analytic McTigue, Analytic Mogi, BEM 3D disclocations, 3D mixed BEM,Comsol 2D FEM, FEM 2D NGSOLVE, FEM 3D Pylith, etc.

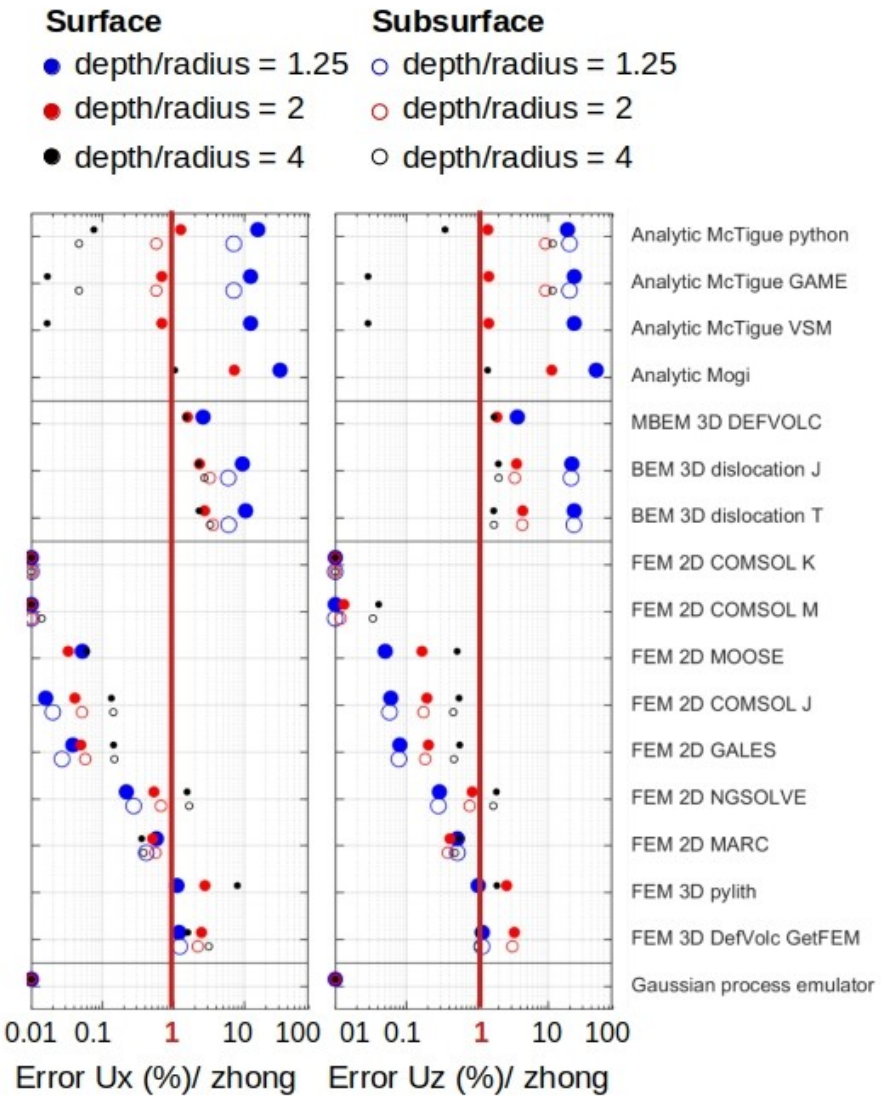

- For deep reservoirs (D/R=4), all solutions are acceptable (1% error).
- For shallow reservoirs (D/R<1.25), Mogi and McTigue have large errors (>10%).
- 2D Finite Element Model (FEM) solutions show the **lowest error** (< 1%).
- 3D solutions show **larger errors** (~1-3%), particularly dislocations Boundary element Methods (BEM) (11%).
- **Several bugs** have been identified in analytic solutions.

Benchmarking : sphere in a homogeneous ½ space

Convergence tests

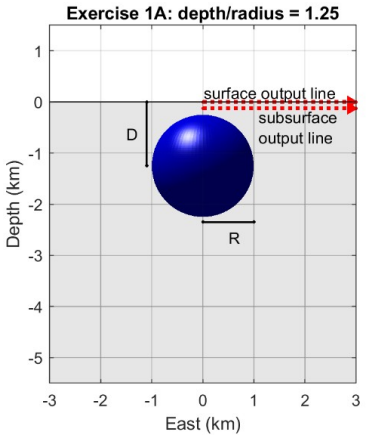

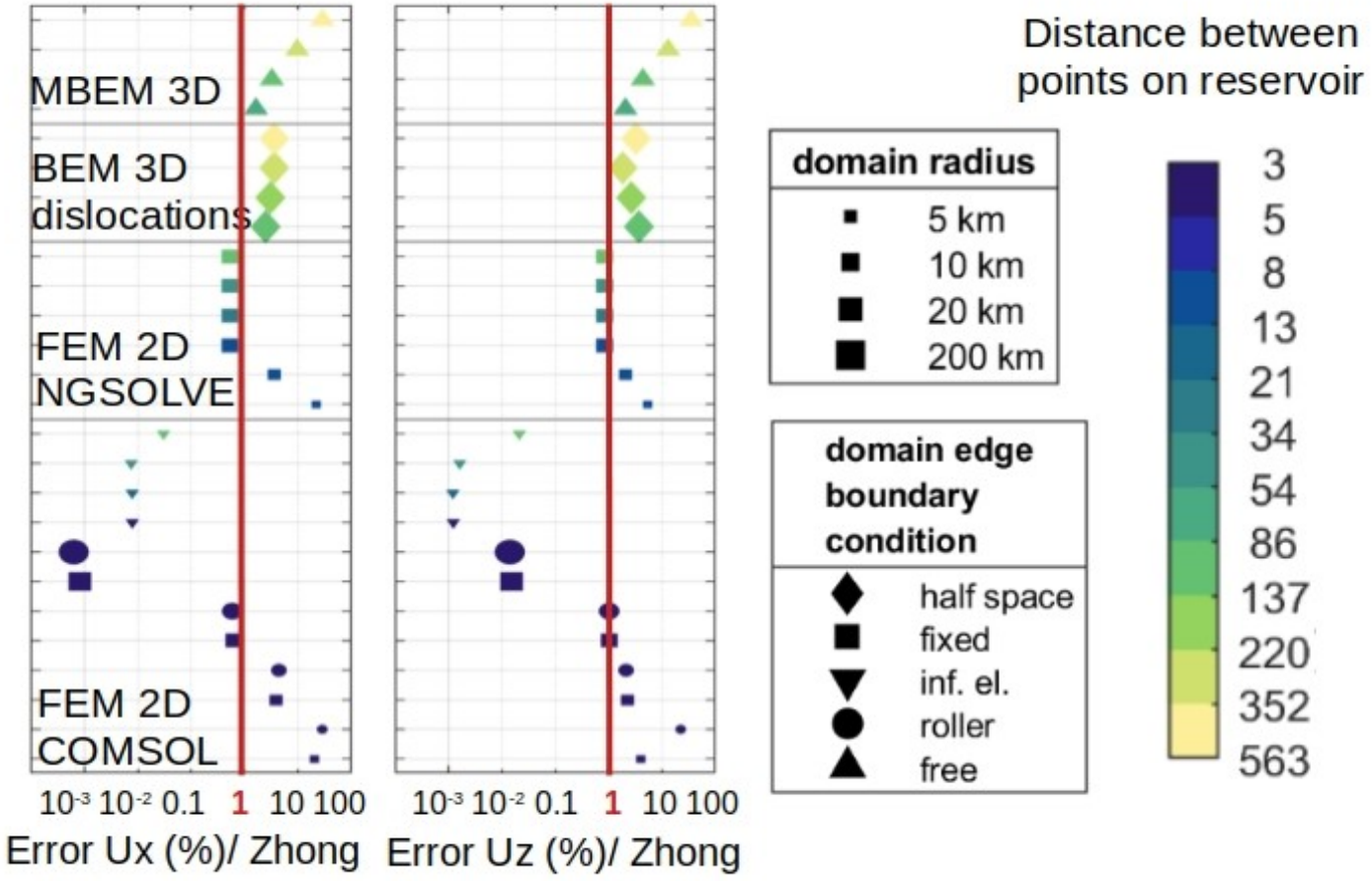

- The domain size must be at least **20 times the source size** (infinite elements are best)
- The **mesh density fine enough** to have solution convergence.
- No significant difference between types of boundary conditions

Validations: adding topographies

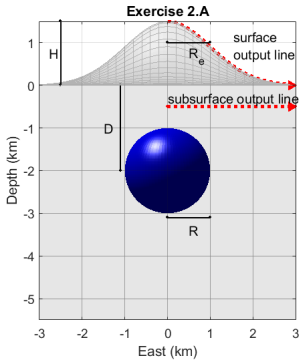

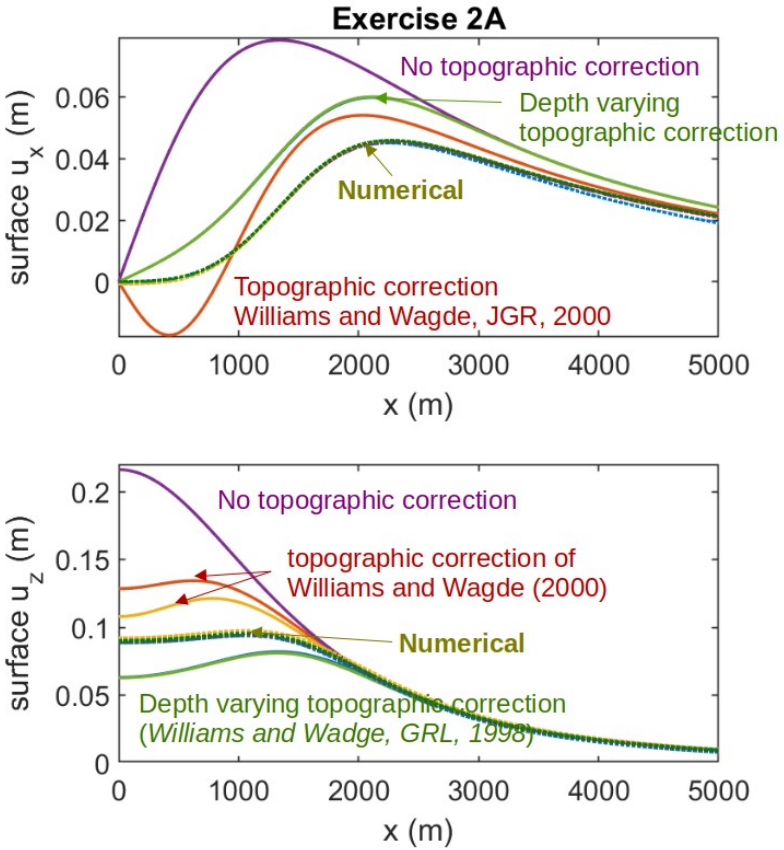

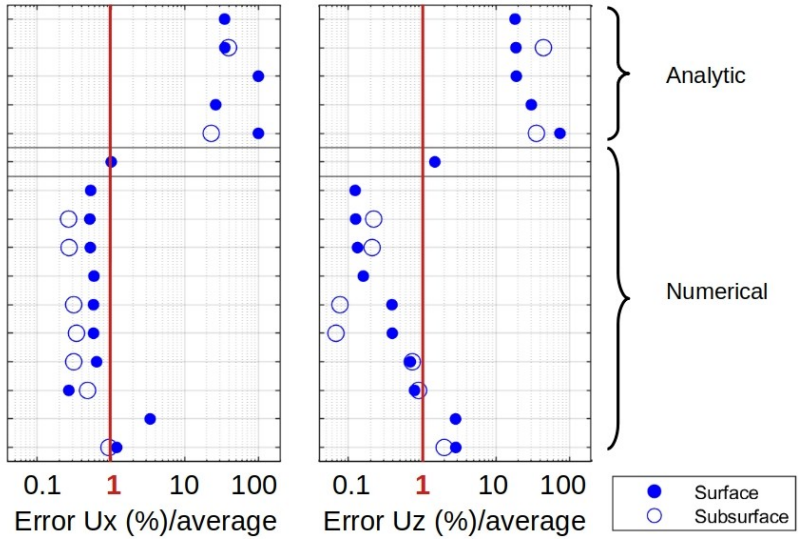

- **Analytic** solutions, with or without topographic corrections, are far from **numerical solutions** (U_z is 66 % larger for no topographic correction, and 30% smaller for depth varying correction)
- **Less than 1%** of difference between numerical solutions;

Validations: heterogeneities in elastic properties resulting from temperatures

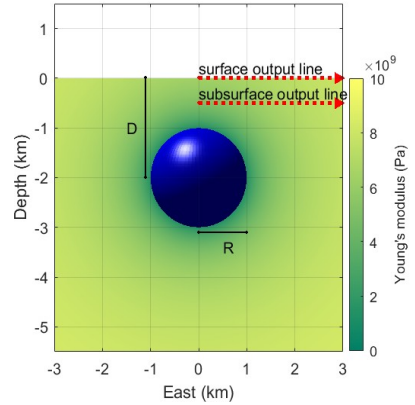

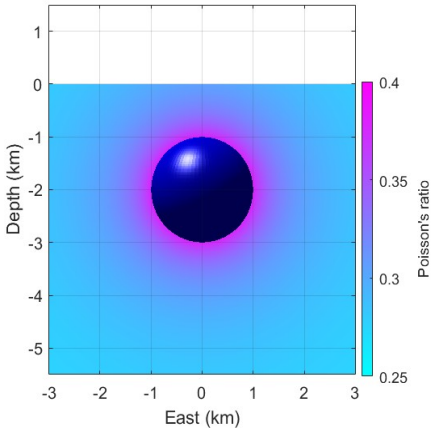

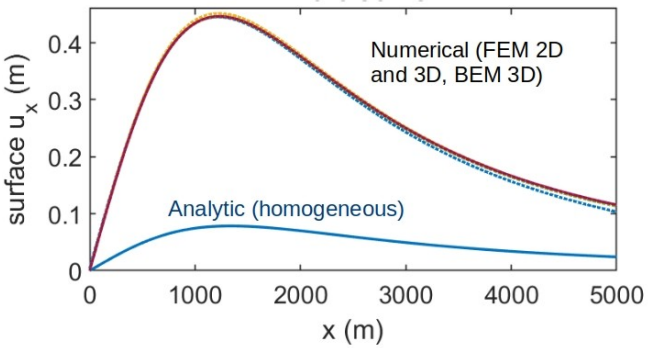

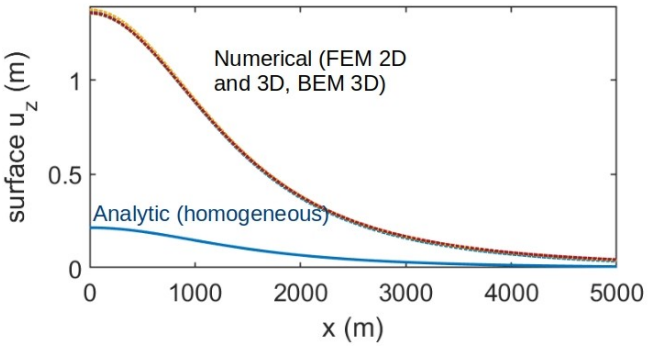

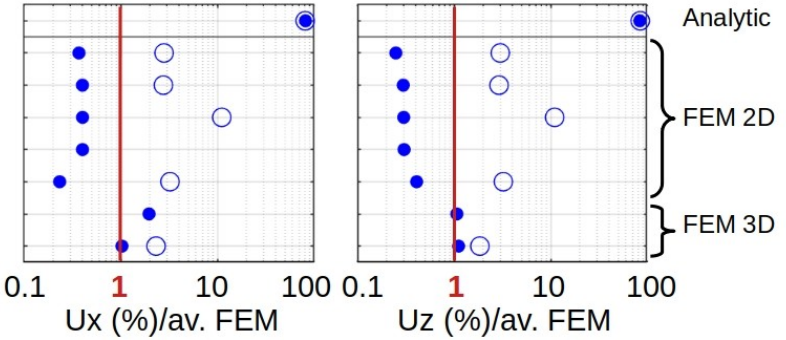

Following *Bakker et al., JGR, 2016*

- Analytic homogeneous solution is **wrong** (U_z is 85% less)
- **2D and 3D FEM** solutions are **close** (< 1% variations)
- Using analytic solutions, the shape of the solution is right, but the amplitude too weak → overpressures might be overestimated.
- However, these heterogeneities might be **second order** relative to **depths varying heterogeneities**

Verification: inversion of InSAR and GNSS data

Sphere in a half-space (*Zhong et al., GJI, 2019*)

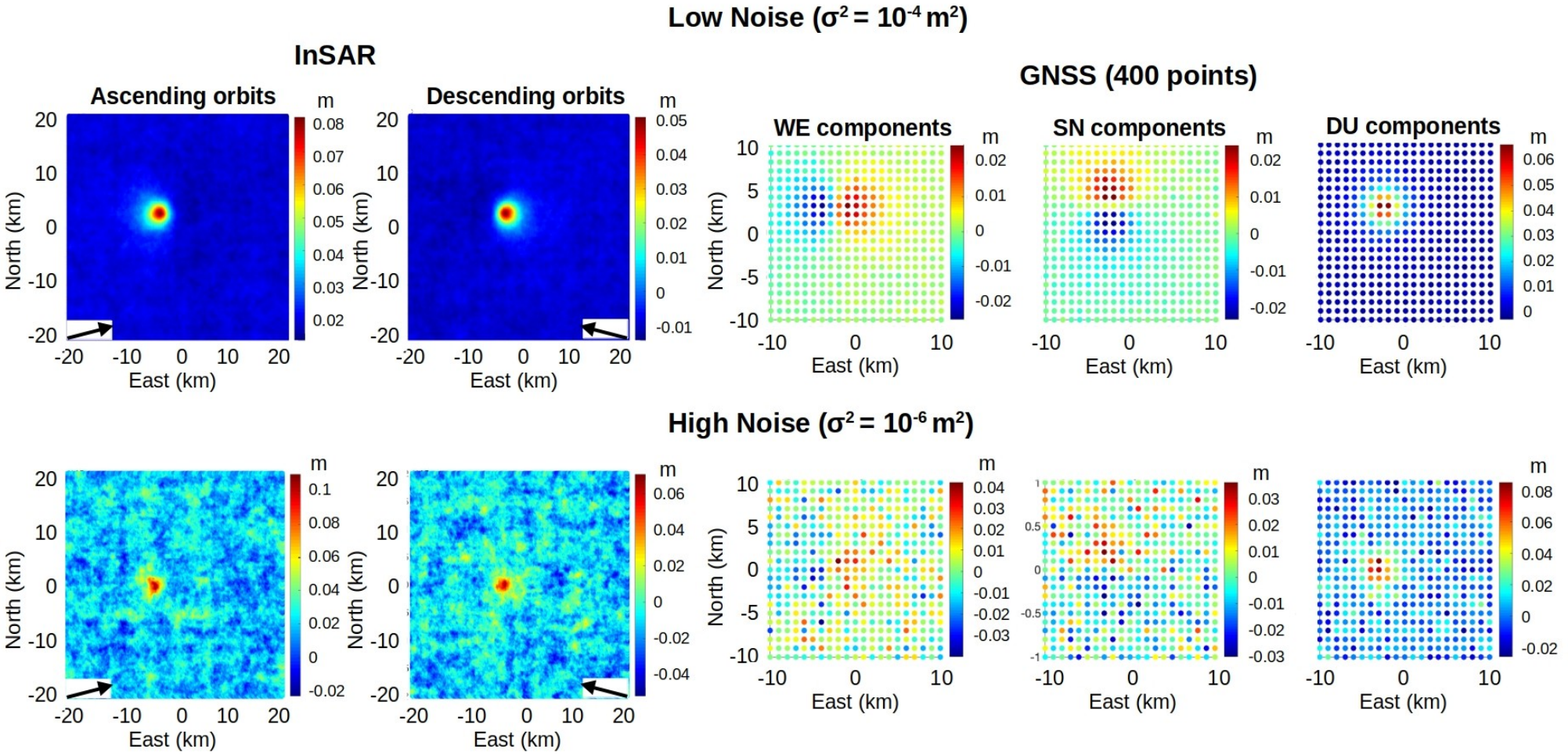

Verification: inversion of InSAR and GNSS data

Results for low noise data (depth/radius = 2.3)

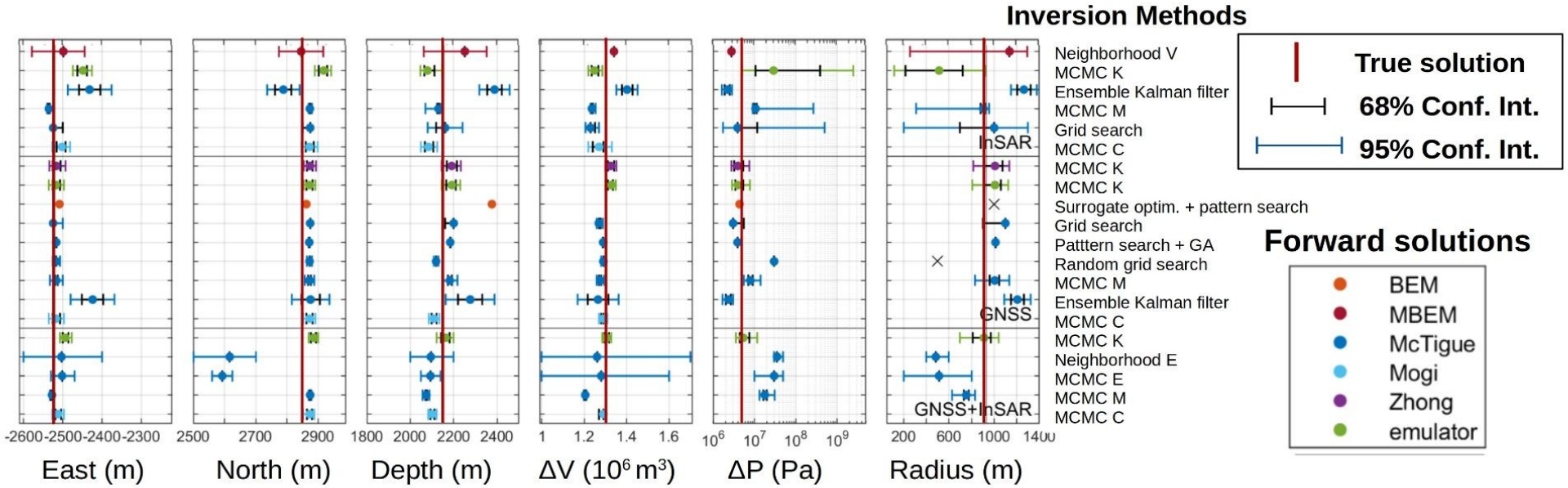

- Large range of forward modelling methods: BEM, FEM, Analytic, Emulator;
- Large range of inverse methods: Neighborhood, Markov Chain Monte Carlo (MCMC), Ensemble Kalman Filter, Genetic algorithm, surrogate search, grid search;
- Best determined parameters are: coordinates, depth (20% of range), and volume changes (30% range);
- As expected, poorly constrained pressure change and reservoir radius;
- Better accuracy for GNSS/InSAR in this exercise, but number of GNSS points is **unrealistic**!
- With high noise, the initial model is well retrieved with larger depth (35%) and larger volume change (50%) ranges than the low noise solution (20 and 30%, respectively);
- Many submissions failed to obtain the solution within **the obtained uncertainties**.
- **Larger variations** related to **inversion methods** rather than **forward model** choice

Verification: inversion of InSAR and GNSS data

Misfit function χ^2 and Probability Densities Functions (PDF) low noise

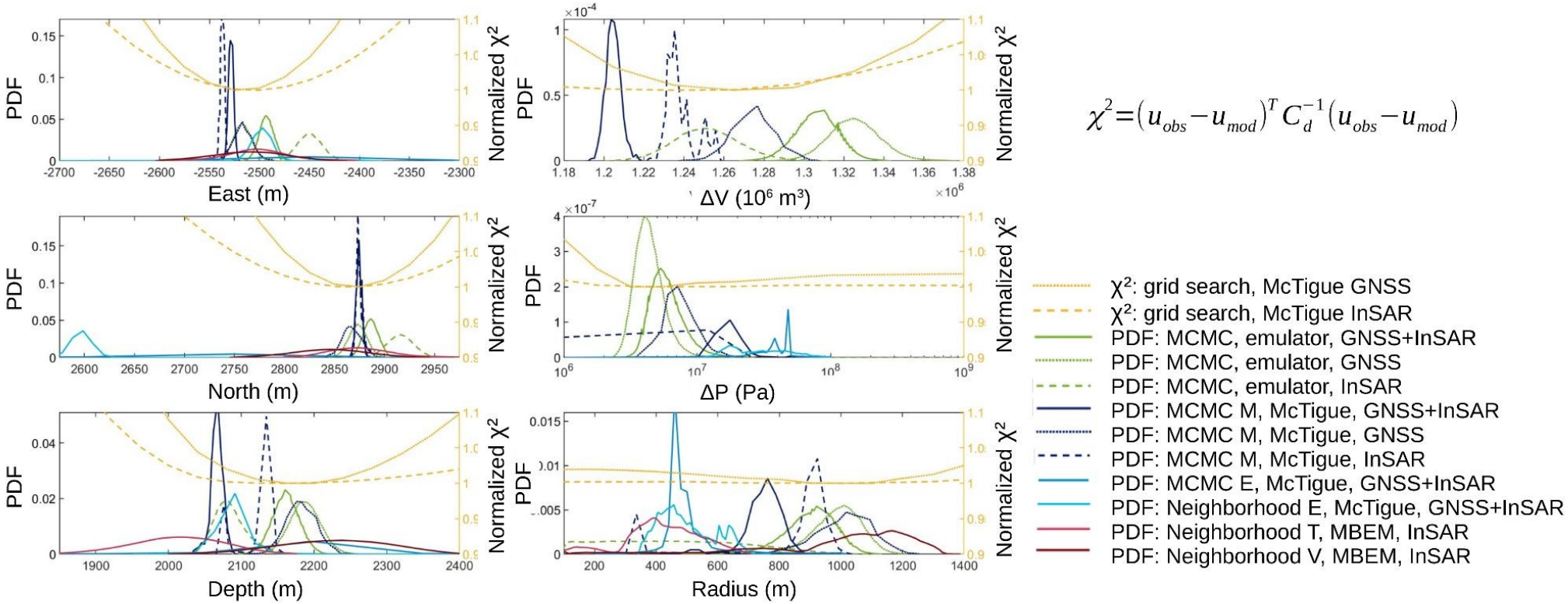

$$\chi^2 = (u_{obs} - u_{mod})^T C_d^{-1} (u_{obs} - u_{mod})$$

- χ^2 reflect poorly resolved parameters (pressure and radius);
- The sharpness of PDF reflect the number of forward models computed using the different inversion methods;
- Emulators used with inversions present interesting alternatives to numerical simulations.

Best practice when analysing volcano deformations

- For deep spherical source (depth/radius>2) at flat volcanoes, Mogi and Mc Tigue solutions are **acceptable**
- For more complex cases, closer to real volcanoes, analytic solutions are **inaccurate**, and **3D numerical solutions** are needed.
- Importance to **benchmark** numerical solutions against exact analytic solutions;
- Importance to **test convergence** of numerical models;
- Because of the large variability related to **inverse methods**, it is important to test new implementations of inversions using **synthetic tests**;
- It is likely that solutions determined have inaccurate parameters and uncertainties estimations: need for **external constraints** on source characteristics, or for **joint inversions** of different parameters.
- For **inversions** with more complex volcanoes, **need** for **fast numerical methods**, such as Gaussian process emulators or Fictitious domains methods.

5. Examples :
5.1. Stress change inversion as gauges for crustal stress

What drives and accommodates rift extension in Kivu ?

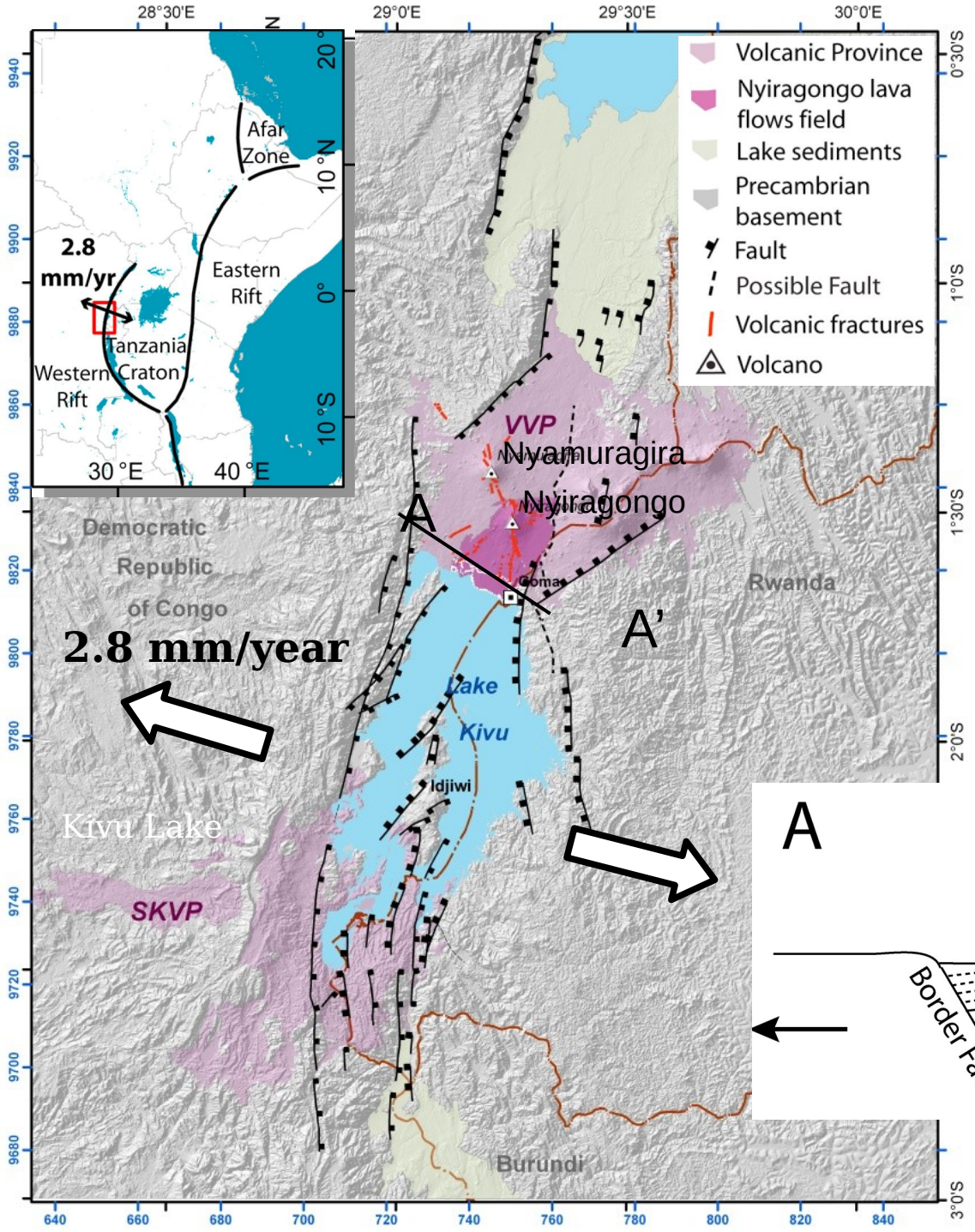

The Virunga volcanic Province (VVP)

Nyiragongo, Goma and its surburb of 2,1 M inhabitants

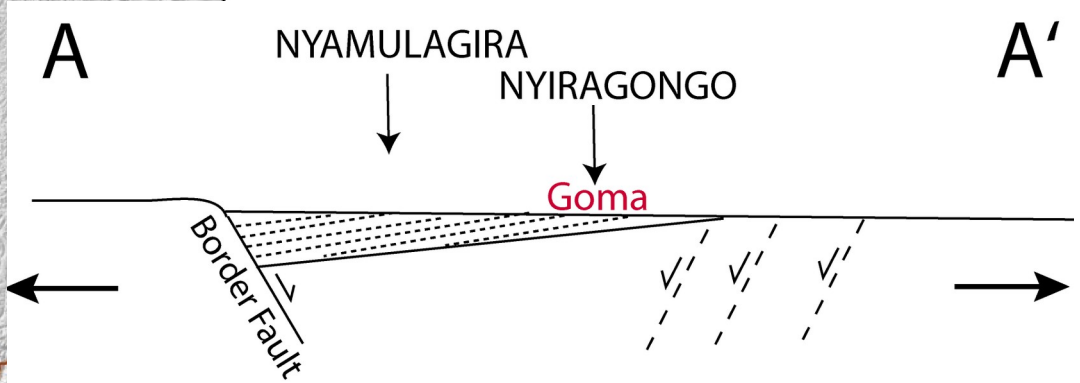

Wauthier et al., JGR, 2012

What drives and accommodates rift extension in Kivu ?

Tectonic stresses and Faulting assisted extension ?

Magma assisted extension ?

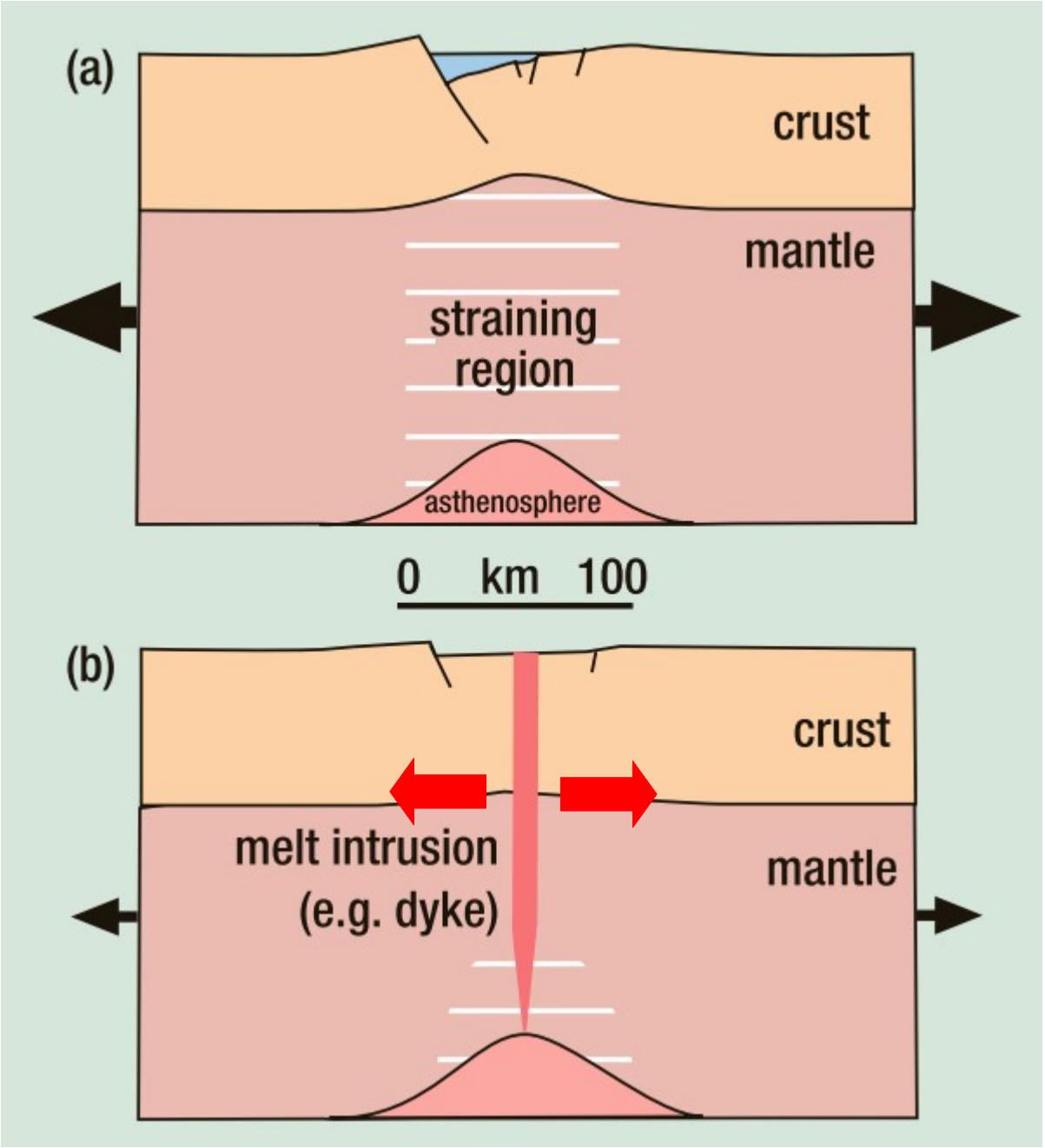

(*Ebinger, Astronomy and Geophysics, 2005*)

What drives and accommodates rift extension in Kivu ?

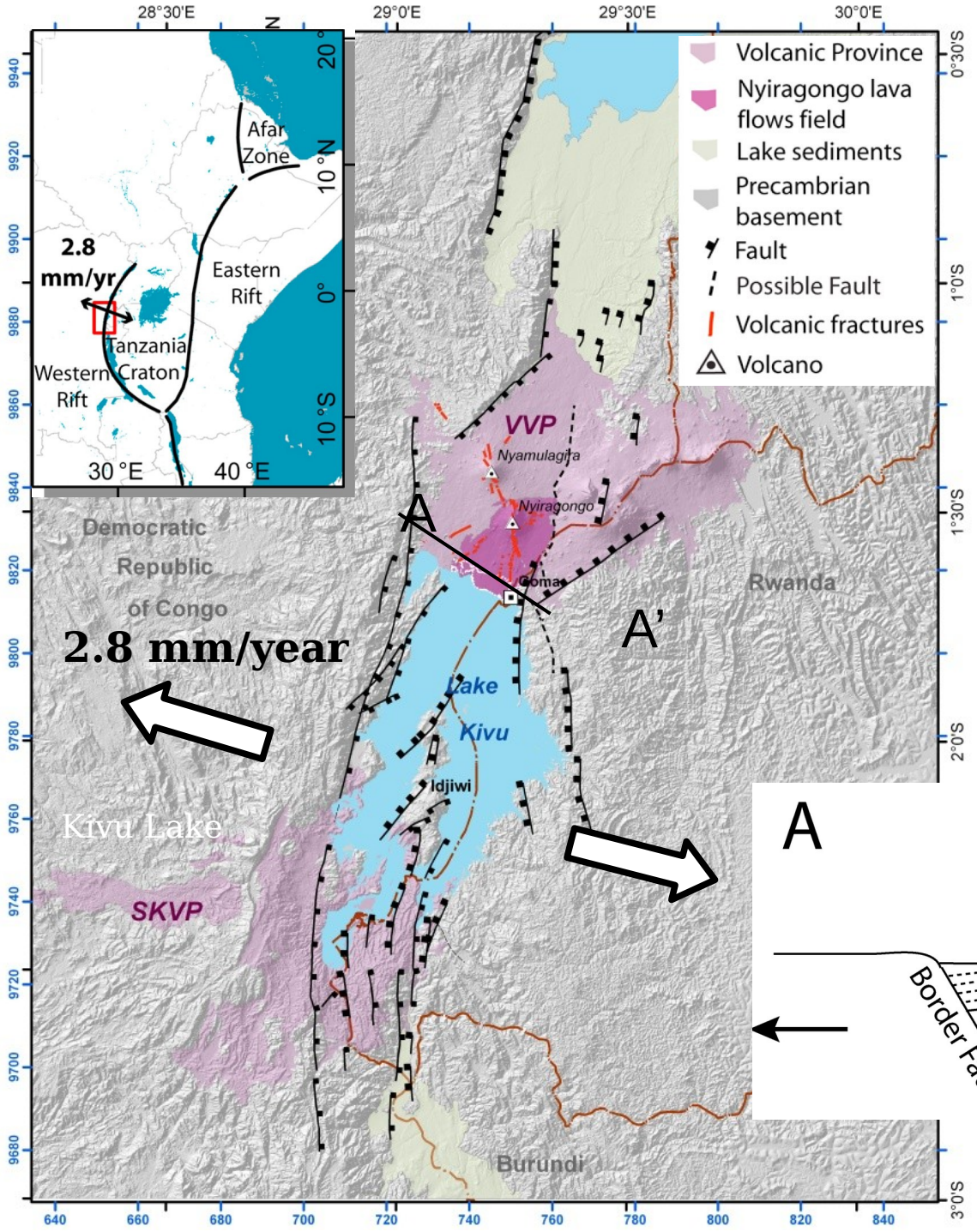

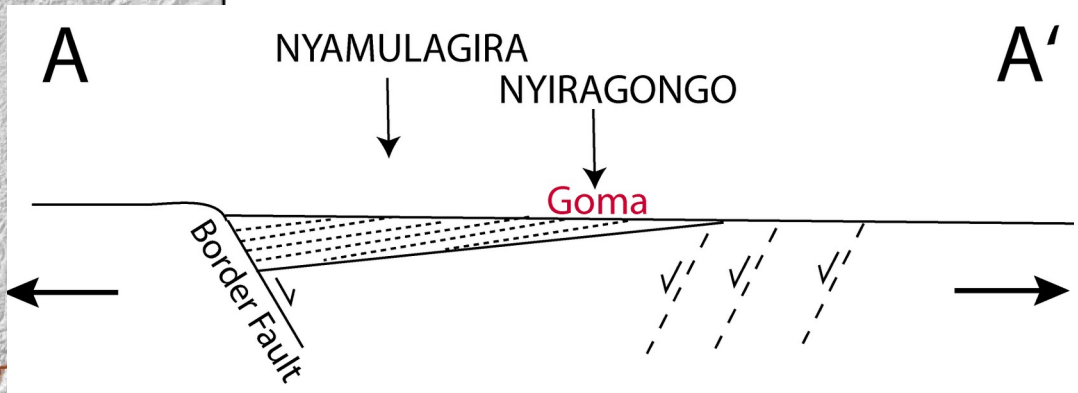

In the Virunga Basin:

- Only 15% of crustal extension
- Extension is accommodated by western border detachment faults,

Ebinger, Geol. Soc. Am. Bull, 1989

Wauthier et al., JGR, 2012

What drives and accommodates rift extension in Kivu ?

Tectonic stresses ?

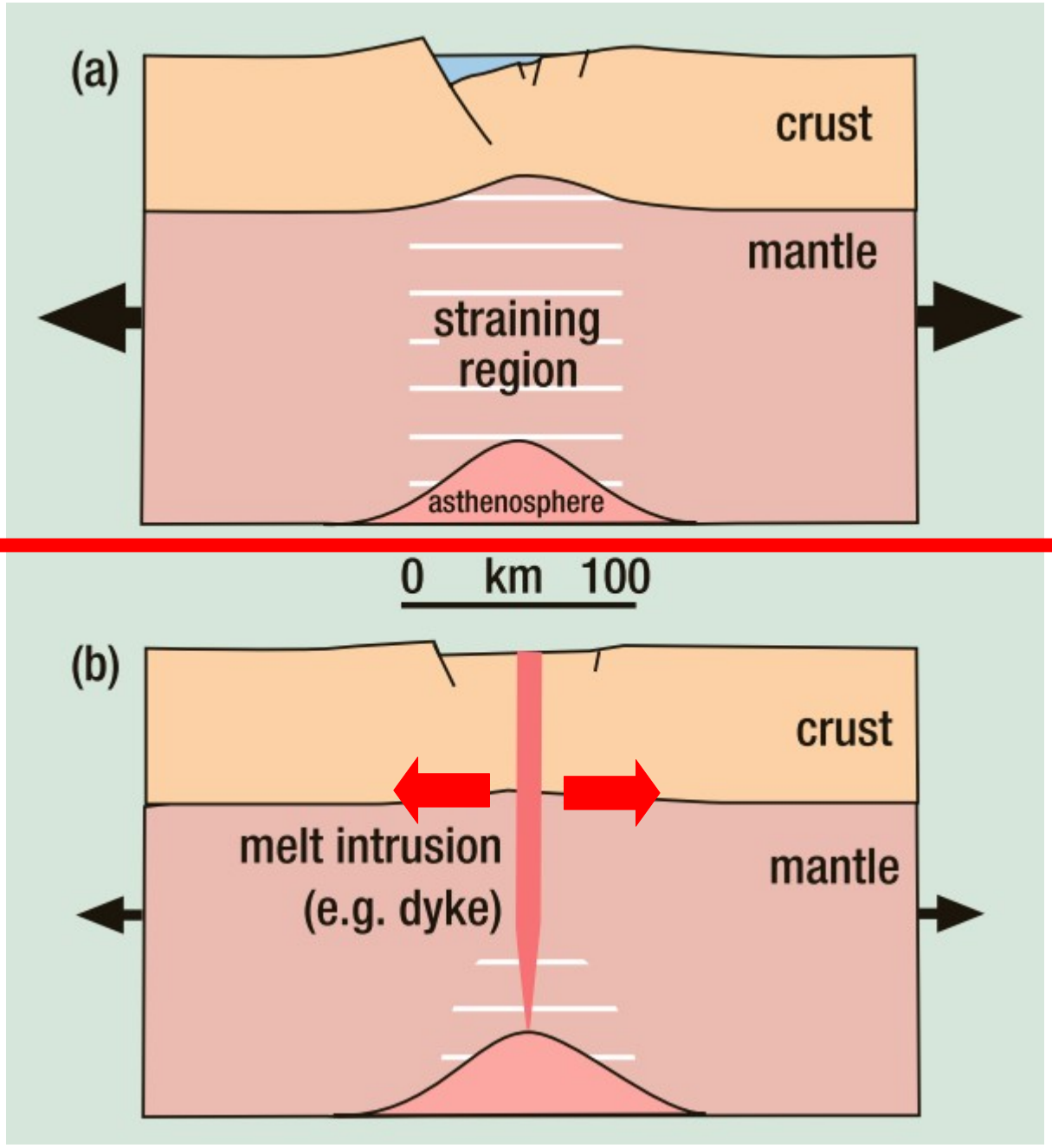

Magma assisted extension ?

(*Ebinger, Astronomy and Geophysics, 2005*)

Nyiragongo 2002 and 2021 eruption
Democratic Republic of the Congo

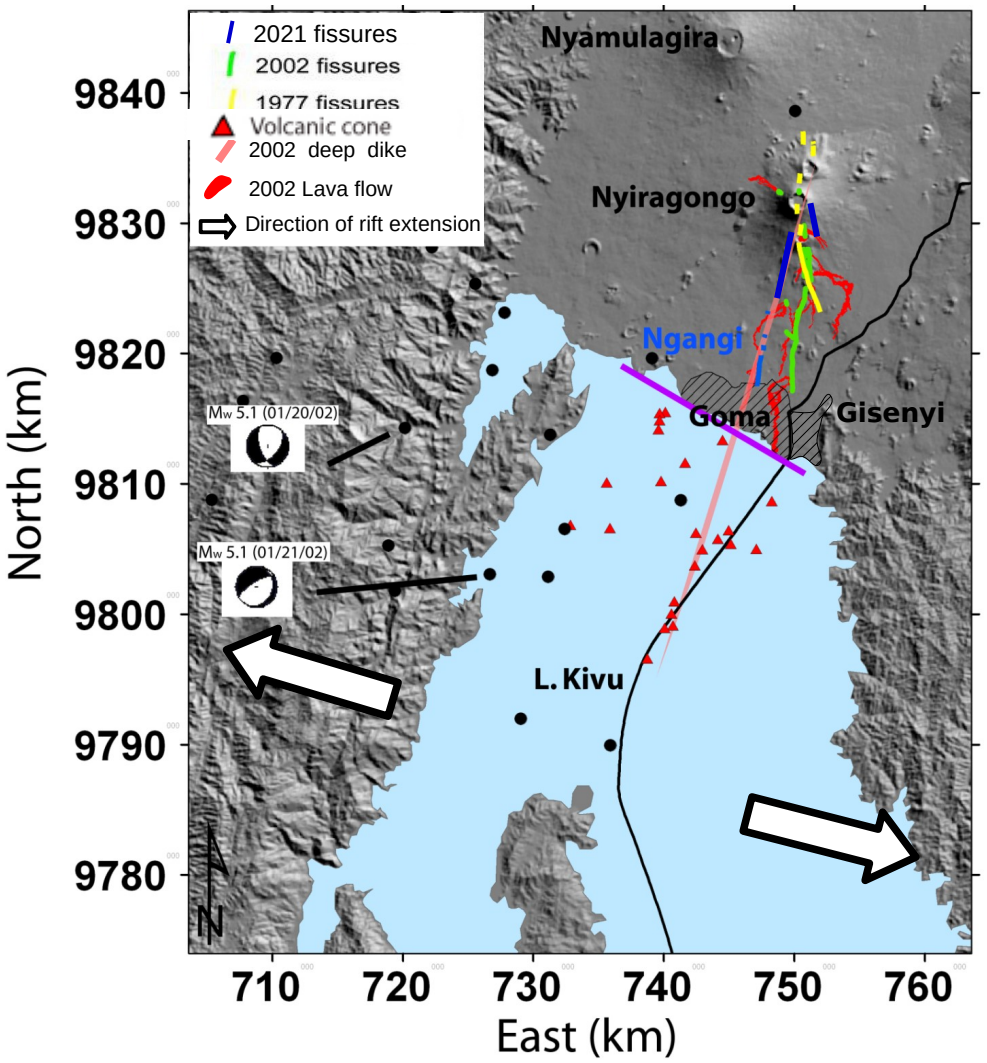

- A strato-volcano with a crater lava Lake

- Three historical eruptions in 1977, 2002 and 2021
- Associated fissures trend NS

Model for Nyiragongo 2002 eruption

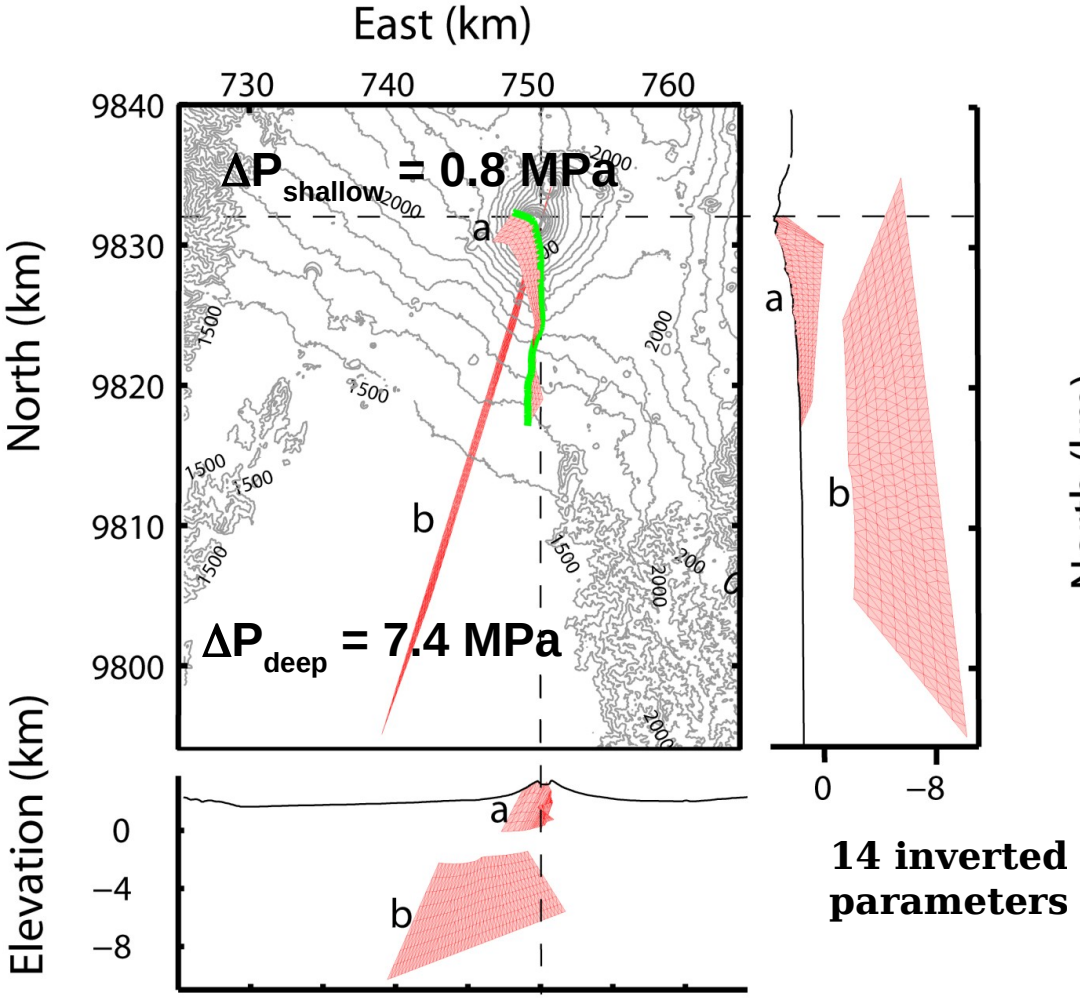

14 inverted parameters

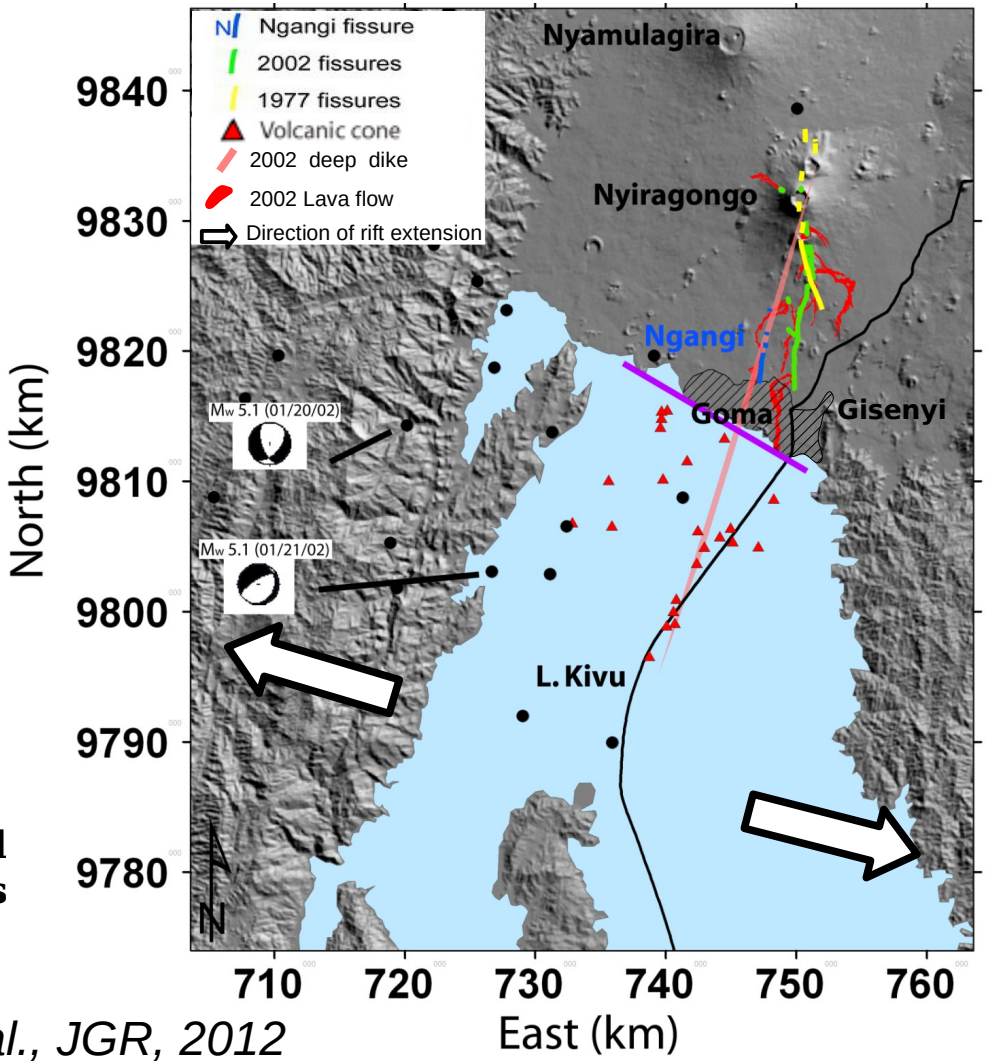

Wauthier et al., JGR, 2012

- **The deep dike is perpendicular to the rift extension direction → Injection direction guided by the rift extension**

The may 2021 eruption confirms the small overpressure

InSAR data

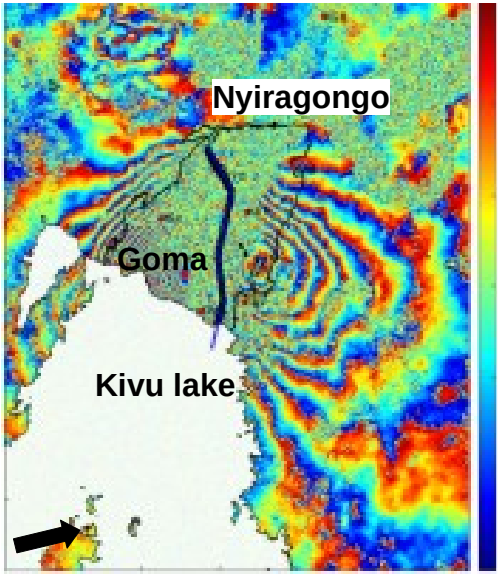

Model

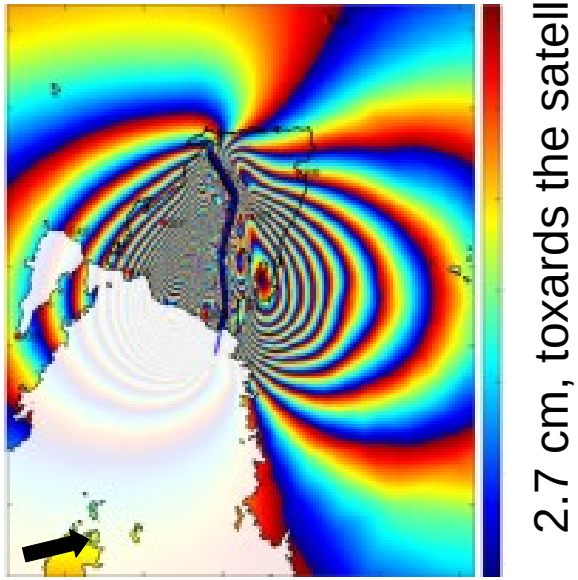

7 inverted parameters

$\Delta P_{shallow}$ = 0.8 MPa

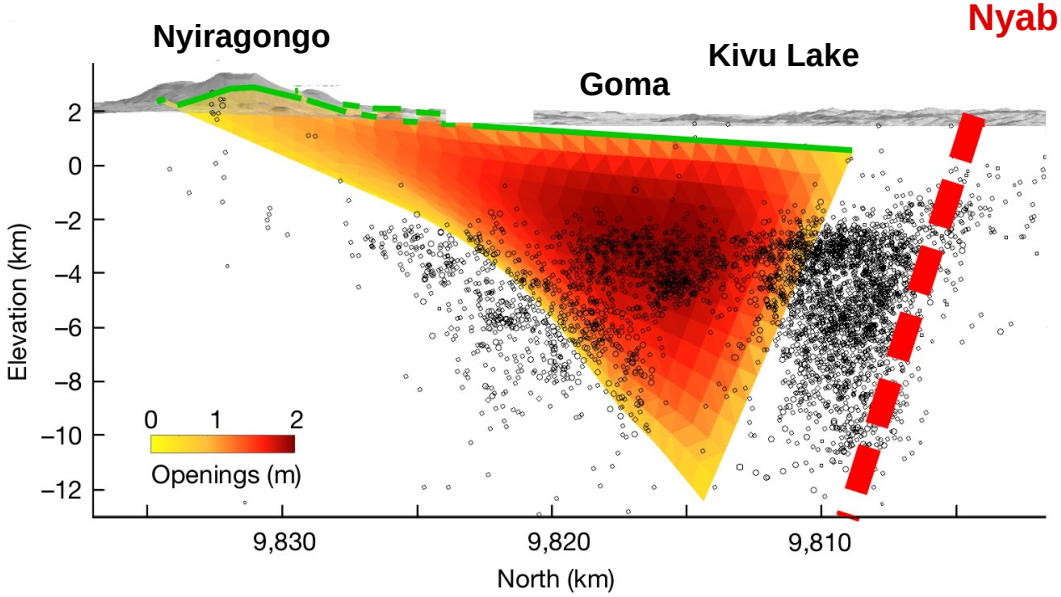

Smittarello et al., Nature, 2022

A magma-assisted rift rextension

Overpressure from InSAR data inversion:

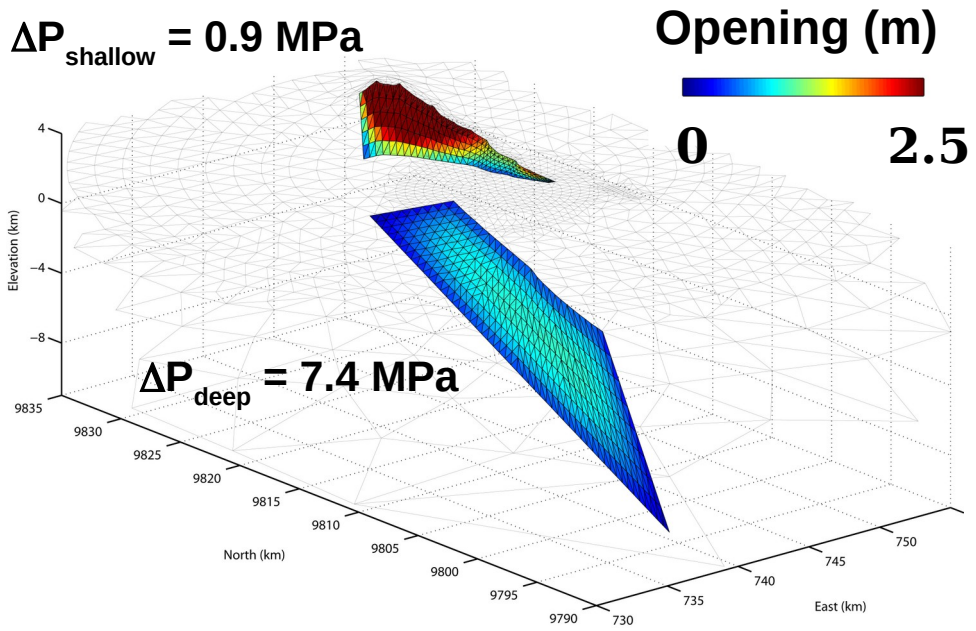

Wauthier et al., JGR, 2012

Overpressure theoretical model:

Assumption: crustal stresses are lithostatic ($\sigma_h \sim \sigma_v \sim P_{rock}$),

$$\Delta P\left(z_{dike}\right) = P_{magma} - P_{rock} = \int \left(\rho_m - \rho_r(z)\right) g dz \,, \qquad \text{with:}$$

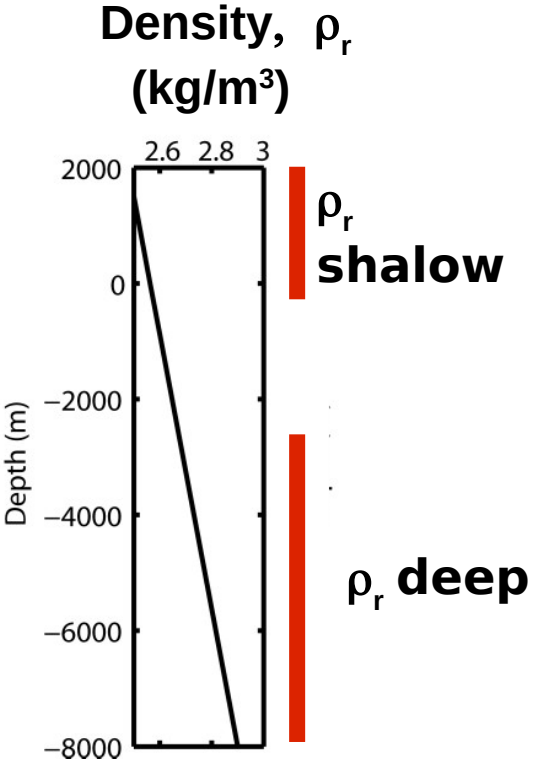

we get $\Delta P_{Shallow} \sim 1$ MPa and $\Delta P_{Deep} = 4.5$ MPa

→ **The crust is at a lithostatic stress state:**
Unconsistent with a rift extension driven by plate separation

→ **The rift extension is driven by the magmatic activity**

What drives and accommodates rift extension in Kivu ?

Tectonic stresses ?

Magma assisted extension ?

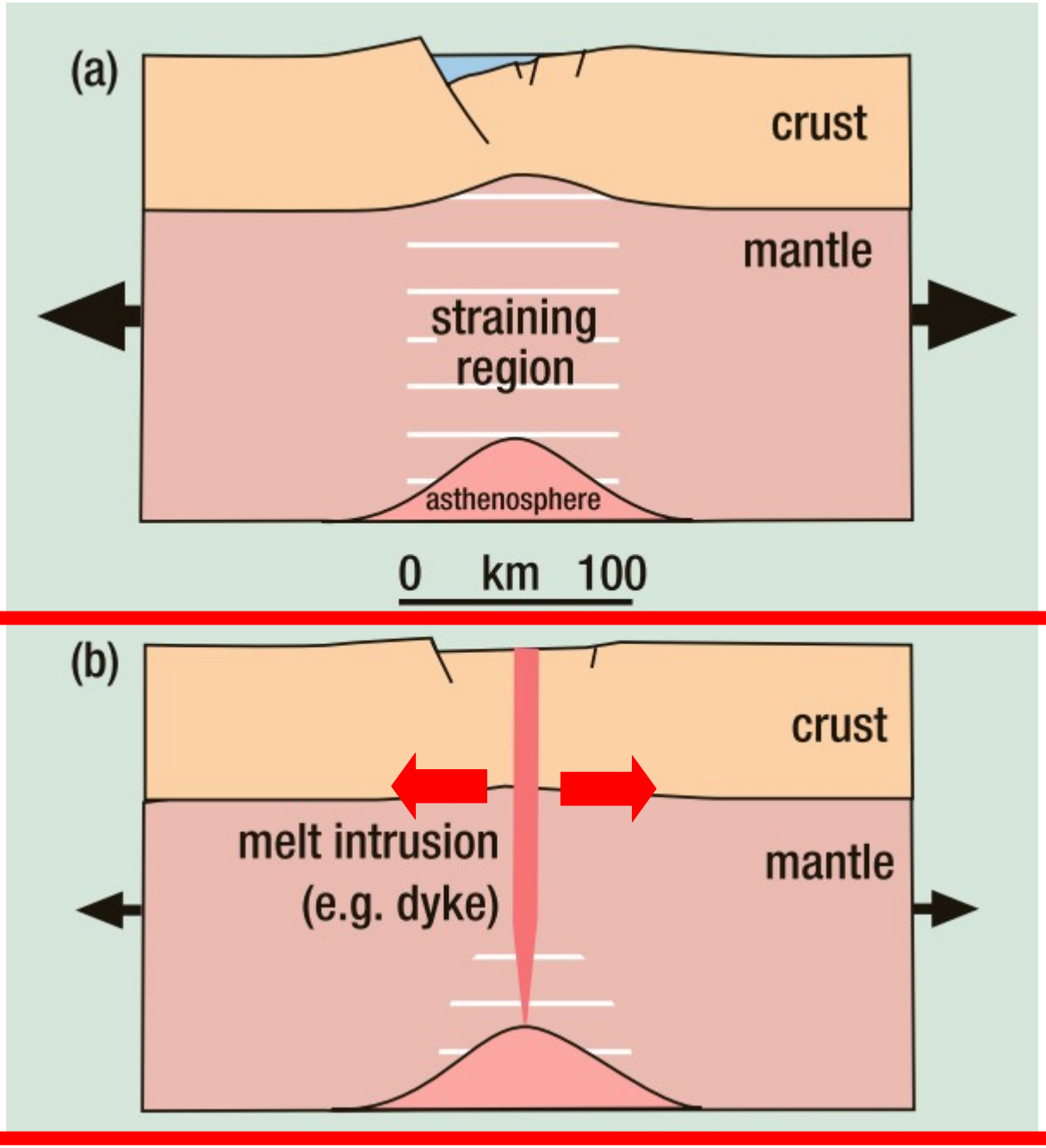

Ebinger, Astronomy and Geophysics, 2005

5. Examples
5.2. Stress change inversion for flank failure mechanisms

Flank failures at Réunion Island

- Induce 24 % of volcano casualties world wide (tsunamis and large earthaquakes)
- Ubiquous at Réunion Island

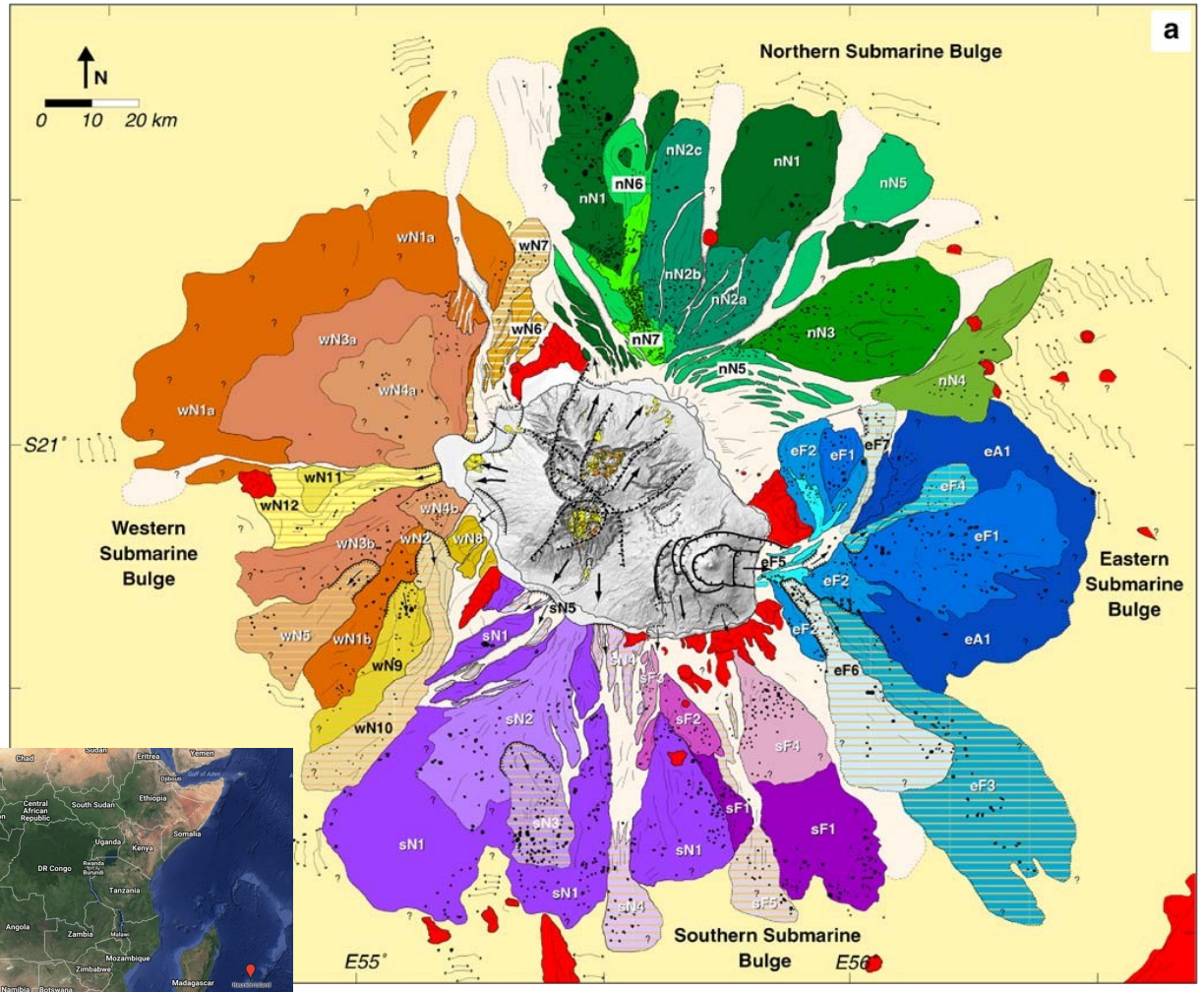

Oehler et al., JVGR, 2008

47 flank failure events
Largest 100 km^3
Oldest 2 My

Piton de la Fournaise is very active: 59 intrusions since 1998 (2.3/year)

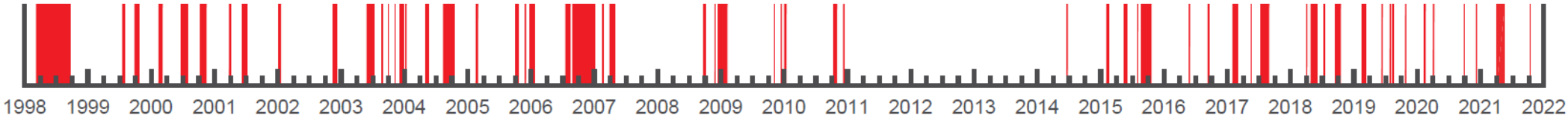

Eruptive fissures : 1932 - 2020

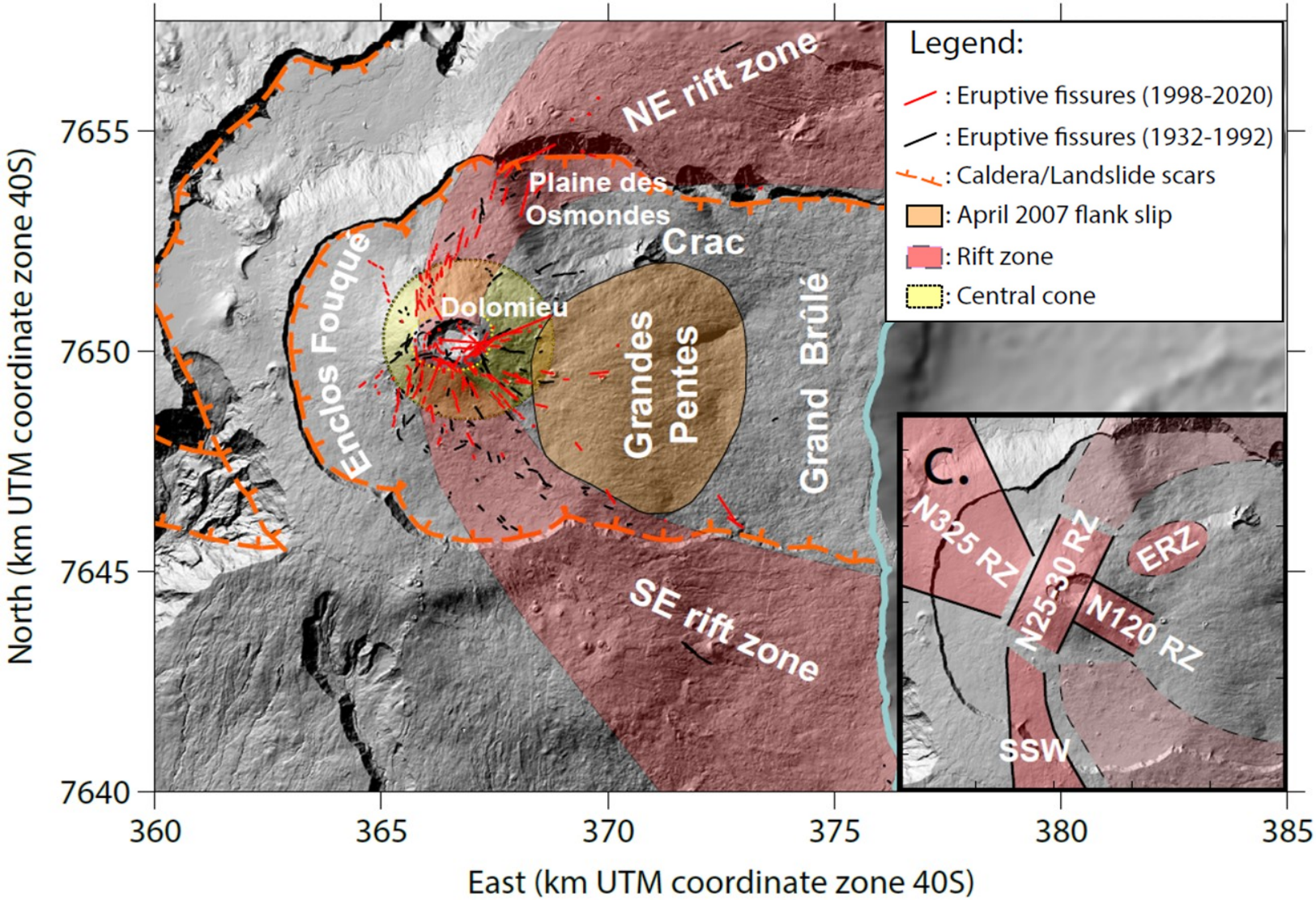

Piton de la Fournaise is one of the best monitored volcanoes

- **since 1998, 57/59 intrusions imaged by at least one InSAR data**

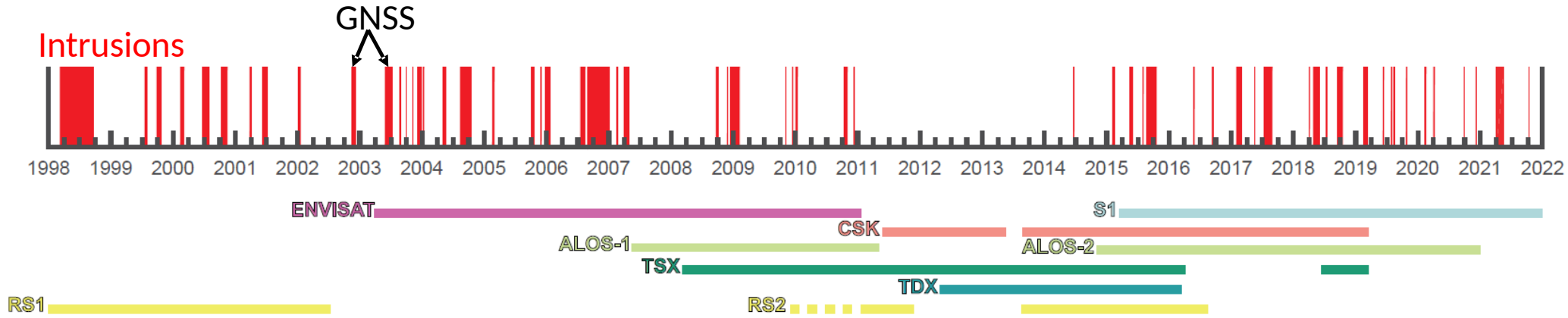

- **GNSS campain + continuous data can be used for non imaged eruptions**

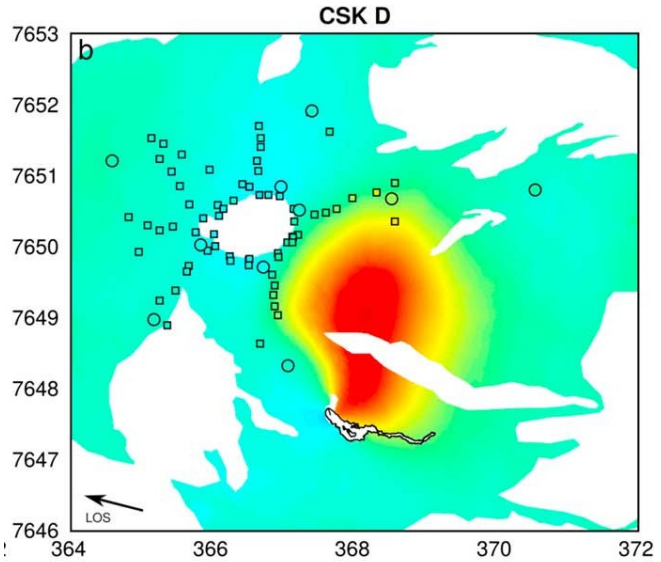

□ Campain GNSS

○ Continuous GNSS

Smittarello et al., JGR, 2019

An unusual flank displacement in 2007

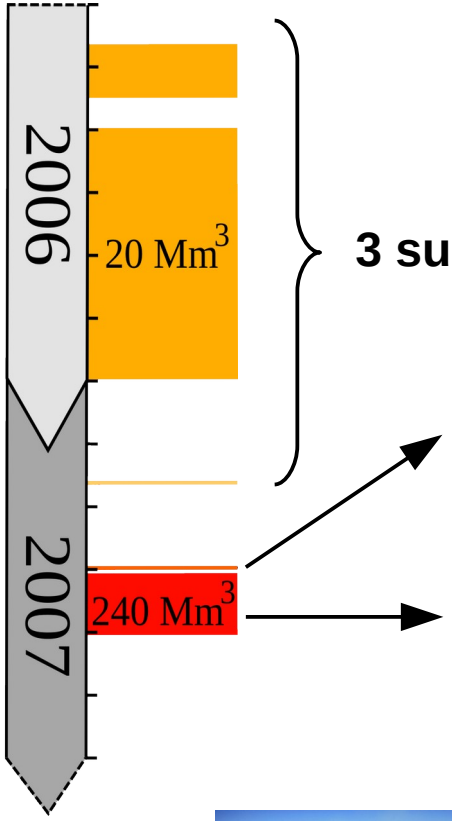

3 summit eruptions

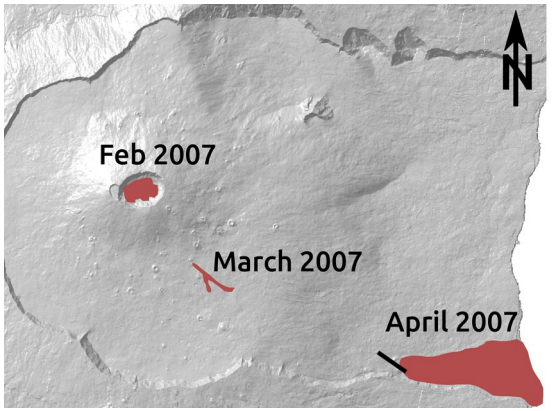

March 30 summit eruption

April 2007: distal eruption

- largest emitted volume of XX, XXI century= 240 Mm^3
- 300 meters high caldera collapse on April 6

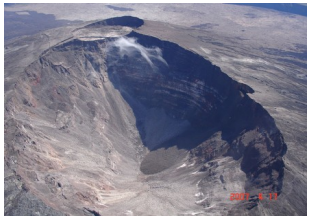

September 2006 **April 2007**

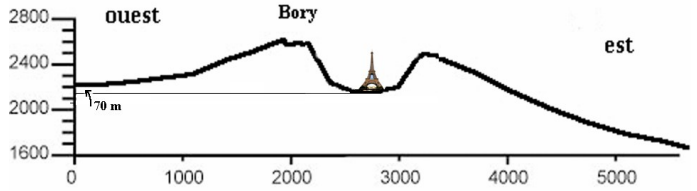

An unusual flank displacement in 2007

Co-eruptive displacement

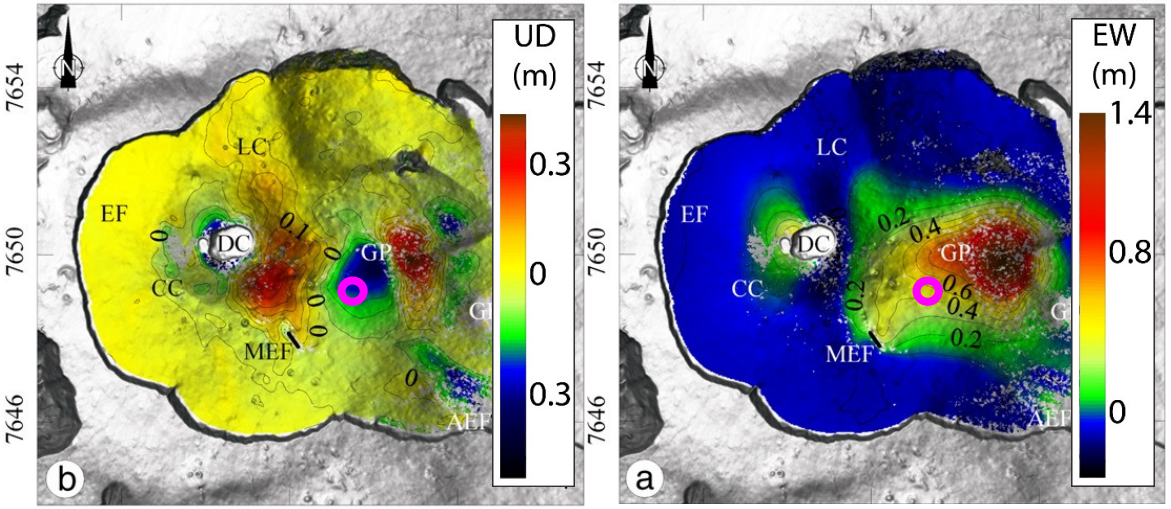

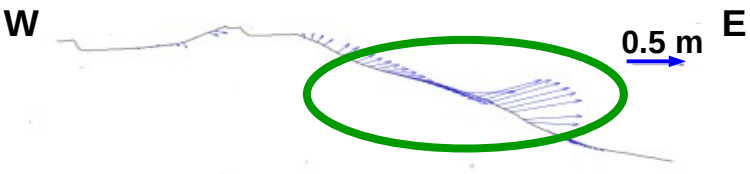

1.4 m eastward / 0.37 m uplift

Froger et al., JVGR, 2015

Long-term EW displacement

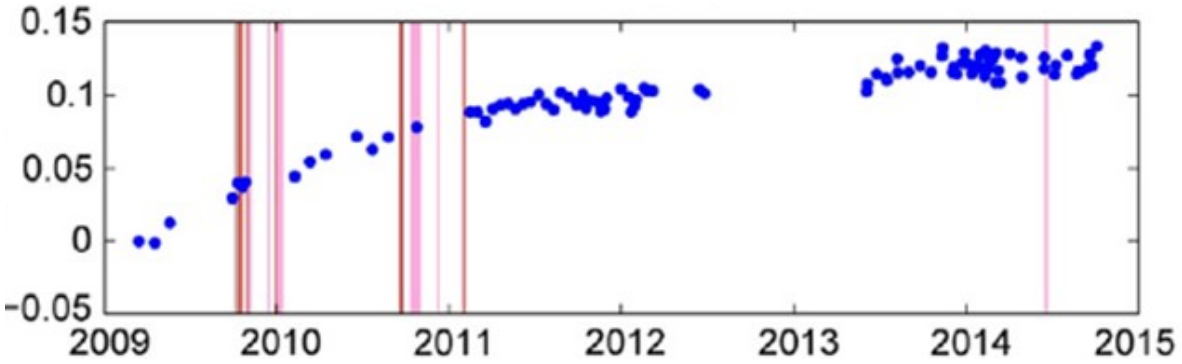

1-2 cm/yr eastward and subsidence

Chen et al., Rem. Sens. Envir., 2017

Origin of the 2007 flank displacement

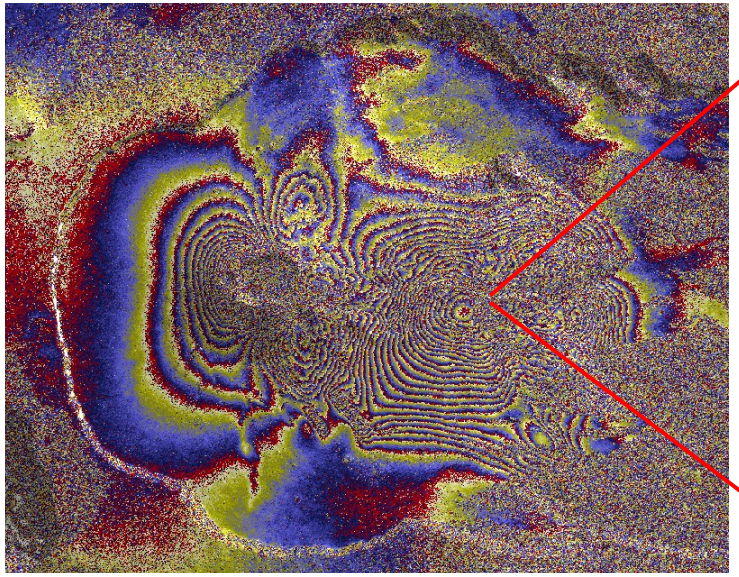

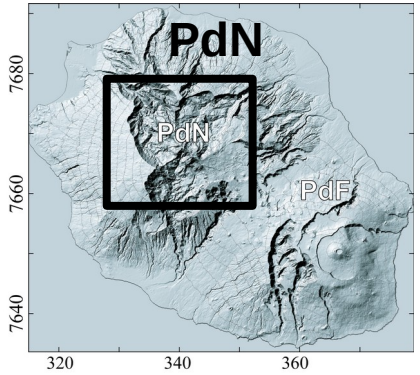

System of faults ?

Hawaï

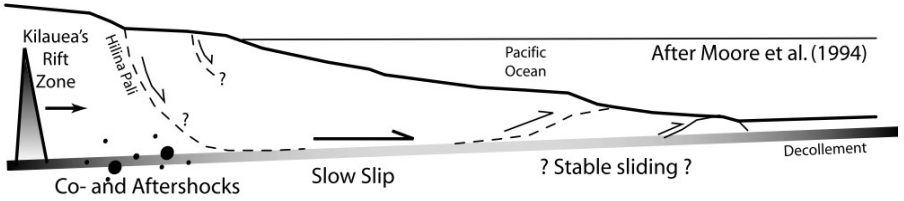

Montgomery-Brown et al., JGR, 2009

Intrusion and shearing of a sill ?

Piton des Neiges

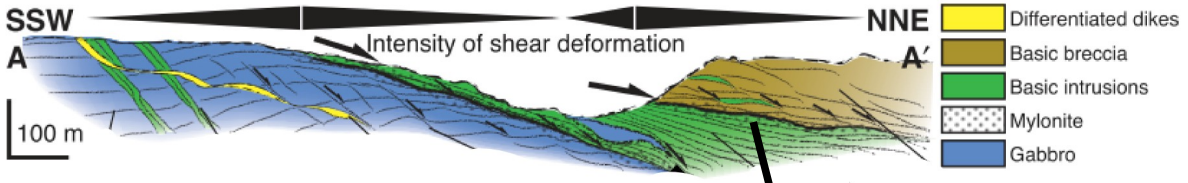

Famin and Michon, Geology, 2010

Evidence of shear ductile and brittle deformation

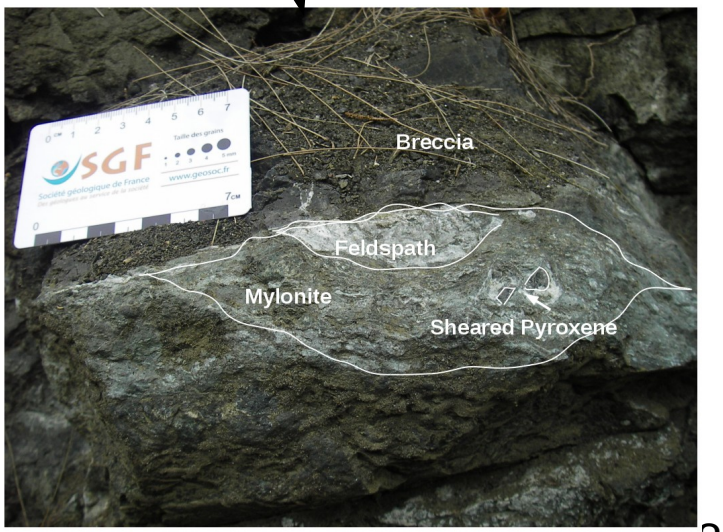

Inverse modeling of 22 years of InSAR and GNSS data

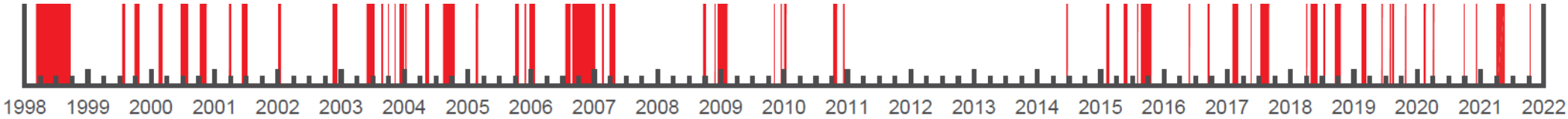

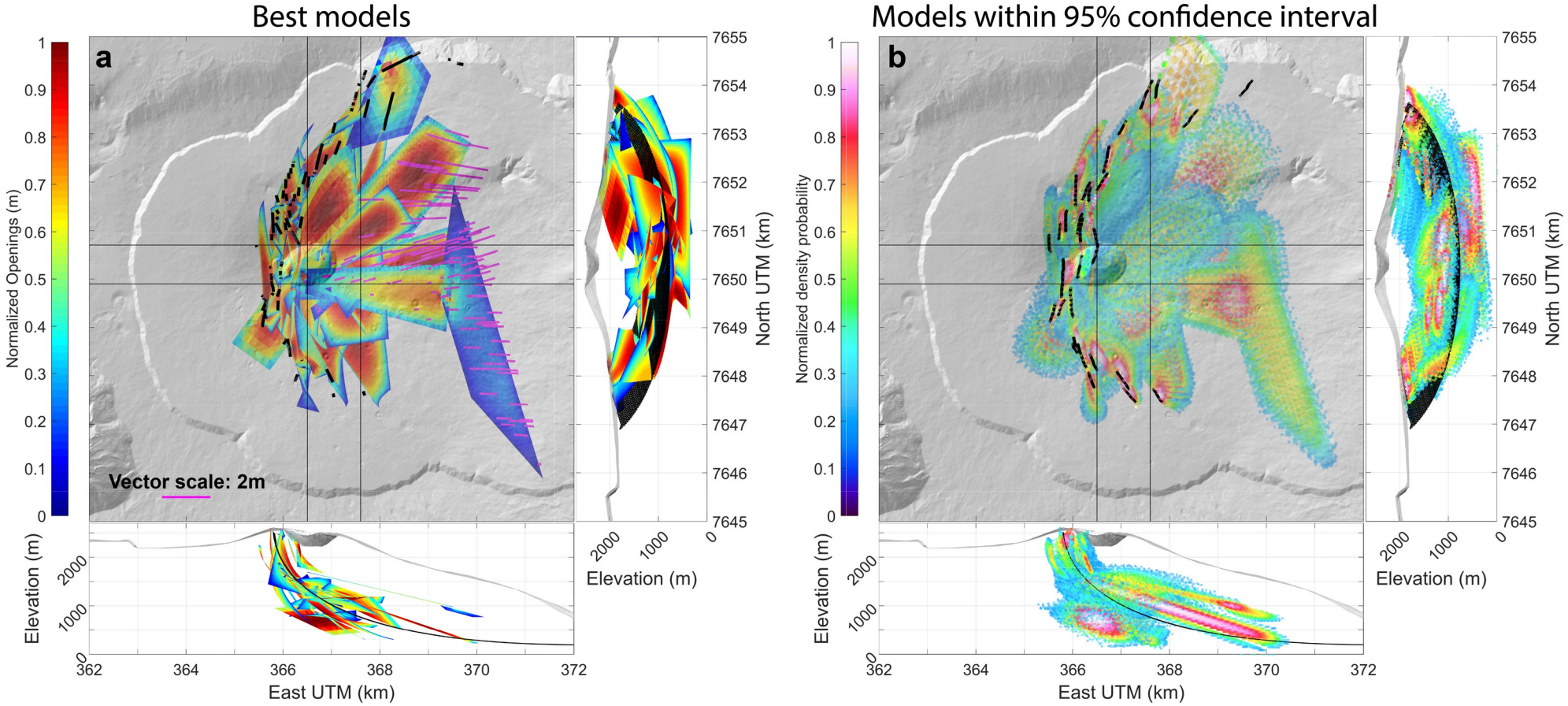

Dumont et al., Nature Communication, 2023 ; EPSL, 2024

➡ **80% of the magma intrudes in a spoon-shaped collapse structure**

A major spoon-shaped collapse structure

Dumont et al., Nature Communication, 2023 ; EPSL, 2024

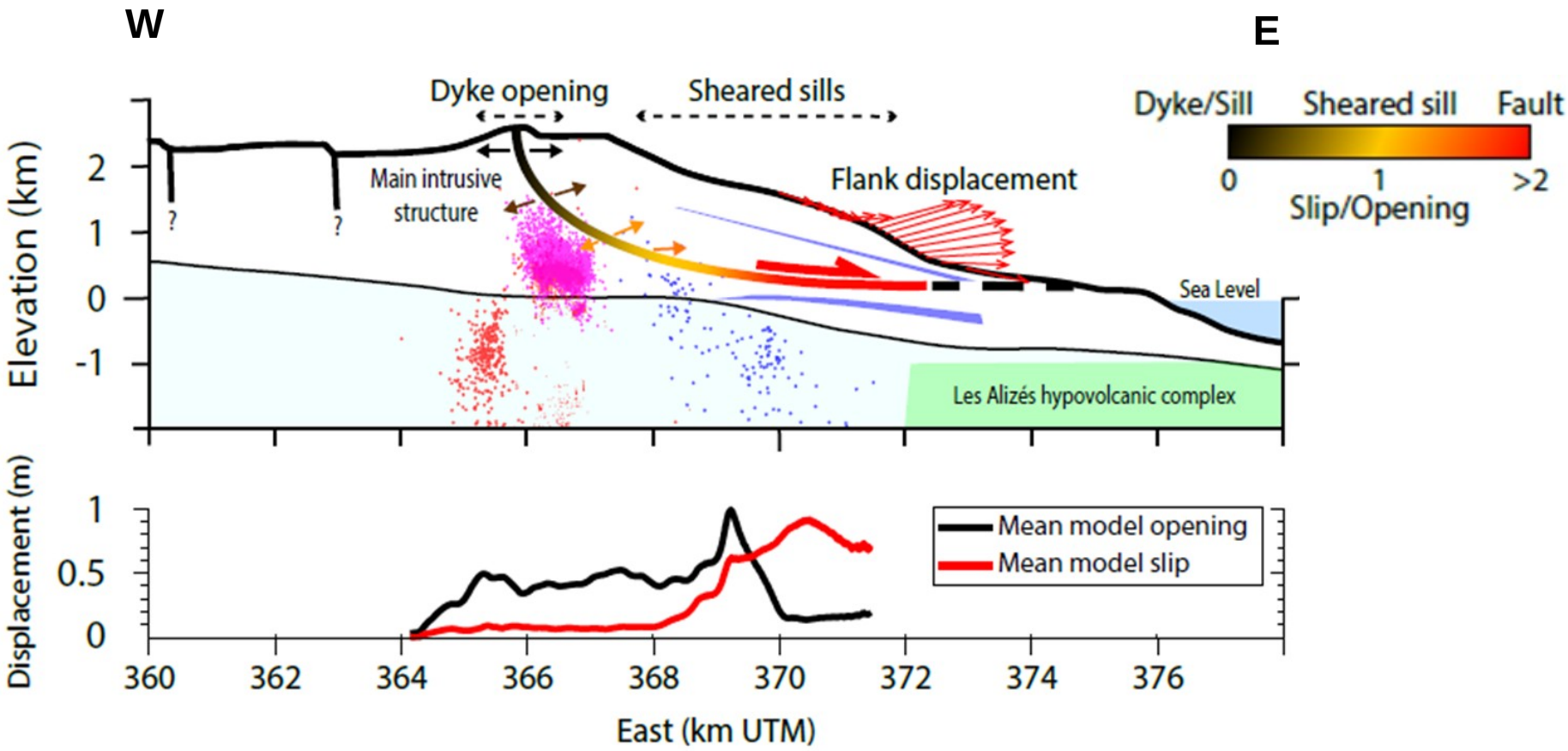

Continuum of displacements from west to east:

- **Pure opening of subvertical curved dykes**
- **Curved sheared sills**
- **Fault slip in the easternmost part (in 2007)**

➡ **Hybrid between previously assumed models;**

➡ **Could accommodate flank failure**

A similar structure may be active at Etna as evidence by the 2018 Christmas event

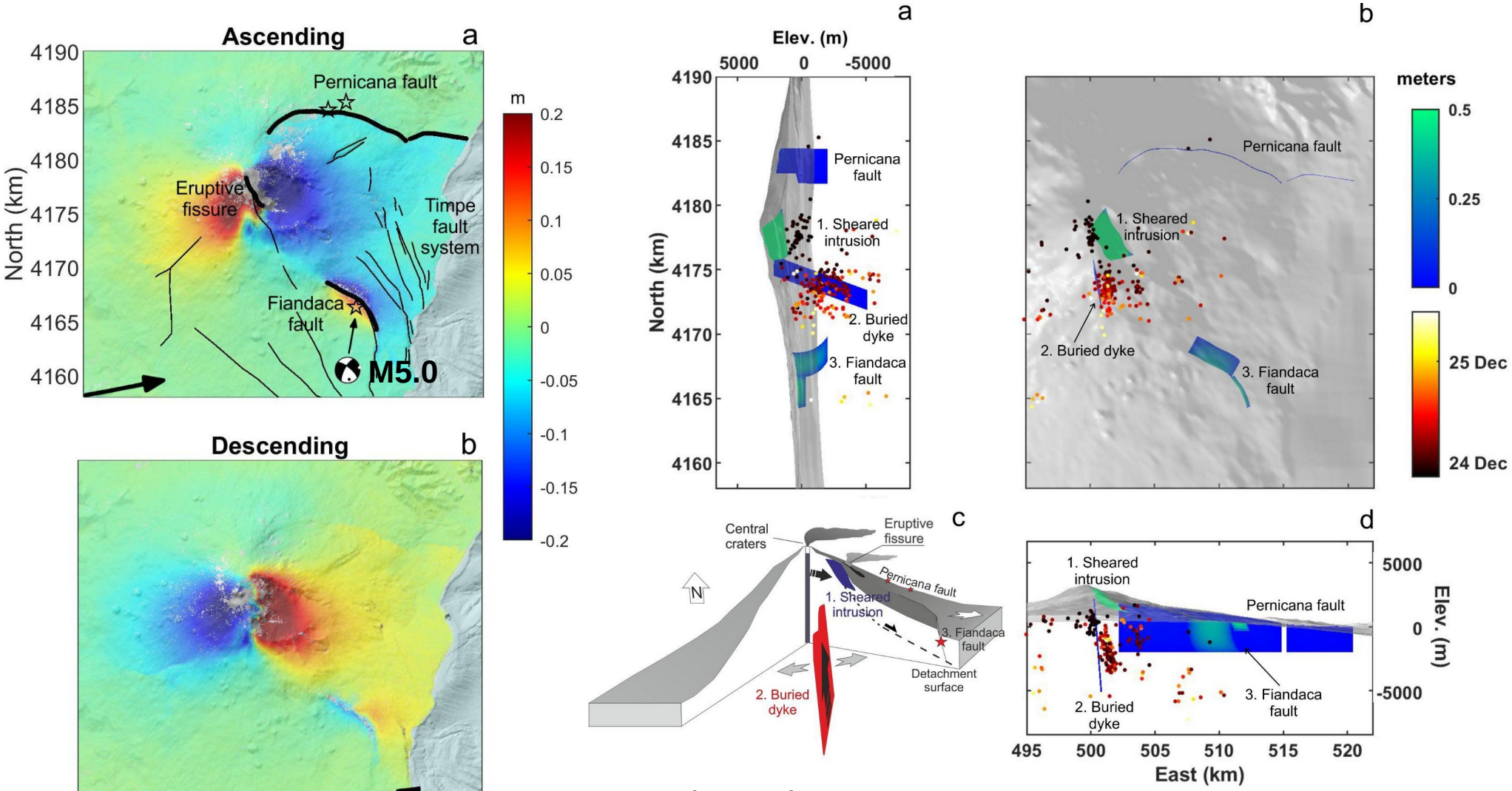

Iozzia et al., GRL, 2024

- A **curved sheared intrusion** and a **buried dyke** explain displacement close to the summit;
- Pernicana fault responded passively; Fiandaca fault released accumulated stress;

What can be learnt from the Inverse modelling of InSAR data ?

Rift extension drive

Wauthier et al., JGR, 2012

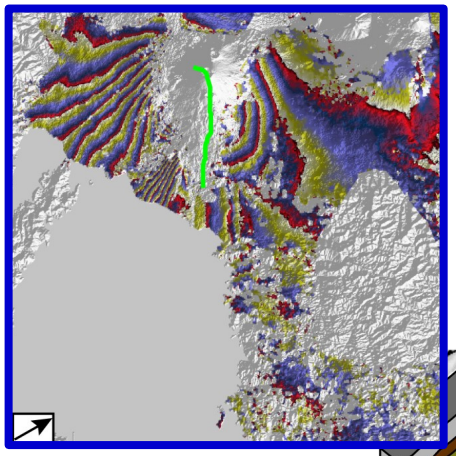

Intrusion pathways

Bagnardi et al., EPSL, 2013

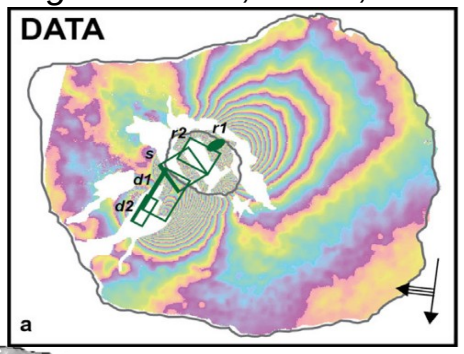

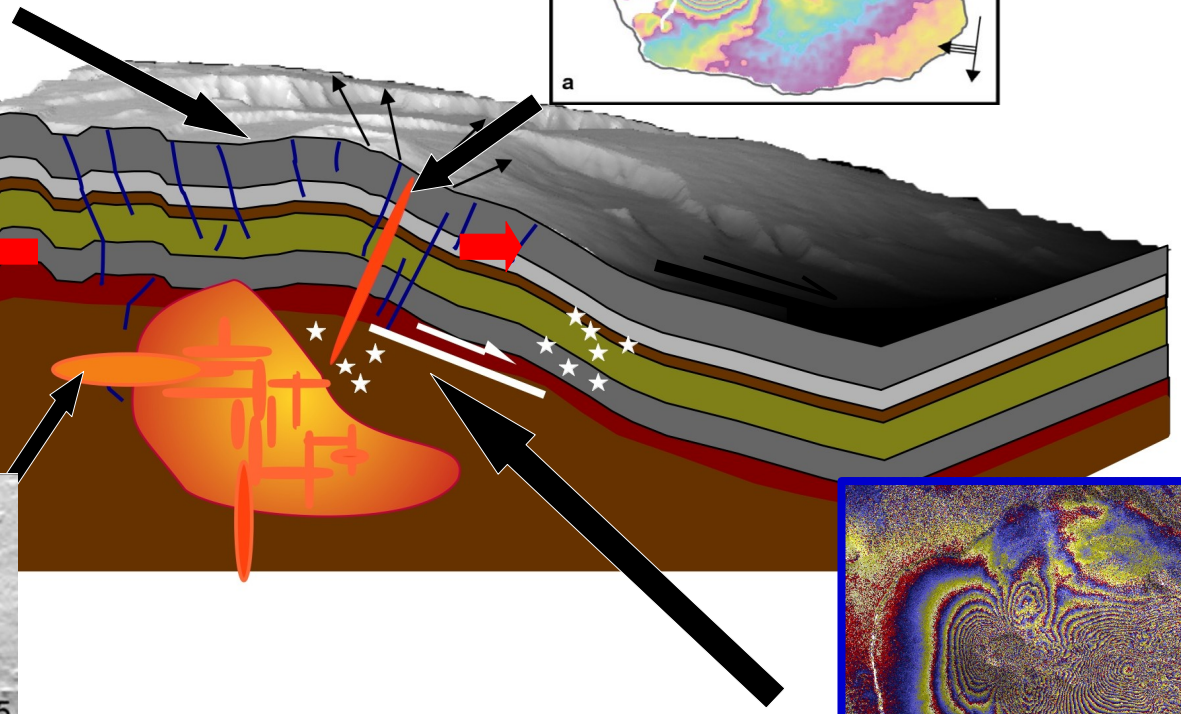

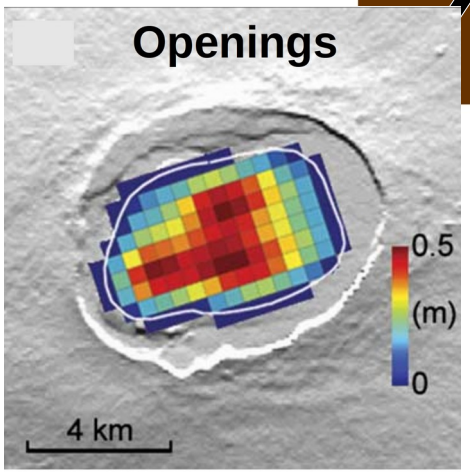

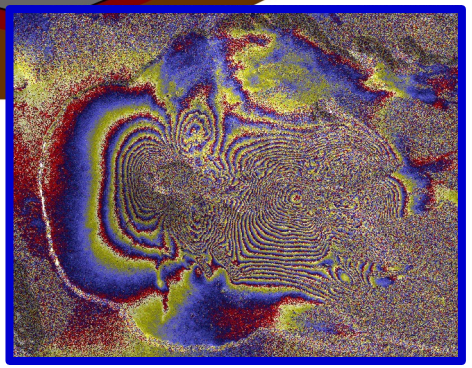

Flank slip mechanism

Tridon et al., JGR, 2016;
Dumont et al., Nat. comm., 2022.

Characteristics of reservoirs

Amelung et al., Science, 2000

Conclusions about inversions with stress boundary conditions

- **Inverting for stress changes:**
  - **is more physical than kinematic inversions;**
  - **leads to more likely models;**
  - **is more informative.**

- **In the Virunga Volcanic Province, the rift extension is driven by magmatic activity rather than plate extension;**
- **At Piton de la Fournaise, we find a continuum of fracture displacement: dike intrusion -> sheared intrusions -> fault slip that accommodates magma intrusions;**
- **Sheared intrusions also seem to be active at Etna.**
- **Sheared intrusions should be searched at other shield volcanoes with evidence of flank slip**


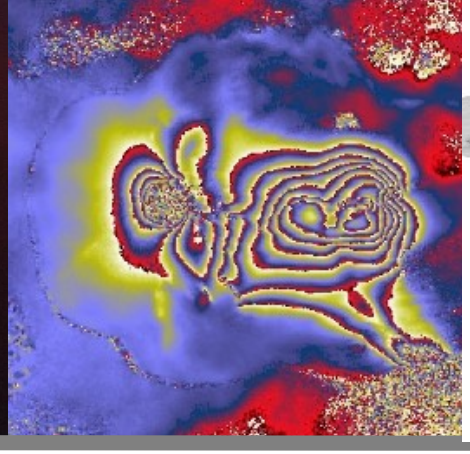
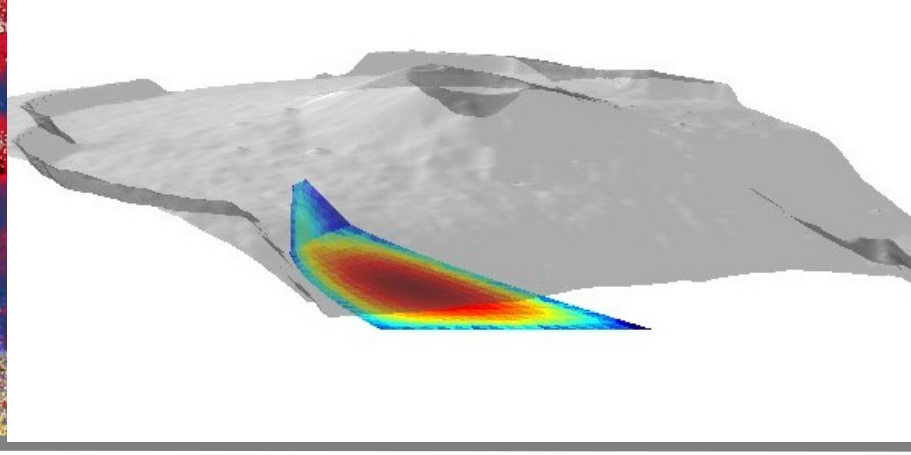

Thank you for your attention !


Quentin Dumont


Christelle Wauthier


Yo Fukushima


Marine Tridon


Gilda Currenti


Jean-Luc Froger


Adriana Iozzia